Dissertation
submitted to the
Combined Faculty of Mathematics, Engineering and Natural Sciences
of Heidelberg University, Germany
and to the
Department of Physics
of the University of Trento, Italy
for the degree of
Doctor of Natural Science

Put forward by
Ricardo Costa de Almeida
born in: Vitória, Espirito Santo, Brazil
Oral examination: November 7, 2022

Entanglement certification in quantum many-body systems

Author:	Ricardo Costa de Almeida
Supervisors:	Philipp Hauke Jürgen Berges
Referees:	Markus Oberthaler Jörg Evers

Zusammenfassung

Verschränkung ist eine grundlegende Eigenschaft von Quantensystemen und ihre Charakterisierung ein zentrales Problem der Physik. Darüber hinaus besteht eine steigende Nachfrage nach skalierbaren Protokollen, die das Vorhandensein von Verschränkung bescheinigen können. Dies liegt vor allem an der Rolle der Verschränkung als entscheidende Ressource für Quantentechnologien. Die systematische Zertifizierung der Verschränkung ist jedoch sehr anspruchsvoll, und dies gilt insbesondere für Quanten-Vielteilchensysteme. In dieser Dissertation stellen wir uns dieser Herausforderung und stellen einige Techniken vor, die die Zertifizierung von mehrteiliger Verschränkung in Vielteilchensystemen ermöglichen. Dies wird mit einer Anwendung auf ein Modell wechselwirkender Fermionen demonstriert, das das Vorhandensein einer elastischen mehrteiligen Verschränkung bei endlichen Temperaturen zeigt. Darüber hinaus diskutieren wir auch einige Feinheiten bezüglich der Definition von Verschränkung in Systemen nicht unterscheidbarer Teilchen und liefern eine formale Charakterisierung der multipartiten Modenverschränkung. Dazu müssen wir mit einem abstrakten Formalismus arbeiten, mit dem sich die Verschränkung in Quanten-Vielteilchensystemen ohne Bezug auf eine bestimmte Struktur der Zustände definieren lässt. Um diese Technik weiter zu demonstrieren, und auch motiviert durch aktuelle Quantensimulationsbemühungen, verwenden wir sie, um den Rahmen von Verschränkungszeugen auf Theorien von Gittereichungen zu erweitern.

Abstract

Entanglement is a fundamental property of quantum systems and its characterization is a central problem for physics. Moreover, there is an increasing demand for scalable protocols that can certify the presence of entanglement. This is primarily due to the role of entanglement as a crucial resource for quantum technologies. However, systematic entanglement certification is highly challenging, and this is particularly the case for quantum many-body systems. In this dissertation, we tackle this challenge and introduce some techniques that allow the certification of multipartite entanglement in many-body systems. This is demonstrated with an application to a model of interacting fermions that shows the presence of resilient multipartite entanglement at finite temperatures. Moreover, we also discuss some subtleties concerning the definition entanglement in systems of indistinguishable particles and provide a formal characterization of multipartite mode entanglement. This requires us to work with an abstract formalism that can be used to define entanglement in quantum many-body systems without reference to a specific structure of the states. To further showcase this technique, and also motivated by current quantum simulation efforts, we use it to extend the framework of entanglement witnesses to lattice gauge theories.

Sommario

L'entanglement è una proprietà fondamentale dei sistemi quantistici e la sua caratterizzazione è un problema centrale per la fisica. Inoltre, vi è una crescente richiesta di protocolli scalabili in grado di certificare la presenza di entanglement. Ciò è dovuto principalmente al ruolo dell'entanglement come risorsa cruciale per le tecnologie quantistiche. Tuttavia, la certificazione sistematica dell'entanglement è molto impegnativa, e questo è particolarmente vero per i sistemi quantistici a molti corpi. In questa dissertazione, affrontiamo questa sfida e introduciamo alcune tecniche che consentono la certificazione dell'entanglement multipartito in sistemi a molti corpi. Ciò è dimostrato con un'applicazione a un modello di fermioni interagenti che mostra la presenza di entanglement multipartito resiliente a temperature finite. Inoltre, discutiamo anche alcune sottigliezze riguardanti la definizione di entanglement in sistemi di particelle indistinguibili e forniamo una caratterizzazione formale dell'entanglement multipartito. Ciò ci richiede di lavorare con un formalismo astratto che può essere utilizzato per definire l'entanglement nei sistemi quantistici a molti corpi senza fare riferimento a una struttura specifica degli stati. Per mostrare ulteriormente questa tecnica, e anche motivata dagli attuali sforzi di simulazione quantistica, la usiamo per estendere la struttura dei testimoni di entanglement alle teorie di gauge del reticolo.

Resumo

O emaranhamento é uma propriedade fundamental dos sistemas quânticos e sua caracterização é um problema central para a física. Além disso, há uma demanda crescente por protocolos escaláveis que possam certificar a presença de emaranhamento. Isso se deve principalmente ao papel do emaranhamento como um recurso crucial para as tecnologias quânticas. No entanto, a certificação sistemática de emaranhamento é altamente desafiadora, e este é particularmente o caso de sistemas quânticos de muitos corpos. Nesta dissertação, abordamos este desafio e apresentamos algumas técnicas que permitem a certificação do emaranhamento multipartido em sistemas de muitos corpos. Isto é demonstrado com uma aplicação a um modelo de férmions interagentes que mostra a presença de emaranhamento multipartido resiliente a temperaturas finitas. Além disso, também discutimos algumas sutilezas sobre a definição de emaranhamento em sistemas de partículas indistinguíveis e fornecemos uma caracterização formal do emaranhamento de modo multipartido. Isso exige que trabalhemos com um formalismo abstrato que pode ser usado para definir o emaranhamento em sistemas quânticos de muitos corpos sem referência a uma estrutura específica dos estados. Para mostrar ainda mais essa técnica, e também motivado pelos atuais esforços de simulação quântica, nós a usamos para estender a estrutura de testemunhas de emaranhamento para teorias de gauge na rede.

Acknowledgments

First, I would like to thank Philipp Hauke for being a fantastic supervisor and researcher. It was a great pleasure to work with you all these years and have so many interesting discussions. Be it in presence or remotely, research or not, you provided constant support and engaging conversations. So thank you for sharing a bit of your knowledge and vision with me. You encouraged me constantly, quite literally all the way to the last minute, and I'm genuinely grateful for that.

Likewise, I thank Jürgen Berges for being my supervisor during the cotutelle, and Markus K. Oberthaler and Jörg Evers for being part of my committee. I appreciate it very much, and I'm certain we will have an interesting discussion during the examination.

Of course, I must also express my gratitude to the group. As a collective, for providing a stimulating research environment, but also to all members individually, for the conversations we had, about physics or otherwise. Fruit breaks, isolated houses, nonsense discussions, struggles with bureaucracy, basements, chairs, food, and all the rest of it. Special mentions go to Veronica, whom I worked with closely in the lattice gauge theory project that is an important part of this dissertation. Before coming to Trento, I also had a great time at the KIP and ITP, where I learned plenty of physics. I'm specially thankful for all the breakfasts that made me (hopefully) less ignorant of experimental physics.

For all my friends, scattered around different cities, countries and continents, you provided me with moments of joy, introspection, and comradery that were essential. Thank you.

My family was extremely supportive during all these years and a source of comfort. I thank you all, but specially my parents Bruno and Sylvia, who instilled in me the thirst for knowledge, and my brothers, Rafael and Victor, ever present in the lively debates during dinner. It was a nice surprise, even if under bad circumstances, to be able to spend some time back home with you. It is also necessary to highlight my time in Cotia with Nicole's family. Thank you, Milton, Mirian and Mathias for welcoming me in your home despite the difficult situation. Nicole was the one supporting me everyday, my partner in life. You were the one saying "Coragem" while I was struggling through the writing and the one that kept me sane during the process. You are a fundamental part of my life and the one that makes me happy with all the love and laughter someone could want.

Contents

1 Introduction

Entanglement is a fundamental feature of quantum mechanics and one of its most striking features. It is a direct byproduct of the basic postulates of quantum mechanics as they were laid down in the 1920s [1–4]. This was already recognized in 1935 by Einstein et al. with their discovery of the Einstein–Podolski–Rosen (EPR) paradox [5]. It demonstrated the puzzling consequences of the principle of quantum superposition when applied to composite systems. Subsequent works further examined this issue and formalized it systematically [6, 7]. It was in this context that Schrödinger introduced the term entanglement to describe certain quantum correlations.

The EPR paradox was part of a broader debate concerning the completeness and validity of quantum mechanics. Specifically, it fueled the side of the debate that argued that quantum mechanics was incomplete. This skepticism was originally caused by the ontic character of probabilities in the quantum mechanical description, as established by the Born rule [8]. But the EPR paradox—and the existence of entanglement—provided additional arguments. Hidden-variables models were introduced as attempts to bypass these perceived issues, while still explaining quantum mechanical phenomenology [9, 10]. However, they were plagued with additional problems and explicitly violated locality.

It took more than three decades after the EPR discovery to resolve the issues it raised. In a seminal work, Bell formalized the philosophical assumptions underpinning the paradox and devise a quantitative way to test them [11]. It demonstrated that local realism imposes strong restrictions on the admissible correlations that can be observed in physical systems [12]. Bell's inequality—and its generalizations [13]—provided an experimentally accessible test for these restrictions.

Remarkable experiments in the 1970s and 1980s showed violations of Bell inequalities [14–16]. These experiments proved that reality cannot be described by a model consistent with local realism. This excluded the possibility of local hidden-variable models, and showed that the counter-intuitive features of quantum mechanics are inevitable. Moreover, follow-up experiments closed various loopholes to ensure that Bell inequalities are indeed violated [17–20]. As such, by now, it is an experimentally verified fact that entanglement is a fundamental part of reality.

The modern perspective on entanglement is completely opposite to the negative connotation it had in the early years of quantum mechanics [21]. It is now widely understood that entanglement plays a crucial role in the description of various systems. And its characterization is one of the central questions of physics [22, 23]. This is particularly the case for quantum many-body physics, for entanglement can explain certain salient phenomena, and shed new light into pressing open problems [24–26]. Moreover, entanglement is an important catalyst for current research efforts. In particular, it is key to the ongoing cross-fertilization between atomic physics, solid state, and quantum information.

A prominent example of the relevance of entanglement in quantum many-body physics is the development of tensor network methods. They originate in the density matrix renormalization group (DMRG) method developed in the early 1990s [27]. This method was instrumental and remains the primary computational tool for studying one-dimensional quantum systems. However, its theoretical understanding was limited until the development of matrix product states (MPS) [28]. This is a class of ansatzes that generalize the Affleck–Kennedy–Lieb–Tasaki (AKLT) state [29]. The advent of MPSs produced new insights about the DMRG method and enabled the development of more general tensor network ansatzes [30]. Examples of this are projected entangled pair states (PEPS) [31], and the multiscale entanglement renormalization ansatz (MERA) [32]. What all tensor network methods have in common is their reliance on knowledge of the entanglement structure of many-body states [33].

Entanglement also provides a signature of quantum phase transitions, which are the quantum counterpart of the familiar concept from statistical mechanics [34]. Quantum phase transitions are driven by quantum fluctuations and exist at zero temperature. At sufficiently small, but finite, temperatures, it is possible to find signatures of the quantum phase transition in the quantum critical regime [35]. This is the region that lies above the quantum critical point (QCP), where the transition takes place. In this region, entanglement displays scaling behaviour [36], and certain measures of entanglement diverge [37–39].

Topological order is another important instance where entanglement determines the properties of a quantum many-body system. It describes the states of topological phases of matter, which are phases that cannot be described by the spontaneous symmetry breaking formalism [40]. Paradigmatic examples include the Toric code [41], and string-net models [42]. Topologically ordered states are characterized by a pattern of long-range entanglement. And they manifest a plethora of unconventional phenomena. The two most emblematic ones are the existence of a topological ground state degeneracy and the presence of anyonic excitations. Both of which are extreme examples of emergent phenomena in many-body physics, and require novel techniques to be studied.

Entanglement also has the potential to fuel various technological applications. As it is the resource necessary to power quantum technologies [43, 44]. The most emblematic example is quantum computation. It is an idea that originates in the 1980s [45, 46], but it is yet to be fully realized. The goal is to leverage the properties of quantum mechanical systems to gain a speedup over classical computers. Shor's algorithm for prime number factorization is possibly the most famous instance of this [47]. Additional examples include the Deutsch–Jozsa algorithm [48], quantum search [49], and more [50]. However, despite rapid progress and increasing capabilities [51], we still lack a scalable platform for quantum computing.

Another potential quantum technology is quantum simulation. It employs highly controllable quantum mechanical systems to simulate quantum many-body systems [52], and probe physics that is otherwise inaccessible. These machines must satisfy various properties to ensure some degree of reliability [53]. Platforms suitable for this task include trapped ions [54] and ultracold atoms [55]. They enable the simulation of paradigmatic models such as the Hubbard model with the help of optical lattices [56–61]. On the experimental side, quantum simulation is only possible due to remarkable advances in experimental atomic, molecular, and optical physics (AMO). The realization of Bose–Einstein condensates (BEC) in the late 1990s being a key moment in this trajectory [62, 63].

Quantum metrology is perhaps the most mature quantum technology in present day [64]. It arises as an extension of the problem of parameter estimation to a quantum mechanical setting [65]. The concept is to use quantum correlations to enhance the metrological sensitivity of a detection apparatus. Thereby increasing the precision of parameter estimation in, e.g., a atomic interferometer. This procedure requires specially engineered states to work, such as squeezed states of light [66, 67] or squeezed spin states [68–70]. It has been successfully demonstrated in various experimental works [71–74], and has important applications [75–77].

The metrological enhancement obtained with squeezed states is due to the presence of entanglement [78, 79]. This has been implemented in multiple experiments with great success [80–86]. And it raises the possibility of using metrology as a tool to detect entangled states [87–89]. It is possible to further characterize the quantum correlations of atomic systems that provide a metrological enhancement. This leads to the concept of multipartite entanglement, which acts as a resource for quantum metrology [90–92]. More rigorously, one can demonstrate that the quantum Fisher information (QFI) [93], a quantifier of metrological enhancement, is bounded by a function of the amount of entanglement in the system. Therefore, the QFI provides a witness for multipartite entanglement in systems described by spin degrees of freedom.

Given the potential technological applications, there is a growing demand for techniques to certify the presence of entanglement [23]. Its importance to quantum many-body physics provides further motivation for this quest. However, many techniques for entanglement detection scale poorly with system size. This is a significant problem and it restricts their application. The scaling problem stems from the exponential growth of the Hilbert space, and reliance on quantum state tomography techniques. State tomography, while a useful tool, has severe limitations and becomes prohibitive for large systems [94, 95]. Thus, it is critical to find scalable techniques that permit the certification of entanglement in quantum many-body systems. In this work, we present our results that contribute to this endeavor. In particular, we demonstrate that it is possible to extract the QFI of quantum many-body system using an experimentally friendly protocol based on engineered dynamics. This enables one certify the presence of multipartite entanglement in quantum many-body systems.

Another crucial question for the characterization of entanglement in quantum many-body systems is how to formally define entanglement. Specifically, how to generalize the usual definition of entanglement for qubits—and distinguishable particles—to systems made up of identical particles. This has been investigated since the early 2000s [96–98], with some debates concerning the physical interpretation of bosonic and fermionic entanglement [99], and known applications to quantum technologies. Particularly to quantum metrology. However, existing works about entanglement of indistinguishable particles have focused on the bipartite case. Our results extends this to the multipartite case using a systematic, and unified formalism, that is system agnostic. This builds up on previous works that demonstrated the relevance of operator algebras to the definition of entanglement [100]. Recently, this technique has also been used to investigate entanglement entropy in lattice gauge theory [101–104]. Motivated by this, we apply our formalism to this setting as well, and use it to construct entanglement witnesses for lattice gauge theories.

Chapter 2 is a summary of the background material for the rest of this dissertation with a review of the theory of entanglement. And a summary of theory of quantum estimation. In chapter 3 we present our protocol for extracting the QFI of states in thermal equilibrium. We derive it, discuss some of its advantages and limitations, and present a extension beyond the scope of thermal states. The two following chapters focus on multipartite entanglement of indistinguishable particles. In chapter 4 we discuss multipartite mode entanglement and derive QFI bounds for separable fermionic states. Chapter 5 contains our numerical results for a model of interacting fermions. The topic of chapter 6 are lattice gauge theories, and how to construct entanglement witnesses for them. Finally, in chapter 7, we summarize the dissertation and discuss some future perspectives.

This dissertation is based on two published works and another in preparation:

- R. Costa de Almeida and P. Hauke, "From entanglement certification with quench dynamics to multipartite entanglement of interacting fermions", Phys. Rev. Research **3**, L032051 (2021) [105].

  In this publication, we present our protocol for extracting the QFI of thermal states using quench dynamics. We also demonstrate that this procedure can be used to certify the presence of multipartite entanglement in a system of interacting fermions. Chapters 3 to 5 are expanded versions of the contents of this publication. I was responsible for the theoretical derivations, and the numerical computations.

- R. Costa de Almeida and P. Hauke, "Probing the quantum Fisher information of passive states", (in preparation) [106]

  This upcoming work is an extension of the previous one. It aims to broaden the scope of our multipartite entanglement certification protocol, so that it applies to non thermal equilibrium states. In particular, we demonstrate that the formula for extracting the QFI holds for a larger class of equilibrium states. And showcase the efficacy of this procedure with numerical results based on random sampling of quantum many-body states. My contributions include the theoretical derivations, and the implementation of the sampling algorithm.

- V. Panizza, R. Costa de Almeida, and P. Hauke, "Entanglement witnessing for lattice gauge theories", J. High Energy Phys. **2022**, 196 (2022) [107]

  Our results for lattice gauge theories are presented in this work. In particular, we demonstrate the possibility of using entanglement witnesses to detect entanglement in lattice gauge theories, and construct an explicit example for a U(1) theory. The techniques introduced in this work are particularly suited for implementation in quantum simulators. My primary responsibility was to develop the theoretical framework for the characterization of entanglement witnesses in the presence of superselection rules, but I also contributed to the development of the optimization procedure. Parts of the results are also published in V. Panizza's master thesis [108].

Additionally, chapter 4 contains a broader discussion of entanglement in systems of indistinguishable particles, and results which have not been published yet. It formalizes and significantly extends our previous results concerning multipartite mode entanglement [105]. Finally, during the course of my Ph.D., I also helped to supervise two masters students, but the contents of the work carried out with them is not presented here and can be found in their thesis [109, 110].

2 Theoretical background

In this chapter, we lay the theoretical foundations and basic toolkit for the dissertation. The central topic is entanglement, in its various incarnations, and some techniques for detecting it. We adopt a bottom up approach, and progressively build up a general formalism for multipartite entanglement. The other focal point is quantum metrology and how entangled states can enhance sensing. Specially because this provides us with a tool to certify the presence of multipartite entanglement. For the sake of conciseness, our presentation focuses on the theoretical aspects that allow us to derive the entanglement bounds.

The first section concerns the bipartite case, the simplest scenario. Afterwards, we move to the multipartite setting and discuss some of the basic results for it. In both cases, we consider systems defined by qubits, or qudits, which is the most familiar case. It is important to emphasize this, for chapters 4 and 6 discuss more complex situations that do not admit such a description. The third section is a summary of some theoretical aspects of quantum metrology, and its relation to multipartite entanglement. This relation provides us with entanglement bounds that will be used, and extended, in the subsequent chapters. Finally, we conclude with a discussion of some mathematical aspects of entanglement from an algebraic point of view. The presentation in the final section is somewhat abstract, but it will be made concrete through out this dissertation with examples.

The classic review by Horodecki et al. [21] is our primary reference for general facts about entanglement. Additionally, the book by Nielsen et al. [43] covers some of the more basic concepts discussed here. We also recommend Wilde's book [111] for technical aspects of quantum information theory. Regarding quantum metrology, we refer to the in-depth review by Pezzé et al. [64], and the one by Tóth et al. [79]. The fourth section builds upon ideas from the theory of operator algebras following the work of Balachandran et al. [100]. It employs some concepts and terminology from algebraic quantum field theory (AQFT) and the theory of C^*-algebras, but it is completely self-contained. Nonetheless, for the interested reader, we suggest the book by Haag [112] which sets the foundations of AQFT, and the one by Murphy [113] for background on operator algebras.

2.1 Entanglement in bipartite systems

Bipartite systems are the prototypical setting to study entanglement. This is the case both for technical and historical reasons. After all, as mentioned in chapter 1, research into quantum entanglement originates from the debate surrounding the EPR paradox [5–7] and the eventual discovery of Bell inequalities [11, 13]. Both of which concern bipartite systems. Moreover, numerous technological applications of quantum information science rely on bipartite entanglement as a resource [43]. This is the case for dense coding [114], some quantum key distribution protocols [115, 116], and quantum teleportation [117–120]. On a more practical note, the theory of bipartite entanglement is necessary to make sense of the multipartite scenario.

2.1.1 Nonlocal quantum correlations

Let us consider a system defined by two qubits, labeled A and B. Each qubit is taken to be a independent subsystem, such that A and B are physically separated. For instance, one can assume that the two qubits are causally disconnected, in the relativistic sense. However, we do not discard the possibility that A and B interacted in the past, so that they can be in an arbitrary state. A general pure state of this system is given by

$$\begin{aligned} |\psi\rangle = \; & \psi(0,0)|\,0_A\rangle \otimes |\,0_B\rangle + \psi(0,1)|\,0_A\rangle \otimes |\,1_B\rangle \\ & + \psi(1,0)|\,1_A\rangle \otimes |\,0_B\rangle + \psi(1,1)|\,1_A\rangle \otimes |\,1_B\rangle\,, \end{aligned} \tag{2.1}$$

which is a superposition of the 4 classical states of a pair of bits. One can imagine that there are agents, typically called Alice and Bob, that have local access to the qubits. Each agent can manipulate their own qubit, but does not have access to the other one.

We can use tensor products to reconstruct all observables by combining Pauli matrices acting locally. Examples of this are

$$\begin{aligned} \hat{\mathrm{O}}_A &= \hat{\sigma}^x_A \otimes \hat{\mathrm{I}}_B \qquad \hat{\mathrm{O}}'_A = \hat{\sigma}^z_A \otimes \hat{\mathrm{I}}_B \\ \hat{\mathrm{O}}_B &= \hat{\mathrm{I}}_A \otimes \hat{\tau}^x_B \qquad \hat{\mathrm{O}}'_B = \hat{\mathrm{I}}_A \otimes \hat{\tau}^z_B\,, \end{aligned} \tag{2.2}$$

where $\hat{\tau}^x$ and $\hat{\tau}^z$ are Pauli matrices rotated by $\exp(i\pi\hat{\sigma}^y/4)$. More generally, it is possible to describe all quantum maps acting on such a bipartite system. But Alice and Bob are only allowed to perform local operations and classical communication (LOCC).

Consider the observable $\hat{\mathrm{T}} = \hat{\mathrm{O}}_A\hat{\mathrm{O}}_B + \hat{\mathrm{O}}'_A\hat{\mathrm{O}}_B + \hat{\mathrm{O}}_A\hat{\mathrm{O}}'_B - \hat{\mathrm{O}}'_A\hat{\mathrm{O}}'_B$, and its expectation value with respect to the state described by equation (2.1). If the wave

function factorizes according to $\psi(i,j) = \psi_A(i)\psi_B(j)$, it is straightforward to check that $\langle \hat{\mathrm{T}} \rangle \leq 2$. This bounds the correlations of pure states that Alice and Bob can produce locally. However, for an arbitrary pure state, the upper bound is higher,

$$\langle \hat{\mathrm{T}} \rangle \leq 2\sqrt{2}\,, \tag{2.3}$$

and it is known as Tsirelson's bound [121]. It holds for arbitrary operators with norm one, as long as the observables acting on A commute with those acting on B. Bell states saturate inequality (2.3), so the bound is tight and cannot be improved. It follows that their wave function does not factorizes. As we already mentioned, this implies that Alice and Bob cannot locally produce pure states that will can the correlations of the Bell states. Moreover, since $\langle \hat{\mathrm{T}} \rangle$ is linear as a function of the states, adding statistical mixtures will not change this. Hence, the two qubits become indissociable if they are in a Bell state, and we say that they are in a entangled state.

It is instructive to consider a classical counterpart of the situation we just described. In a classical system, a state amounts to an assignment of objective values to the observables features of the system. The observables amount to binary variables in the classical scenario, since they have eigenvalues ± 1. Hence, a classical state assigns variables $o_A, o'_A, o_B, o'_B \in \{-1, +1\}$ to the system. Rearranging the terms of $\hat{\mathrm{T}}$, we have

$$\begin{aligned} &\langle o_A o_B \rangle + \langle o'_A o_B \rangle + \langle o_A o'_B \rangle - \langle o'_A o'_B \rangle \\ &\qquad = \langle (o_A + o'_A) o_B \rangle + \langle (o_A - o'_A) o'_B \rangle \leq 2\,. \end{aligned} \tag{2.4}$$

The bound above comes from the fact that either $o_A = o'_A$ or $o_A = -o'_A$, so the two terms cannot contribute simultaneously. This is essentially the content of Bell's theorem [11]. It states that inequality (2.4) holds for any description of reality consistent with local realism. Thus, the existence of quantum states that violate it, implies that quantum mechanics is inconsistent with local realism.

Experimental tests showing violations of Bell inequalities demonstrate that local realism does not describe reality [14–17]. And they exclude the possibility of local hidden-variables models [12]. This is a very strong result. In particular, it means that any theory consistent with experiments must also have the counter-intuitive features of quantum mechanics. It also shows that entanglement is a fundamental feature of nature, since only entangled states can violate Bell inequalities. However, it is important to notice that not all entangled states are Bell nonlocal [122]. This means that there are entangled states that admit a description with a local hidden-variables model.

2.1.2 Reduced states and entanglement

Let us consider a more general setting for a bipartite system and formally define bipartite entanglement. Specifically, we fix a Hilbert space $\mathcal{H}_{AB}$ that admits a decomposition into

$$\mathcal{H}_{AB} = \mathcal{H}_A \otimes \mathcal{H}_B \,, \tag{2.5}$$

a tensor product of local Hilbert spaces $\mathcal{H}_A$ and $\mathcal{H}_B$. For concreteness, assume that each subsystem is a qudit,

$$\mathcal{H}_A = \bigoplus_{\mu} \mathbb{C}|\,\mu_A\rangle = \mathbb{C}|\,0_A\rangle \oplus \cdots \oplus \mathbb{C}|\,d_A - 1\rangle \cong \mathbb{C}^{d_A} \tag{2.6}$$

$$\mathcal{H}_B = \bigoplus_{\nu} \mathbb{C}|\,\nu_B\rangle = \mathbb{C}|\,0_B\rangle \oplus \cdots \oplus \mathbb{C}|\,d_B - 1\rangle \cong \mathbb{C}^{d_B} \,, \tag{2.7}$$

with dimensions d_A and d_B, respectively. It is possible to use qudits to model various physical systems, and they can be experimentally realized in multiple ways. But no further specification is necessary for our purposes.

Pure states can be decomposed according to equation (2.5) into

$$|\,\psi\rangle = \sum_{\mu,\nu} \psi(\mu_A, \nu_B)|\,\mu_A\rangle \otimes |\,\nu_B\rangle \,, \tag{2.8}$$

where $\psi(\mu_A, \nu_B)$ is a wave function corresponding to some local bases. Furthermore, it is possible to regard $\psi(\mu_A, \nu_B)$ as a matrix and simplify equation (2.8) with a singular value decomposition (SVD). This procedure yields bases $\{|\,\kappa_A\rangle\}$ and $\{|\,\kappa_B\rangle\}$, with a common index κ, such that

$$|\,\psi\rangle = \sum_{\kappa} \sqrt{\mathrm{p}(\kappa)}|\,\kappa_A\rangle \otimes |\,\kappa_B\rangle \,, \tag{2.9}$$

for a $\mathrm{p}(\kappa)$ that defines a probability distribution. Equation (2.9) is known as a Schmidt decomposition and it is an indispensable tool for analysing bipartite systems. It is also used extensively to implement tensor networks numerical methods [30].

Product states are the simplest instance of a Schmidt decomposition. They correspond to a delta probability distribution $\mathrm{p}(\kappa) = \delta(\kappa)$ and we can write

$$|\,\psi\rangle = |\,\psi_A\rangle \otimes |\,\psi_B\rangle \,, \tag{2.10}$$

so that the wave function factorizes $\psi(\mu_A, \nu_B) = \psi_A(\mu_A)\psi_B(\nu_B)$. We showed that they cannot violate a Bell inequality, so they do not have nonlocal correlations.

In fact, this follows directly from their most important property, namely that the correlations of all local observables vanish. Specifically,

$$\langle\psi\,|\,\hat{O}_A\otimes\hat{O}_B\,|\,\psi\rangle = \langle\psi_A\,|\,\hat{O}_A\,|\,\psi_A\rangle\langle\psi_B\,|\,\hat{O}_B\,|\,\psi_B\rangle\,, \tag{2.11}$$

for every observable $\hat{O}_A$ and $\hat{O}_B$ with local support in A and B. As a consequence, local states encode all expectation values and correlations. And there is no loss of information when we restrict a product state to one of the subsystems. This implies that product states are not entangled.

For an arbitrary state, the restriction to subsystems is more complicated and there is loss of information. Using equation (2.9) we see that

$$\begin{aligned}\langle\psi\,|\,\hat{O}_A\otimes\hat{1}_B\,|\,\psi\rangle &= \sum_{\kappa,\kappa'} p(\kappa)^{\frac{1}{2}}\,p(\kappa')^{\frac{1}{2}}\langle\kappa'_A\,|\,\hat{O}_A\,|\,\kappa_A\rangle\langle\kappa'_B\,|\,\kappa_B\rangle \\ &= \sum_{\kappa} p(\kappa)\langle\kappa_A\,|\,\hat{O}_A\,|\,\kappa_A\rangle = \mathrm{Tr}\Big(\sum_{\kappa} p(\kappa)|\,\kappa_A\rangle\langle\kappa_A\,|\hat{O}_A\Big)\,,\end{aligned} \tag{2.12}$$

so the restriction of $|\,\psi\rangle$ to A is a mixed state,

$$\hat{\rho}_A = \sum_{\kappa} p(\kappa)|\,\kappa_A\rangle\langle\kappa_A\,|\,, \tag{2.13}$$

and some information is lost. It is this loss that indicates that the two subsystems become indissociable and that the state is entangled. The entropy of $\hat{\rho}_A$,

$$S_A(|\,\psi\rangle\langle\psi\,|) = S(\hat{\rho}_A) = -\sum_{\kappa} p(\kappa)\ln p(\kappa)\,, \tag{2.14}$$

quantifies this and it is known as the entanglement entropy. Of course, the same reasoning applies to B and one can check that $S_A(|\,\psi\rangle\langle\psi\,|) = S_B(|\,\psi\rangle\langle\psi\,|)$.

Equation (2.13) is indicative of the presence of correlations between A and B, i.e., violations of equation (2.11). Indeed, for a general state, correlations between A and B are given by

$$\begin{aligned}&\langle\psi\,|\,\hat{O}_A\otimes\hat{O}_B\,|\,\psi\rangle - \langle\psi\,|\,\hat{O}_A\otimes\hat{1}_B\,|\,\psi\rangle\langle\psi\,|\,\hat{1}_A\otimes\hat{O}_B\,|\,\psi\rangle \\ &\qquad = \sum_{\mu,\nu}\sum_{\mu',\nu'}\langle\mu_A\,|\,\hat{O}_A\,|\,\mu'_A\rangle\langle\nu_B\,|\,\hat{O}_B\,|\,\nu'_B\rangle\cdot \\ &\qquad \sum_{\mu''\nu''}\begin{pmatrix}\psi^\dagger(\mu_A,\nu_B)\psi(\mu'_A,\nu'_B)\psi^\dagger(\mu''_A,\nu''_B)\psi(\mu''_A,\nu''_B) \\ - \\ \psi^\dagger(\mu_A,\nu''_B)\psi(\mu'_A,\nu''_B)\psi^\dagger(\mu''_A,\nu_B)\psi(\mu''_A,\nu'_B)\end{pmatrix},\end{aligned} \tag{2.15}$$

so there can be nonzero contributions depending on the wave function. Fixing local bases that diagonalize $\hat{O}_A$ and $\hat{O}_B$, the expression becomes

$$= \sum_{\mu',\nu'}\langle\mu'_A\,|\,\hat{O}_A\,|\,\mu'_A\rangle\langle\nu'_B\,|\,\hat{O}_B\,|\,\nu'_B\rangle\sum_{\mu'',\nu''}\begin{pmatrix}p(\mu'_A,\nu'_B)\,p(\mu''_A,\nu''_B) \\ - \\ p(\mu'_A,\nu''_B)\,p(\mu''_A,\nu'_B)\end{pmatrix}, \tag{2.16}$$

where $p(\mu_A, \nu_B) = |\psi(\mu_A, \nu_B)|^2$ is the probability of measuring a specific basis state. If, and only if, the state is a product state, equation (2.16) vanishes for all local bases. As a consequence, equation (2.11) can only hold for all local observables for product states. This shows that the two subsystems A and B will be entangled whenever the state of the composite system is not a product state, since there will be correlations between local observables. Therefore, we say that a pure state is entangled if it is not a product state.

2.1.3 Bipartite entanglement detection

To extend the definition of entanglement to mixed states, we need an appropriate generalization of equation (2.10). As it turns out, there is an easy solution. It is to define separable states as those that can be written as a mixture of product states,

$$\hat{\rho} = \sum_{\lambda} p_\lambda |\, \lambda_A\rangle\langle\lambda_A \,| \otimes |\, \lambda_B\rangle\langle\lambda_B \,| \,. \tag{2.17}$$

If a state is not separable then it is impossible to model it with a statistical ensemble of product states, and we say it is entangled [21]. The set of separable states is manifestly convex, since it is given by the convex hull of the subset of product states. Hence, the set of entangled states is the difference of two convex sets, the set of all states $\mathcal{S}(AB)$ and the set of separable states Sep (see figure 2.1).

Notice that simple correlations cannot distinguish entangled mixed states from separable ones. This is because

$$\langle \hat{O}_A \otimes \hat{O}_B\rangle_{\hat{\rho}} - \langle \hat{O}_A\rangle_{\hat{\rho}}\langle \hat{O}_B\rangle_{\hat{\rho}} = \sum_{\lambda} p_\lambda \langle \hat{O}_A \hat{O}_B\rangle_{\hat{\rho}_\lambda} - \sum_{\lambda,\lambda'} p_\lambda p_{\lambda'} \langle \hat{O}_A\rangle_{\hat{\rho}_\lambda}\langle \hat{O}_B\rangle_{\hat{\rho}_{\lambda'}}, \tag{2.18}$$

can achieve non zero values even if all $\hat{\rho}_\lambda$ are product states. However, there are alternative methods that can be used to detect entangled states [22], such as those based on the Peres–Horodecki criterion [123, 124]. It is also possible to use entanglement witnesses to detect entanglement [125–127]. To define one, it is necessary to find an operator $\hat{W}$ whose $\mathrm{Tr}(\hat{\rho}\hat{W}) = 0$ hyperplane appropriately splits $\mathcal{S}(AB)$ (see figure 2.1). Specifically, $\hat{W}$ must be chosen such that $\mathrm{Tr}(\hat{\rho}\hat{W}) \geq 0$ for all separable states, so that a negative expectation value signals entanglement. The operator $\hat{W} = 2 - \hat{T}$ is an example of this.

Of course, Bell inequalities also diagnose entangled states, but only Bell non-local ones [122, 128]. We can leverage this to obtain a finer description of $\mathcal{S}(AB) \setminus \mathsf{Sep}$ through a series of strict inclusions $\mathsf{Sep} \subset \mathsf{Loc} \subset \mathcal{S}(AB)$, as in figure 2.1. The convex set Loc contains all states that admit a description by a local hidden-variables model and includes some entangled states.

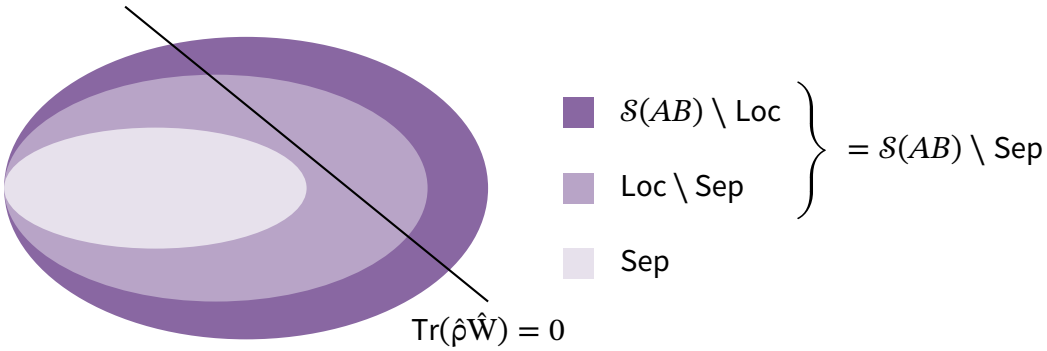

Figure 2.1: Pictorial depiction of $\mathcal{S}(AB)$ for a bipartite system. Separable states are shown in a lighter shade displaying the convexity of Sep. Bell nonlocal states, which are entangled, are represented with the darkest shade. The intermediate color depicts $\mathsf{Loc} \setminus \mathsf{Sep}$, i.e., states that are entangled but admit a description with a local hidden-variables model. We also represent the hyperplane defined by an entanglement witness $\hat{\mathrm{W}}$. States in the upper right corner region are witnessed by $\hat{\mathrm{W}}$, whereas those in the bottom left are not.

2.2 Multipartite entanglement

The multipartite case is a natural extension of the bipartite setting. Understanding it is a major line of research in the field of quantum information. Moreover, it is also central to the characterization of entanglement in quantum many-body systems [26]. And this is our primary motivation for studying it. However, the characterization of multipartite entanglement is much more intricate [129].

The added complexity of multipartite systems leads to a rich classification theory [130]. Such that even the three qubit case is already qualitatively different compared to the two qubit one. This is because it admits a different class of entangled states that is inequivalent to Bell states [131]. Adding more qubits further increases the possibilities, so that the classification difficulty also increases. This approach also requires extensive knowledge of the states, so it is hard to translate into directly observable features.

We present a different strategy here that does no rely on a full classification of multipartite entangled states. Instead, it characterizes multipartite entanglement with a hierarchy of different separability notions. It provides less information about the structure of entanglement, but it is manageable.

2.2.1 Partitions of many-body systems

Consider a quantum many-body system S composed of N qudits. And assume that the degrees of freedom of the system are homogeneous so that each qudit has the same dimension d. Thus, the Hilbert space $\mathcal{H}_S$ is given by

$$\mathcal{H}_S = \bigotimes_{i=1}^{N} \mathcal{H}_i = \mathcal{H}_1 \otimes \cdots \otimes \mathcal{H}_N \cong \mathbb{C}^{d^N} . \tag{2.19}$$

Similarly to equation (2.8), all pure states $|\psi\rangle \in \mathcal{H}_S$ admit a wave function description,

$$|\psi\rangle = \sum_{\mu_i} \psi(\mu_1, \dots, \mu_N) |\mu_1\rangle \otimes \cdots \otimes |\mu_N\rangle , \tag{2.20}$$

with respect to a local bases. However, there is an important difference relative to the bipartite case. The wave function is a tensor with multiple indices, instead of a matrix with only two indices. This is a byproduct of the exponential growth of $\dim \mathcal{H}_S = d^N$, but it also signals another difficulty. The definition of entanglement explicitly relies on a choice of subsystem, but there are multiple possibilities for S that are all equally valid. Therefore, we require a systematic formmalism to treat all possible partitions of S on equal footing.

A partition of the system amounts to a division of the qudits into separate groups, i.e., into subsystems. Formally, we may regard a subsystem R as a subset $R \subset \{1 \dots N\}$ labelling the qudits that are a part of it. So a partition P is just a set of subsets $P \subset 2^{\{1 \dots N\}}$. The sets of the partition must be pairwise disjoint, $R \cap Q = \varnothing$ if $R \neq Q \in P$, so that each subsystem is independent of each other. They must also cover $\{1 \dots N\}$, so that all qudits are included.

Given a fixed partition P, we consider a wave function ψ such that

$$\psi(\mu_1 \dots \mu_N) = \prod_{R \in P} \psi_R(\mu_{r_1}, \dots, \mu_{r_{|R|}}) , \tag{2.21}$$

for some choice of subsystem wave functions ψ_R (see figure 2.2). The indices $r_1, \dots, r_{|R|}$ are just labels for the qudits that belong to R and the specific ordering does not matter. As one might expect, expectation values factorize according to

$$\langle\psi| \Big(\prod_{R \in P} \hat{O}_R \Big) |\psi\rangle = \prod_{R \in P} \langle\psi_R| \hat{O}_R |\psi_R\rangle , \tag{2.22}$$

as long as each observable $\hat{O}_R$ has support in R [1]. The simplest case occurs when $R \in P$ is a singleton set. This can be understood as a mean-field wave function

[1] We say that $\hat{O}_R$ has support in R if it can be written as $\hat{O}_R = \sum_z O^z \hat{O}_1^z \otimes \cdots \otimes \hat{O}_N^z$ such that, for all $i \notin R$, $\hat{O}_i^z = \hat{1}_i$.

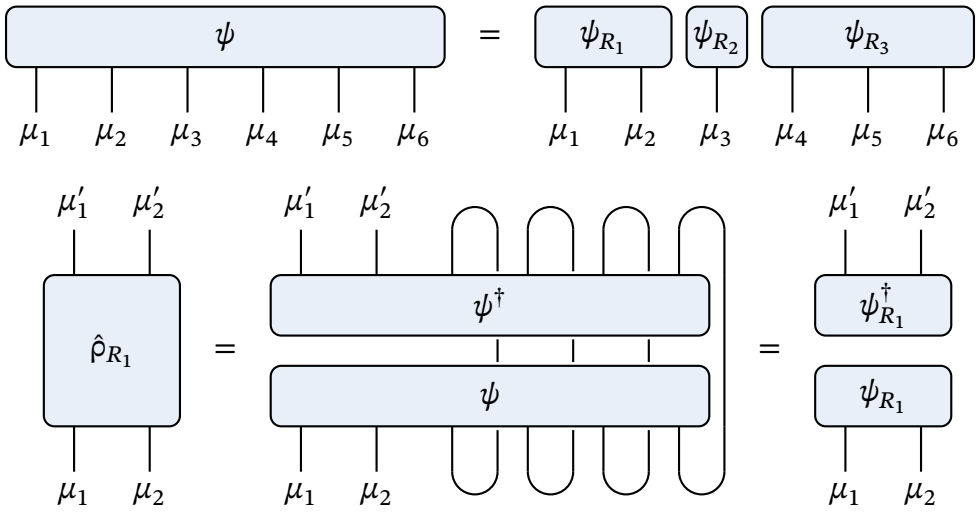

Figure 2.2: An example of a 3-producible state in a system with $N = 6$. The partition in this example is $P = \{R_1, R_2, R_3\}$ with $R_1 = \{1, 2\}$, $R_2 = \{3\}$ and $R_3 = \{4, 5, 6\}$. The bottom panel shows the reduced state associated to R_1 and how it is obtained. The diagrammatic notation makes it explicit that it is pure.

ansatz,

$$\psi(\mu_1 \dots \mu_N) = \prod_i \psi_i(\mu_i) = \psi_1(\mu_1) \dots \psi_N(\mu_N) \,, \tag{2.23}$$

since correlations between different qudits vanish. States that obey equation (2.21) are called P-product states, or P-producible, by analogy with the bipartite case. Equation (2.22) guarantees that they do not have correlations between different subsystems. Hence, one can apply the same strategy as before and define Sep_P as the convex hull of all P-producible states.

We can use the tricks from the last section to study P-entanglement, i.e., deviations from the P-producible behaviour. In particular, given any state $|\psi\rangle$, the reduce state associated to some subsystem $R \in P$ always exists. It is given by

$$\begin{aligned} \hat{\rho}_R &= \mathsf{Tr}_{S\setminus R}(|\psi\rangle\langle\psi|) \\ &= \sum_{\mu_i, \mu'_i} \psi(\mu_1, \dots, \mu_N) \Big(\prod_{z \notin R} \delta(\mu_z = \mu'_z) \Big) \psi^\dagger(\mu'_1, \dots, \mu'_N) \bigotimes_{r \in R} |\mu_r\rangle\langle\mu'_r| \,, \end{aligned} \tag{2.24}$$

where the partial trace runs over all $z \notin R$. It is implemented by contractions between μ_z and μ'_z enforced with $\delta(\mu_z = \mu'_z)$. This operation maps P-producible states into pure states, so $S_R(|\psi\rangle\langle\psi|) = S(\hat{\rho}_R)$ measures deviations from this

behaviour (see figure 2.2). However, the entropy $S_R(\cdot)$ simply measures entanglement between R and $S \setminus R$. So one is measuring bipartite entanglement, and not a truly multipartite feature. Nonetheless, in specific situations it is possible to combine the entanglement entropy of multiple subsystems to obtain information that goes beyond the bipartite framework. The topological entanglement entropy is a prominent example of this [132, 133]. It provides a tool that can detect topologically ordered states.

2.2.2 k-Entanglement hierarchy

In order to obtain the multipartite entanglement hierarchy, it is necessary to consider more flexible separability criteria. Instead of assuming a specific decomposition, as in equation (2.21), we only restrict the complexity of the ψ_R tensors. So that different partitions are allowed to coexist in statistical mixtures. This enables us to derive a measure of the degree to which a certain entangled states is multipartite entangled, or not.

Concretely, a partition P is a k-partition if each $R \in P$ contains at most k elements. This implies that the dimension of

$$\mathcal{H}_R = \bigotimes_{r \in R} \mathcal{H}_r \tag{2.25}$$

is bounded by d^k for all $R \in P$. The complexity of the ψ_R tensors is limited by this constraint, and this changes the overall scaling of the problem. For instance, the number of parameters that specify a state scales like d^N in general. But for states described by a k-partition, the number scales like $f(N/k)d^k$, for some polynomial function $f(\cdot)$.

A k-producible state is a state that is P-producible for some k-partition P. The physical picture is that a k-producible state can be described by an anstaz that only uses k-body wave functions. To define k-separability, we use the same strategy as the bipartite case. The set of k-separable states Sep_k is defined as the convex hull of the set of all k-producible states. And a k-separable state $\hat{\rho}$ is given by

$$\hat{\rho} = \sum_\lambda p_\lambda |\psi_\lambda\rangle\langle\psi_\lambda| = \sum_\lambda p_\lambda \bigotimes_{R \in P_\lambda} |\psi_R\rangle\langle\psi_R| , \tag{2.26}$$

a mixture of k-producible states $|\psi_\lambda\rangle$. Each $|\psi_\lambda\rangle$ is P_λ-producible with respect to some k-partition P_λ, but these partitions do not have to be same. Therefore, properties that hold for k-separable states cannot reference properties of a specific k-partition. In this sense, the k-separability criteria does not privilege any particular partition.

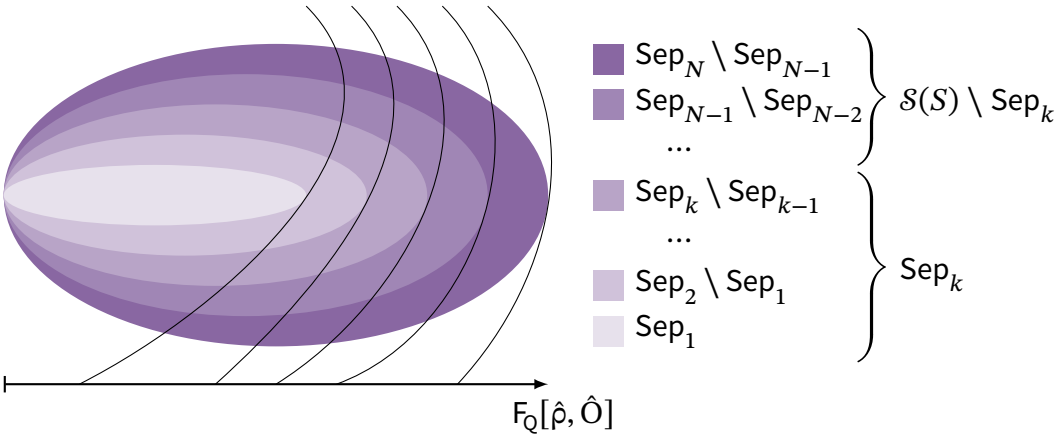

Figure 2.3: Pictorial depiction of $\mathcal{S}(S)$ for a multipartite system. Each set $\mathsf{Sep}_k \setminus \mathsf{Sep}_{k-1}$ contains all states with entanglement depth k. Genuine multipartite entangled states belong to the outermost layer $\mathsf{Sep}_N \setminus \mathsf{Sep}_{N-1}$. We also represent represent the contour levels of $\mathsf{F}_Q[\hat{\rho}, \hat{O}]$ defined by inequality (2.48). The leftmost curve corresponds to the SQL that realizes shot-noise $\mathsf{F}_Q[\hat{\rho}, \hat{O}] \propto N$, and the rightmost to the HL when $\mathsf{F}_Q[\hat{\rho}, \hat{O}] \propto N^2$.

Each set Sep_k contains Sep_{k-1} by construction, since it is defined by a weaker constraint. Thus, the k-separability criteria define a hierarchy of convex sets as

$$\mathsf{Sep}_1 \subset \mathsf{Sep}_2 \subset \cdots \subset \mathsf{Sep}_{N-1} \subset \mathsf{Sep}_N = \mathcal{S}(S)\,, \tag{2.27}$$

and we can use it to define multiple notions of entanglement. In particular, a state is k-entangled if it is not $(k-1)$-separable, and it has entanglement depth k if it is k-separable and k-entangled simultaneously (see figure 2.3). Hence, states of entanglement depth k can be described by k-body wave functions, but nothing less, whereas k-entangled states might require higher order wave functions. If a state is 1-separable then it is called completely separable. By contrast, if a state is N-entangled then it is a genuine multipartite entangled (GME) state.

It is not possible to naively extend entanglement measures from bipartite partition to the k-partite case. This is because the k-partitions in equation (2.26) can be different for each state in the mixture. It is harder to detect k-entanglement because of this. But it also guarantees that the entanglement observed is actually multipartite in nature. Nonetheless, some measures of multipartite entanglement exist [129, 134, 135], but rely on additional assumptions.

2.3 Entanglement-enhanced metrology

As discussed in the introduction, multipartite entanglement is a resource for quantum metrology. And we can use this to obtain a tool for certifying multipartite entanglement. However, in order to make this statement rigorous, we must derive the basic result of quantum estimation theory. This will give us the definition of the quantum Fisher information (QFI) and allow us to derive multipartite entanglement bounds for it.

2.3.1 Classical Estimation theory

Let us quickly review some concepts from classical estimation theory. The starting point is a conditional probability distribution $\mathsf{p}(\mu \,|\, \theta)$ that encodes the experimental apparatus. An estimator $\bar{\theta}$ is simply a random variable on the possible outcomes μ and its prediction for the parameter is given by

$$\mathbb{E}\big(\bar{\theta} \,|\, \theta\big) = \sum_{\mu} \mathsf{p}(\mu \,|\, \theta)\bar{\theta}(\mu) \,. \tag{2.28}$$

It is unbiased if $\mathbb{E}\big(\bar{\theta} \,|\, \theta\big) = \theta$, that is, if it predicts the correct value of the parameter. The variance $\Delta^2\big(\bar{\theta} \,|\, \theta\big) = \mathbb{E}\big(\bar{\theta}^2 \,|\, \theta\big) - \mathbb{E}\big(\bar{\theta} \,|\, \theta\big)^2$ quantifies the precision of the estimator, and provides a figure of merit for its quality.

Our goal is to determine the quality of the measurement scheme itself, not of a specific estimator. Therefore, we need a quantity that only depends on the probability distribution. The Fisher information (FI) is precisely this [136, 137]. It is defined as

$$\mathsf{F}(\theta) = \Delta^2\Big(\partial_\theta \ln \mathsf{p}(\mu \,|\, \theta) \,\Big|\, \theta\Big) = \sum_{\mu} \mathsf{p}(\mu \,|\, \theta)\Big(\partial_\theta \ln \mathsf{p}(\mu \,|\, \theta)\Big)^2 \,. \tag{2.29}$$

and measures the sensitivity of $\mathsf{p}(\mu \,|\, \theta)$ to changes of the parameter. The random variable $s(\mu \,|\, \theta) = -\partial_\theta \ln \mathsf{p}(\mu \,|\, \theta)$ is the score of the distribution, and measures the change in likelihood function with respect to θ. A direct calculation show that $\mathbb{E}(s(\mu \,|\, \theta) \,|\, \theta) = 0$. Thus, $\mathsf{F}(\theta) = \Delta^2(s(\mu \,|\, \theta) \,|\, \theta)$ is the simplest non trivial measure of the properties of the score.

The Cramér–Rao inequality is a universal bound on the precision of any estimator in terms of the FI [138, 139]. For any unbiased estimator $\bar{\theta}$, we have

$$\Delta^2\big(\bar{\theta} \,|\, \theta\big) \geq \mathsf{F}(\theta)^{-1} \,, \tag{2.30}$$

which bounds the precision an estimator.

An important property of the FI is that it is convex in the probability distribution. This means that the FI of a distribution $\mathsf{p}(\mu\,|\,\theta) = \sum_\lambda \mathsf{p}(\lambda) c_\lambda(\mu\,|\,\theta)$ is bounded from above,

$$\mathsf{F}(\theta) \leq \sum_\lambda c_\lambda \, \mathsf{F}_\lambda(\theta) \tag{2.31}$$

by the convex sum of the FI of each $\mathsf{p}_\lambda(\mu\,|\,\theta)$. Convexity is extremely useful as it allow us to bound the FI without having to calculate it directly. It is also conceptually meaningful and consistent with inequality (2.30). This is because convexity ensures one cannot improve the precision of parameter estimation by simply adding statistical uncertainty.

2.3.2 Quantum Fisher information

Now we develop the quantum analogue of estimation theory. The basic object is a parameter dependent state $\hat{\rho}(\theta)$, which is quantum version of the conditional probability distribution. Given a quantum channel Φ_θ parameterized by θ, we can write $\hat{\rho}(\theta) = \Phi_\theta(\hat{\rho})$. And for a unitary channel, we have

$$\hat{\rho}(\theta) = \hat{\mathrm{U}}_\theta \hat{\rho} \hat{\mathrm{U}}_\theta^\dagger = \exp(-i\theta\hat{\mathrm{O}})\hat{\rho}\exp(+i\theta\hat{\mathrm{O}}) \,, \tag{2.32}$$

where $\hat{\mathrm{O}}$ is the observable that generates the unitary rotations by $\hat{\mathrm{U}}_\theta$. The problem of extracting the value of θ from $\hat{\rho}(\theta)$ is known as quantum parameter estimation. It is the basic setup for quantum metrology. In particular, a central question is to determine the metrological enhancement provided by $\hat{\rho}$.

Positive operator-valued measures (POVM) generalize the more common notion of projective measurements. We can use them to build probability distributions, and apply the machinery of estimation theory. This provides us with a formalism to describe experimental setups in a systematic way. Formally, a POVM is a set of positive semi-definite operators $\{\hat{\Pi}_\mu\}$ that satisfies

$$\sum_\mu \hat{\Pi}_\mu = \hat{1} \,. \tag{2.33}$$

The labels μ denote the possible experimental outcomes, and

$$\mathsf{p}(\mu\,|\,\theta) = \mathsf{Tr}\big(\hat{\rho}(\theta)\hat{\Pi}_\mu\big) \tag{2.34}$$

is the probability of observing a certain event. Equation (2.33) guarantees that the probabilities are properly normalized.

Using equations (2.29) and (2.34), we can calculate the metrological sensitivity associated to each POVM. However, it is necessary to remove the explicit dependence on POVM's. This will produce a metrological bound intrinsic to the state.

Optimizing over all possible POVM's,

$$F_Q\big[\hat{\rho}_\theta\big] = \max_{\{\hat{\Pi}_\mu\}} F(\theta) \tag{2.35}$$

realizes this and defines the quantum Fisher information (QFI). This definition has a clear operational meaning. It describes the metrological sensitivity of a completely optimized experimental setup. In particular, we have the quantum Cramér–Rao bound,

$$\Delta^2\big(\bar{\theta}\,|\,\theta\big) \geq F(\theta)^{-1} \geq F_Q\big[\hat{\rho}_\theta\big]^{-1} , \tag{2.36}$$

which is, by construction, a generic bound on the precision of parameter estimation. The FI in inequality (2.36) is associated to the probability distribution of some arbitrary POVM.

Equation (2.35) enables one to derive many of the properties of the QFI. In particular, inequality (2.31) implies that

$$\max_{\{\hat{\Pi}_\mu\}} F(\theta) \leq \sum_\lambda p_\lambda \max_{\{\hat{\Pi}_\mu\}} F_\lambda(\theta) , \tag{2.37}$$

for any state $\hat{\rho} = \sum_\lambda p_\lambda \hat{\rho}_\lambda$. Therefore, the QFI is also convex. This is consistent with the intuition from the classical scenario, but it only accounts for classical correlations. We will see that it is possible to use quantum correlations to improve the metrological sensitivity, i.e., increase the QFI.

The original definition of the QFI is different from the one we just presented [93]. It defines the QFI as geometrical measure of statistical distinguishability in the space of states. In particular, one can show that the QFI is the metric associated to the Bures metric. And it is connected to the fidelity of two states $\hat{\rho}_{\theta_1}$ and $\hat{\rho}_{\theta_2}$. Of course, the definition we presented is equivalent to the geometrical one.

Despite its advantages, equation (2.35) has drawbacks. The most severe is that it does not give an explicit formula for the QFI. But it is possible to obtain one with the help of the geometric perspective. To derive it, we first define the symmetric logarithmic derivative (SLD) $\hat{L}(\theta)$ implicitly through

$$\partial_\theta \hat{\rho}(\theta) = \frac{1}{2}\big\{\hat{\rho}(\theta), \hat{L}(\theta)\big\} = \frac{1}{2}\big(\hat{\rho}(\theta)\hat{L}(\theta) + \hat{L}(\theta)\hat{\rho}(\theta)\big) . \tag{2.38}$$

Explicit calculation shows that $\partial_\theta\, p(\mu\,|\,\theta) = \mathrm{Re}\,\mathrm{Tr}\big(\hat{\rho}(\theta)\hat{\Pi}_\mu\hat{L}(\theta)\big)$ for any POVM.

Applying this to equation (2.29), it follows that

$$\begin{aligned} F(\theta) &= \sum_{\mu} \frac{\left(\mathrm{Re}\,\mathrm{Tr}\left(\hat{\rho}(\theta)\hat{\Pi}_{\mu}\hat{L}(\theta)\right)\right)^2}{\mathrm{Tr}\left(\hat{\rho}(\theta)\hat{\Pi}_{\mu}\right)} \leq \sum_{\mu} \frac{\left|\mathrm{Tr}\left(\sqrt{\hat{\rho}(\theta)}\sqrt{\hat{\Pi}_{\mu}}\sqrt{\hat{\Pi}_{\mu}}\hat{L}(\theta)\sqrt{\hat{\rho}(\theta)}\right)\right|^2}{\mathrm{Tr}\left(\hat{\rho}(\theta)\hat{\Pi}_{\mu}\right)} \\ &\leq \sum_{\mu} \frac{\mathrm{Tr}\left(\hat{\rho}(\theta)\hat{\Pi}_{\mu}\right)}{\mathrm{Tr}\left(\hat{\rho}(\theta)\hat{\Pi}_{\mu}\right)} \mathrm{Tr}\left(\hat{\rho}(\theta)\hat{L}(\theta)\hat{\Pi}_{\mu}\hat{L}(\theta)\right) = \mathrm{Tr}\left(\hat{\rho}(\theta)\hat{L}(\theta)^2\right), \end{aligned} \tag{2.39}$$

where we used the Schwartz inequality to get to the second line. It is easy to show that there is a POVM that realizes the bound above so

$$F_Q\left[\hat{\rho}(\theta)\right] = \mathrm{Tr}\left(\hat{\rho}(\theta)\hat{L}(\theta)^2\right), \tag{2.40}$$

and it is sufficient to obtain the SLD to calculate the QFI.

The SLD operates as a quantum analogue of the score. For the unitary case, we can use equations (2.32) and (2.40) to obtain

$$F_Q\left[\hat{\rho}(\theta=0)\right] = F_Q\left[\hat{\rho}, \hat{O}\right] = 2\sum_{\mu,\nu} \frac{\rho_\mu - \rho_\nu}{\rho_\mu + \rho_\nu}(\rho_\mu - \rho_\nu)|\langle\mu\,|\,\hat{O}\,|\,\nu\rangle|^2, \tag{2.41}$$

where we fix a bases that diagonalizes $\hat{\rho}$, and consider $\theta = 0$ for simplicity. If the state is pure then we have a particularly simple formula,

$$F_Q\left[|\,\psi\rangle\langle\psi\,|, \hat{O}\right] = 4\sum_{\mu\neq\psi} |\langle\mu\,|\,\hat{O}\,|\,\psi\rangle|^2 = 4\left(\langle\psi\,|\,\hat{O}^2\,|\,\psi\rangle - \langle\psi\,|\,\hat{O}\,|\,\psi\rangle^2\right), \tag{2.42}$$

that shows that the QFI is proportional to the quantum mechanical variance. More generally, we have

$$F_Q\left[\hat{\rho}, \hat{O}\right] \leq 4\sum_{\lambda} \rho_\lambda\left(\langle\psi_\lambda\,|\,\hat{O}^2\,|\,\psi_\lambda\rangle - \langle\psi_\lambda\,|\,\hat{O}\,|\,\psi_\lambda\rangle^2\right) \tag{2.43}$$

if the state $\hat{\rho}$ is a mixture of pure states $|\,\psi_\lambda\rangle$. In fact, one can recover the QFI of a state by taking the infimum of the right-hand side of inequality (2.43) over all possible decompositions into mixtures of pure states [140].

Equation (2.41) is more approachable compared to equation (2.35), but it is still hard to use. In particular, the need for a diagonal basis introduces a substantial obstacle. In a experimental setting it forces one to perform state tomography for a generic state. As such, the resources involved scale exponentially with system size. This makes the procedure unfeasible for general quantum many-body systems. However, some groundbreaking experiments have been able to circumvent this restriction and obtain positive results [83–86]. In chapter 3, we will discuss a technique that allow us to calculate the QFI of certain equilibrium states. It bypasses the need for access to a diagonal basis, and provide us with an experimentally friendly protocol.

2.3.3 Multipartite entanglement bounds

Besides technological applications, our main interest in the QFI is its ability to detect multipartite entanglement [79, 90–92]. In chapter 1, we already discussed the concept of squeezing and its relations to entanglement. Now we will formally derive bounds for the QFI that relate it to the k-separability criteria of section 2.2.

Consider the system defined by the multipartite Hilbert space of equation (2.19). Let us fix a local observable $\hat{O}$ that acts on a single qudit and define the generator

$$\hat{O}_S = \sum_{i=1}^{N} \hat{O}_i = \sum_{i=1}^{N} \hat{1}_1 \otimes \cdots \otimes \hat{1}_{i-1} \otimes \hat{O} \otimes \hat{1}_{i+1} \otimes \cdots \otimes \hat{1}_N \tag{2.44}$$

that acts on the entire multipartite system. If we consider a partition P together with a P-producible state $|\psi\rangle$, then equation (2.22) implies

$$\begin{aligned} F_Q\big[|\psi\rangle\langle\psi|, \hat{O}_S\big] &= 4\big(\langle\psi|\hat{O}_S^2|\psi\rangle - \langle\psi|\hat{O}_S|\psi\rangle^2\big) \\ &= 4\sum_{ij}\big(\langle\psi|\hat{O}_i\hat{O}_j|\psi\rangle - \langle\psi|\hat{O}_i|\psi\rangle\langle\psi|\hat{O}_j|\psi\rangle\big) \\ &= 4\sum_{R\in P}\sum_{ij\in R}\big(\langle\psi_R|\hat{O}_i\hat{O}_j|\psi_R\rangle - \langle\psi_R|\hat{O}_i|\psi_R\rangle\langle\psi_R|\hat{O}_j|\psi_R\rangle\big) \\ &= \sum_{R\in P} F_Q\big[|\psi_R\rangle\langle\psi_R|, \hat{O}_R\big]\,, \end{aligned} \tag{2.45}$$

where we have used the factorization to go from the second line to the third one. The observable $\hat{O}_R$ introduced in the last line of equation (2.45) is just the sum of $\hat{O}_i$ over all $i \in R$. Of course, there is a slight abuse of notation since we use the same symbol do denote the observable acting on S and its restriction to R. This does not cause problems, since each $\hat{O}_i$ is a tensor product of local observables.

Assume the absolute value of the eigenvalues of $\hat{O}$ is bounded by some constant $C/2 \in \mathbb{R}^+$. This constrains the eigenvalues of $\hat{O}_R$ to $-C|R|/2 \leq O_\mu \leq C|R|/2$. The maximum variance is reached by a uniform superposition of the eigenstates with maximum and minimum eigenstates. Hence,

$$\langle\psi_R|\hat{O}_i\hat{O}_j|\psi_R\rangle - \langle\psi_R|\hat{O}_i|\psi_R\rangle\langle\psi_R|\hat{O}_j|\psi_R\rangle \leq \frac{\big(C|R|/2 - (-C|R|/2)\big)^2}{4}\,, \tag{2.46}$$

and combining this with equation (2.45) yields

$$F_Q\big[|\psi\rangle\langle\psi|, \hat{O}_S\big] \leq \sum_{R\in P} C|R|^2\,, \tag{2.47}$$

which bounds the QFI of every P-producible state.

It is necessary to remove the partition dependence from inequality (2.47). We can do this by optimizing over all k-partite partitions. The result is a bound that holds for all k-producible states. It is given by

$$\mathsf{F}_{\mathrm{Q}}\big[|\psi\rangle\langle\psi|, \hat{\mathrm{O}}_S\big] \leq \max_{P} \sum_{R\in P} C|R|^2 = C(dk^2 + r^2)\,, \tag{2.48}$$

where $N = dk + r$ [90–92]. Inequality (2.48) also holds for k-separable states due to the convexity of the QFI. Therefore, this inequality detects states which are not k-separable and whose multipartite entanglement leads to a metrological enhancement (see figure 2.3).

The two extreme cases occur for $k = 1$ and $k = N$. In the first one, the QFI can only scale linearly $\mathsf{F}_{\mathrm{Q}} \leq CN \propto N$ and this is the usual classical behaviour. This scaling can be replicated with a probability distribution by taking N independent copies of it. Hence, there is no quantum advantage, and this scenario corresponds to the standard quantum limit (SQL). This should be the case, since $k = 1$ implies the system has no entanglement. The Heisenberg limit (HL) is the other side of the coin. It occurs for $k = N$ and corresponds to a quadratic scaling of the QFI [141]. This is the maximum metrological enhancement a quantum mechanical system can achieve.

In applications with atomic interferometers, one typically consider a linear generator such as in equation (2.44). The most common case is the spin 1/2 with

$$\hat{\mathrm{O}}_S = \frac{1}{2}\sum_i \vec{n}_i \cdot \hat{\sigma}_i\,, \tag{2.49}$$

so that $C = 1$ in inequality (2.48). Each local spin operator $\vec{n}_i \cdot \hat{\sigma}_i$ acts in some arbitrary direction $\vec{n}_i = \big(n_i^x, n_i^y, n_i^z\big)$. Greenberger–Horne–Zeilinger (GHZ) states violate inequality (2.48) so they are multipartite entangled. In particular,

$$|\,\mathrm{GHZ}\rangle = \frac{1}{2^{1/2}}\big(|\downarrow\rangle \otimes \cdots \otimes |\downarrow\rangle + |\uparrow\rangle \otimes \cdots \otimes |\uparrow\rangle\big) \tag{2.50}$$

is a quantum state of entanglement depth N, i.e., it is a GME state. However, notice that not all multipartite states violate inequality (2.48) for some observable. The primary example of an entangled state that cannot be detected by the QFI is the W state,

$$|\,W\rangle = \frac{1}{N^{1/2}}(|\downarrow\rangle \otimes |\uparrow\rangle \cdots \otimes |\downarrow\rangle + \cdots + |\downarrow\rangle \otimes \ldots |\uparrow\rangle \otimes |\downarrow\rangle)\,, \tag{2.51}$$

which arises as one of the equivalency classes of entangled states in the three qubit case [131]. Hence, the QFI can certify that a state is multipartite entangled, but a negative outcome does not exclude this possibility.

2.4 Algebraic perspective

In general, whenever a tensor product decomposition exists, one can utilize the techniques of sections 2.1 and 2.2 to define entangled states. However, there are physical systems that do not admit a tensor product structure. This was already considered in various works in the early 2000s [142–145]. And it was shown that the factorization conditions of equations (2.11) and (2.22) provide a solution. In particular, they provide a separability criteria that generalizes to general systems regardless of the Hilbert space structure. This was elegantly formulated in the work by Bañuls et al. [98] for the case of fermions, and formalized by Balachandran et al. [100] using an algebraic formalism.

In this section, we present the algebraic characterization of separability and entanglement in a self-contained manner. It will be used in chapter 4 to derive multipartite mode entanglement bounds for indistinguishable particles. And in chapter 6 to construct entanglement witnesses for lattice gauge theories. The terminology we introduce here will provide an unified perspective for both cases.

Let us consider a quantum mechanical system S. We can use the factorization condition to define entanglement. Specifically, given a partition P of S, we say that a state factorizes with respect to the partition whenever

$$\langle \prod_{R\in P} \hat{O}_R \rangle_{\hat{\rho}_S} = \prod_{R\in P} \langle \hat{O}_R \rangle_{\hat{\rho}_R} \,, \tag{2.52}$$

for all local observables $\hat{O}_R$. This is just the definition of P-producible states from section 2.2, so we can use the same procedure to define multipartite entanglement. But it is necessary to have some ingredients in order to make sense of equation (2.52). In particular, we need a consistent notion of subsystems and some procedure to translate between the system and its subsystems.

From an algebraic point of view, the system S is defined by an algebra, which we denote by $\mathcal{A}(S)$, that specifies its observables. The simplest and most familiar example occurs when one considers the algebra $\mathcal{A}(S) = \mathcal{B}(S)$ formed by bounded linear operators acting on some Hilbert space $\mathcal{H}_S$. However, in general, one has to consider C^*-algebras [113], which generalize the properties of operator algebras to a more abstract setting. The Gelfand–Naimark theorem [146] provides a bridge between this formalism, and the Hilbert space approach. In particular, it allows one to construct a Hilbert space $\mathcal{H}_S$ from the algebra $\mathcal{A}(S)$ such that $\mathcal{A}(S) \subset \mathcal{B}(S)$. Thus, it is always possible to realize an abstract C^*-algebra as a set of operators that satisfy some property. Nonetheless, it is advantageous to keep the abstract point of view in mind, since it puts the observable features of the system in center stage. An allows us to easily define the ingredients required for equation (2.52).

Every C^*-algebra carries an involution $\dagger : \mathcal{A}(S) \to \mathcal{A}(S)$ structure and we can use it to define self-adjoint and positive elements. In particular, the self-adjoint elements of the algebra,

$$\{\hat{O} \in \mathcal{A}(S) \mid \hat{O} = \hat{O}^\dagger\} \subset \mathcal{A}(S) \,, \tag{2.53}$$

coincides with the observables of the system. Positive elements are those of the form $\hat{Q}^\dagger\hat{Q}$ for some $\hat{Q} \in \mathcal{A}(S)$ and they allow us to define states. Formally, a state of the system is a linear functional $\hat{\rho} \in \mathcal{A}(S)^*$ that assigns probability amplitudes $\langle\hat{O}\rangle_{\hat{\rho}} \in \mathbb{C}$ to elements of the algebra. A state must assign positive values to positive elements, that is,

$$\langle\hat{Q}^\dagger\hat{Q}\rangle_{\hat{\rho}} \geq 0 \tag{2.54}$$

for all operators $\hat{Q} \in \mathcal{A}(S)$. It also needs to be unital, i.e., preserve the unit of the algebra. In concrete terms, this means that the state is normalized according to

$$\langle\hat{1}_S\rangle_{\hat{\rho}} = 1 \,, \tag{2.55}$$

where $\hat{1}_S \in \mathcal{A}(S)$ is the unit of the algebra. Inequality (2.54) and equation (2.55) are physical assumptions that ensure that the assignment of probability amplitudes is consistent with the Born rule.

The choice of notation is suggestive of the more familiar density matrix formalism, and we can replicate the usual constructions with it. For instance, given a set of projectors $\{\hat{\Pi}_\mu\}$ that add up to unit, we have

$$\mathsf{p}(\mu) = \langle\hat{\Pi}_\mu\rangle_{\hat{\rho}} = \langle\hat{\Pi}_\mu^\dagger\hat{\Pi}_\mu\rangle_{\hat{\rho}} \geq 0 \tag{2.56}$$

and

$$\sum_\mu \mathsf{p}(\mu) = \sum_\mu \langle\hat{\Pi}_\mu\rangle_{\hat{\rho}} = \langle\hat{1}_S\rangle_{\hat{\rho}} = 1 \,, \tag{2.57}$$

so $\mathsf{p}(\mu)$ can be interpreted as the probability of the event μ occurring. Moreover, the set of states $\mathcal{S}(S)$ is convex. This is easy to check for the familiar case of a finite dimensional Hilbert space $\mathcal{H}_S$, but it also holds for arbitrary C^*-algebras. The extremal points of the set correspond to pure states, the states that define irreducible representations of $\mathcal{A}(S)$ under the Gelfand–Naimark–Segal (GNS) construction [146, 147].

We can recover the usual formalism when $\mathcal{A}(S) = \mathcal{B}(S)$. In particular, in the usual setting, the definition of states as linear functionals is equivalent to the one with density matrices. This follows from Gleason's theorem [148], which demonstrates that any function that assigns probabilities to projectors—in a way compatible with equations (2.56) and (2.57)—can be written as

$$\hat{\Pi} \mapsto \mathsf{Tr}(\hat{\rho}\hat{\Pi}) \in [0, 1] \,, \tag{2.58}$$

where $\hat{\rho}$ is some positive semi-definite operator with trace one.

2.4.1 Nets of observables

To define entanglement, we need a systematic way of tracking the subsystems of S. We do it by employing the concept of a local net of observables. This is a mathematical structure that was originally introduced in the context of the Haag–Kastler axioms [149]. It formalizes the physical intuition that a quantum field theory (QFT) assigns observables to subregions of space-time in a way consistent with relativity. For our purposes, it is not necessary to go into the details of the axioms, but they provide us with our basic motivations.

Given a subsystem $R \subset S$, we can also assign a C^*-algebra $\mathcal{A}(R)$ that describes its observables. After all, it is also a quantum mechanical subsystem. The observables of the subsystem R are also observables of the system$S$, so there must be an embedding of $\mathcal{A}(R)$ into $\mathcal{A}(S)$. Thus, we have a map

$$\iota_R^S : \mathcal{A}(R) \hookrightarrow \mathcal{A}(S) \,, \tag{2.59}$$

that converts observables of R into observables of S. This map has to preserve the structure of $\mathcal{A}(R)$, i.e., it is a $*$-monomorphism. In particular, $\mathcal{A}(R)$ and $\iota_R^S(\mathcal{A}(R))$ are isomorphic as C^*-algebras, and we can regard them as the same algebra and omit the embedding when there is no risk of ambiguity. Notice that embeddings should be consistent, i.e., if we have $Q \subset R \subset S$, then $\iota_Q^S = \iota_R^S \circ \iota_Q^R$.

If we consider the collection of all subsystems, and their associated algebras, we have a net of observables. In the case of the bipartite systems of section 2.1 this is very simple. We have an algebra $\mathcal{A}(S) = \mathcal{B}(A) \otimes \mathcal{B}(B)$ for the entire system, and assign $\mathcal{A}(A) = \mathcal{B}(A)$ and $\mathcal{A}(B) = \mathcal{B}(B)$ to the two subsystems. The embeddings are given by

$$\begin{aligned} \hat{\mathrm{O}}_A \in \mathcal{A}(A) &\hookrightarrow \hat{\mathrm{O}}_A \otimes \hat{\mathrm{I}}_B \in \mathcal{A}(S) \\ \hat{\mathrm{O}}_B \in \mathcal{A}(B) &\hookrightarrow \hat{\mathrm{I}}_A \otimes \hat{\mathrm{O}}_B \in \mathcal{A}(S) \,, \end{aligned} \tag{2.60}$$

so A and B are indeed subsystems of S. Of course, this can be extended to the multipartite case with qudits in a straightforward way.

An important property of the net of observables is that the algebras of independent subsystems must commute. To formalize this, it is convenient to introduce the set

$$\mathcal{A}(R)' = \{\hat{\mathrm{O}} \in \mathcal{A}(S) \mid \forall \hat{\mathrm{O}}_R \in \mathcal{A}(R) \left[\hat{\mathrm{O}}, \hat{\mathrm{O}}_R\right] = 0\} \subset \mathcal{A}(S) \tag{2.61}$$

known as the commutant of $\mathcal{A}(R)$. The operators in $\mathcal{A}(R)'$ commute with all the operators acting on R, so they are compatible with $\mathcal{A}(R)$. Thus, we say that two subsystems $R_1, R_2 \subset R$ are independent if $\mathcal{A}(R_1) \subset \mathcal{A}(R_2)'$ and $\mathcal{A}(R_2) \subset \mathcal{A}(R_1)'$. As such, the commutant contains the algebra of the complementary subsystem, i.e., $\mathcal{A}(S \setminus R) \subset \mathcal{A}(R)'$.

Finally, we also need to replicate the notion a partition of the system. We already have a definition of subsystem—at least at the algebraic level—and a criteria to determine when two subsystems are independent. Therefore, the only missing ingredient is how to determine when some collection of subsystems cover the entire system. The commutant can also help us with this task. If we have a subsystem with an algebra $\mathcal{A}(R)$, then its bicommutant $\mathcal{A}(R)'' = (\mathcal{A}(R)')'$ is the algebra generated by the observables of R inside S. Hence, given a collection of subsystems P, we can associate an algebra to it according to

$$\mathcal{A}(P) = \Big(\bigcup_{R\in P} \mathcal{A}(R)\Big)'' \,, \tag{2.62}$$

which is the algebra generated by all subsystems. We say that P is a partition of S if all subsystems in it are pairwise independent, and $\mathcal{A}(S) = \mathcal{A}(P)$.

2.4.2 Separability criteria

Now we have all the components to use equation (2.52) to define entanglement using the local net of observables. Given a partition P and state $\hat{\rho} \in \mathcal{S}(S)$, we say that the state is a P-product state if

$$\Big\langle \prod_{R\in P} \iota_S^R(\hat{O}_R)\Big\rangle_{\hat{\rho}} = \prod_{R\in P} \big\langle \iota_S^R(\hat{O}_R)\big\rangle_{\hat{\rho}} = \prod_{R\in P} \big\langle \hat{O}_R\big\rangle_{\hat{\rho}_R} \,, \tag{2.63}$$

for all local observables $\hat{O}_R \in \mathcal{A}(R)$. The reduced states $\hat{\rho}_R \in \mathcal{S}(R)$ in the equation above are defined according to

$$\hat{\rho} \in \mathcal{S}(S) \mapsto \hat{\rho}_R = \hat{\rho} \circ \iota_S^R \in \mathcal{S}(R) \,, \tag{2.64}$$

the restriction of the state $\hat{\rho}$ to the subsystems. Contrast this to equation (2.13) and equation (2.24), which define the same quantity for qudit systems, but in a concrete manner.

The set of P-separable states Sep_P is defined just like before, i.e., it is the convex hull of the set of states that obey equation (2.63). And we can use the GNS construction to bound the complexity of the partition and recover the definition of k-separability. Specifically, let d_R be the dimension of the Hilbert space associated to $\mathcal{A}(R)$ by the GNS representation, then we say that P is a k-partition if $\log d_R \leq k$ for all subsystems $R \in P$. The base of the log is not important as it just provides us with a normalization to account for local degrees of freedom. A k-entangled state, with respect to the chosen local net of observables, is a state that cannot be written as a mixture of states that factorize with respect to a k-partition.

3 Entanglement certification protocol

In this chapter, we present our protocol for certifying multipartite entanglement with the help of the QFI. It leverages linear response theory to extract data that would normally require full knowledge of the quantum state. This is particularly valuable for applications to many-body systems. After all, although lower bounds of the QFI have been obtained in some groundbreaking experiments [83–86], general and scalable procedures to directly extract the QFI remain in great demand. Thus, the protocol we describe in this chapter allows us to use the QFI as a tool for certifying the presence of multipartite entanglement in regimes where this was previously inaccessible.

The technique we present here builds upon previous work by Hauke et al. [39]. However, in contrast to it, our protocol only requires measuring the short-time dynamics of mean expectation values after a quench. As such, it does not require access to higher moments and does not rely on frequency-dependent dynamic susceptibilities, as previous proposals. Moreover, to realize such a simplified protocol only requires a weak, abrupt quench, as can be conveniently implemented, e.g., in cold-atom experiments [53, 150, 151]. Notice that various other theoretical works have also used the relation between the QFI and linear response theory [152–154]. And very recently there have been some experimental results [155, 156].

This chapter is an extended account of the results published in reference [105]. We begin with a review of the essential concepts requires from linear response theory. In particular, we derive all the standard results for arbitrary equilibrium states, except for those that are specific to thermal states. Afterwards, we proceed to derive our main result, namely, the formula that powers the quench protocol. We derive the results in full generality first, describing the deconvolution procedure in detail, and then discuss some properties of the quench protocol. We emphasize the experimental advantages of the protocol and its limited requirements. Finally, section 3.3 contains unpublished results that extend the protocol beyond thermal states.

3.1 Linear response theory

Linear response theory is a powerful tool for studying quantum many-body systems. It relates the time evolution of a perturbed system to correlation functions and can be used to obtain various quantities of interest. In this section we are going to briefly summarize the main concepts and techniques of linear response theory. Emphasis will be given to what is necessary for presenting our results in sections 3.2 and 3.3. The book by Coleman [157] contains further details that complement our presentation.

3.1.1 Kubo linear response function

Suppose we have a Hamiltonian $\hat{\mathrm{H}}$ that describes a quantum mechanical system in equilibrium. The initial state of the system corresponds to a density matrix $\hat{\rho}$ that commutes with the Hamiltonian, to ensure that the system is actually in equilibrium. If one applies a time-dependent pertubation, the Hamiltonian of the system becomes time-dependent and we can write it as

$$\hat{\mathrm{H}}(\tau) = \hat{\mathrm{H}} - f(\tau)\hat{\mathrm{O}}' \,, \tag{3.1}$$

where $f(\tau)$ is an external drive that couples to the system through an observable $\hat{\mathrm{O}}'$. The von Neumann equation of the pertubed system is given by

$$\partial_\tau \hat{\rho}_{\mathrm{S}}(\tau) = i[\hat{\rho}_{\mathrm{S}}(\tau), \hat{\mathrm{H}}(\tau)] \tag{3.2}$$

and it governs the dynamics of $\hat{\rho}_{\mathrm{S}}(\tau)$, the Schrödinger picture state. Therefore, it allows us to calculate the expectation value of observables as they fluctuate in time.

To find a formal solution to equation (3.2), it is convenient to move to the Dirac picture, defined by

$$\hat{\rho}_{\mathrm{D}}(\tau) = \exp\big(+i\hat{\mathrm{H}}\tau\big)\hat{\rho}_{\mathrm{S}}(\tau)\exp\big(-i\hat{\mathrm{H}}\tau\big) \tag{3.3}$$

$$\hat{\mathrm{O}}'_{\mathrm{D}}(\tau) = \exp\big(+i\hat{\mathrm{H}}\tau\big)\hat{\mathrm{O}}'\exp\big(-i\hat{\mathrm{H}}\tau\big) \,. \tag{3.4}$$

We have that

$$\begin{aligned} \partial_\tau \hat{\rho}_{\mathrm{D}}(\tau) &= \exp\big(+i\hat{\mathrm{H}}\tau\big)\Big(-i[\hat{\rho}_{\mathrm{S}}(\tau), \hat{\mathrm{H}}] + i[\hat{\rho}_{\mathrm{S}}(\tau), \hat{\mathrm{H}}(\tau)]\Big)\exp\big(-i\hat{\mathrm{H}}\tau\big) \\ &= -if(\tau)[\hat{\rho}_{\mathrm{D}}(\tau), \hat{\mathrm{O}}'_{\mathrm{D}}(\tau)] \,, \end{aligned} \tag{3.5}$$

so the generator of the time evolution in the Dirac picture is the perturbation operator. This yields a self-consistent integral equation

$$\hat{\rho}_{\mathrm{D}}(\tau) = \hat{\rho}_{\mathrm{D}}(-\infty) - i\int_{-\infty}^{\tau} \mathrm{d}\tau' f(\tau')[\hat{\rho}_{\mathrm{D}}(\tau'), \hat{\mathrm{O}}'_{\mathrm{D}}(\tau')] \tag{3.6}$$

which we can expand into the Dyson series to get an exact solution.

Initially the system was in equilibrium so $\hat{\rho}_D(-\infty) = \hat{\rho}$. Plugging this into equation (3.6) results in

$$\hat{\rho}_D(\tau) = \hat{\rho} - i\int_{-\infty}^{\tau} d\tau' f(\tau')[\hat{\rho}, \hat{O}'_D(\tau')] + \dots \tag{3.7}$$

and we get the solution up to linear order in $f(\tau)$ if we truncate the series. The time evolution of an observable $\hat{O}$ can now be easily calculated according to

$$\begin{aligned}\langle \hat{O}(\tau)\rangle &= \mathrm{Tr}\big(\hat{\rho}_S(\tau)\hat{O}\big) = \mathrm{Tr}\big(\hat{\rho}_D(\tau)\hat{O}_D(\tau)\big)\\ &= \mathrm{Tr}\big(\hat{\rho}\hat{O}\big) - i\int_{-\infty}^{\tau} d\tau' f(\tau')\,\mathrm{Tr}\big([\hat{\rho}, \hat{O}'_D(\tau')]\hat{O}_D(\tau)\big)\\ &= \mathrm{Tr}\big(\hat{\rho}\hat{O}\big) + i\int_{-\infty}^{\tau} d\tau' f(\tau')\,\mathrm{Tr}\big(\hat{\rho}[\hat{O}_D(\tau), \hat{O}'_D(\tau')]\big)\\ &= \langle \hat{O}\rangle_0 + i\int_{-\infty}^{\tau} d\tau' f(\tau')\langle[\hat{O}_D(\tau), \hat{O}'_D(\tau')]\rangle_0 ,\end{aligned} \tag{3.8}$$

where $\langle\cdot\rangle_0$ denotes the trace with respect to the equilibrium state. Equation (3.8) is the famous Kubo formula for the linear response of a quantum system [158, 159]. It is most commonly formulated using the Kubo response function,

$$\chi_{\hat{O}\hat{O}'}(\tau - \tau') = i\theta(\tau - \tau')\langle[\hat{O}_D(\tau), \hat{O}'_D(\tau')]\rangle_0 , \tag{3.9}$$

as a convolution with the drive

$$\Delta O(\tau) = \langle \hat{O}(\tau)\rangle - \langle \hat{O}\rangle_0 = (f * \chi_{\hat{O}\hat{O}'})(\tau) = \int_{-\infty}^{+\infty} d\tau' f(\tau')\chi_{\hat{O}\hat{O}'}(\tau - \tau') . \tag{3.10}$$

The Heaviside function $\theta(\tau - \tau')$ is necessary to ensure causality, since it eliminates contributions coming from the future.

3.1.2 Expressions in frequency space

The diagonal basis of the equilibrium Hamiltonian gives an useful expression for the Kubo response function $\chi_{\hat{O}\hat{O}'}(\tau - \tau')$. Fixing $\hat{H} = \sum_\mu \varepsilon_\mu |\mu\rangle\langle\mu|$, it is

$$\chi_{\hat{O}\hat{O}'}(\tau - \tau') = i\theta(\tau - \tau')\sum_{\mu,\nu} e^{-i(\tau-\tau')\omega_{\mu\nu}}(\rho_\mu - \rho_\nu)\langle\mu|\hat{O}|\nu\rangle\langle\nu|\hat{O}'|\mu\rangle , \tag{3.11}$$

where $\omega_{\mu\nu} = \varepsilon_\nu - \varepsilon_\mu$ is the energy difference between two levels and we use the fact that the initial state is diagonal in the energy bases. Equation (3.11) allows

us to obtain the Fourier transform of the Kubo response function with the help of the convolution theorem. In particular, we can write

$$\chi_{\hat{O}\hat{O}'}(\omega) = i\sum_{\mu,\nu}(\delta_{\omega_{\mu\nu}} * \check{\theta})(\omega)(\rho_\mu - \rho_\nu)\langle\mu\,|\,\hat{O}\,|\,\nu\rangle\langle\nu\,|\,\hat{O}'\,|\,\mu\rangle\,, \tag{3.12}$$

using $\delta_{\omega_{\mu\nu}}(\omega) = \delta(\omega - \omega_{\mu\nu})$ and $\check{\theta}(\omega)$, the Fourier transforms of the plane wave and the Heaviside function.

The main subtlety of equation (3.12) is $\check{\theta}(\omega) = \pi\delta(\omega) + P[1/i\omega]$, since the Cauchy principal value $P[1/i\omega]$ needs to be handled with care. Regardless, the outcome of the convolution is

$$\begin{aligned}(\check{\theta} * \delta_{\omega_{\mu\nu}})(\omega) &= \int_{-\infty}^{+\infty} \mathrm{d}\omega'\,\delta(\omega' - \omega_{\mu\nu})\Big(\pi\delta(\omega - \omega') + P[1/i(\omega - \omega')]\Big) \\ &= \pi\delta(\omega - \omega_{\mu\nu}) - i\int_{-\infty}^{+\infty} \mathrm{d}\omega'\,\delta(\omega' - \omega_{\mu\nu})P[1/(\omega - \omega')]\end{aligned} \tag{3.13}$$

and we can use it to express the Kubo response function in frequency space. The imaginary contribution $\chi''_{\hat{O}\hat{O}'}(\omega) = \mathrm{Im}\,\chi_{\hat{O}\hat{O}'}(\omega)$ is given by

$$\chi''_{\hat{O}\hat{O}'}(\omega) = \pi\sum_{\mu,\nu}\delta(\omega - \omega_{\mu\nu})(\rho_\mu - \rho_\nu)\langle\mu\,|\,\hat{O}\,|\,\nu\rangle\langle\nu\,|\,\hat{O}'\,|\,\mu\rangle \tag{3.14}$$

and it is known as the dissipative part. We have to be a bit careful with the real part $\chi'_{\hat{O}\hat{O}'}(\omega) = \mathrm{Re}\,\chi_{\hat{O}\hat{O}'}(\omega)$ due to the Cauchy principal value in equation (3.13). For $\omega \neq 0$, the formula is

$$\chi'_{\hat{O}\hat{O}'}(\omega) = \sum_{\mu,\nu}\frac{1}{\omega - \omega_{\mu\nu}}(\rho_\mu - \rho_\nu)\langle\mu\,|\,\hat{O}\,|\,\nu\rangle\langle\nu\,|\,\hat{O}'\,|\,\mu\rangle\,, \tag{3.15}$$

where we only sum over the indices that satisfy $\omega_{\mu\nu} \neq 0$. However, this is not the correct expression for $\chi'_{\hat{O}\hat{O}'}(\omega = 0)$, which needs to be properly regularized. We will not discuss this regularization here, as our main interest is in the dissipative part. In any case, we mention that $\chi'_{\hat{O}\hat{O}'}(\omega)$ is known as the reactive part of the response and $\chi'_{\hat{O}\hat{O}'}(\omega = 0)$ is the elastic contribution contribution to it.

Contrasting equation (3.11) with equation (3.14) leads to

$$\chi_{\hat{O}\hat{O}'}(\tau) = \frac{i}{\pi}\theta(\tau)\int_{-\infty}^{+\infty}\mathrm{d}\omega\,\exp(-i\omega\tau)\chi''_{\hat{O}\hat{O}'}(\omega)\,, \tag{3.16}$$

so it seems that knowledge of the dissipative part is sufficient to determine the response. Indeed, performing another Fourier transform, we obtain

$$\chi_{\hat{O}\hat{O}'}(\omega) = \underbrace{\frac{1}{\pi}P\int_{-\infty}^{+\infty}\mathrm{d}\omega'\,\frac{\chi''_{\hat{O}\hat{O}'}(\omega')}{\omega' - \omega}}_{=\chi'_{\hat{O}\hat{O}'}(\omega)} + i\chi''_{\hat{O}\hat{O}'}(\omega)\,, \tag{3.17}$$

where we've used our standard trick with the convolution theorem and $\check{\theta}(\omega)$ to resolve the Fourier transform. Equation (3.17) is the Kramers–Kronig relation and it implies that the reactive part of the response is fully determined by the dissipative part. This procedure also shows that the Kubo response function admits an analytic extension to the upper half-plane in frequency space. As it turns out, this is a direct consequence of the causality condition satisfied by equation (3.9).

3.1.3 Kubo–Martin–Schwinger condition

So far we worked with an arbitrary state initial state $\hat{\rho}$ that commutes with the equilibrium Hamiltonian. Now we will discuss a property specific to thermal states. Therefore, we fix an inverse temperature $\beta = 1/T$ and set our initial state to the canonical ensemble. The density matrix is defined by the Gibbs state,

$$\hat{\rho} = \frac{1}{Z(\beta)} \exp(-\beta \hat{\mathrm{H}}) \,, \tag{3.18}$$

with a normalization given by the partition function $Z(\beta) = \mathsf{Tr}(\exp(-\beta\hat{\mathrm{H}}))$. The derivation of the Boltzmann weights formula usually relies on an entropy argument. Specifically, given a fixed a energy constraint $\mathsf{Tr}(\hat{\rho}\hat{\mathrm{H}}) = \varepsilon$, the thermal state is the one that maximizes entropy while satisfying the energy constraint. This optimization problem is easy to solve and the outcome is equation (3.18) with β appearing as a Lagrange multiplier. Different ensembles, such as the grand canonical, can be derived with a similar argument, but with additional constraints.

Linear response theory provides an alternative derivation of the Boltzmann ensemble. The argument is based on the boundary conditions of certain correlation functions in imaginary time. To understand it, let us first notice that

$$\begin{aligned}
\left\langle \hat{\mathrm{O}}'_D(0)\hat{\mathrm{O}}_D(\tau + i\beta)\right\rangle_0 &= \frac{1}{Z(\beta)} \mathsf{Tr}\big(e^{-\beta\hat{\mathrm{H}}}\hat{\mathrm{O}}' e^{+i\hat{\mathrm{H}}(\tau+i\beta)}\hat{\mathrm{O}} e^{-i\hat{\mathrm{H}}(\tau+i\beta)}\big) \\
&= \frac{1}{Z(\beta)} \mathsf{Tr}\big(e^{+i\hat{\mathrm{H}}(\tau+i\beta)}\hat{\mathrm{O}} e^{-i\hat{\mathrm{H}}(\tau+i\beta)} e^{-\beta\hat{\mathrm{H}}}\hat{\mathrm{O}}'\big) \\
&= \frac{1}{Z(\beta)} \mathsf{Tr}\big(e^{-\beta\hat{\mathrm{H}}} e^{+i\hat{\mathrm{H}}\tau}\hat{\mathrm{O}} e^{-i\hat{\mathrm{H}}\tau}\hat{\mathrm{O}}'\big) = \left\langle \hat{\mathrm{O}}_D(\tau)\hat{\mathrm{O}}'_D(0)\right\rangle_0 \,,
\end{aligned} \tag{3.19}$$

where we have used analytic continuation into the strip $I^+_\beta = \{\tau + i\gamma \in \mathbb{C} \mid 0 < \gamma < \beta\}$ for the first expectation value. Equation (3.19) is the Kubo–Martin-Schwinger (KMS) condition and it completely characterizes thermal states [158, 160, 161]. As we shall demonstrate.

For $\tau = 0$, the KMS condition reduces to

$$\left\langle \hat{O}' e^{-\beta \hat{H}} \hat{O} e^{+\beta \hat{H}} \right\rangle_0 = \mathrm{Tr}\left(\hat{O}' e^{-\beta \hat{H}} \hat{O} e^{+\beta \hat{H}} \hat{\rho}\right) = \mathrm{Tr}\left(\hat{O}' \hat{\rho} \hat{O}\right) = \left\langle \hat{O} \hat{O}' \right\rangle_0 \tag{3.20}$$

and this has to hold for all $\hat{O}$ and $\hat{O}'$. The trace is non degenerate so $\mathrm{Tr}(\hat{O}'\hat{X}) = \mathrm{Tr}(\hat{O}'\hat{Y})$ can only be true for all $\hat{O}'$ if $\hat{X} = \hat{Y}$. Hence, $e^{-\beta \hat{H}} \hat{O} e^{+\beta \hat{H}} \hat{\rho} = \hat{\rho} \hat{O}$ and, once again, this should be the case for all operators $\hat{O}$. Rearranging this expression, we see that it is equivalent to $[\hat{O}, e^{+\beta \hat{H}} \hat{\rho}] = 0$ so $e^{+\beta \hat{H}} \hat{\rho}$ must be in the center of the algebra. We conclude that $\hat{\rho} = e^{-\beta \hat{H}} \hat{N}$ for some observable $\hat{N}$ in the center. In the usual case, $\hat{N}$ has to be a number, so we recover equation (3.18) with $\hat{N} = 1/Z(\beta)$, after enforcing the normalization. Thus, the thermal state with inverse temperature β is the only one that fulfills the KMS condition, as we set out to prove.

Formally, equation (3.19) implies the existence of an analytic function $F_{\hat{O}\hat{O}'}(z)$, defined for $z \in I_\beta^+$, that fulfills the boundary conditions given by equation (3.19). The function is defined by

$$F_{\hat{O}\hat{O}'}(\tau) = \left\langle \hat{O}'_D(0) \hat{O}_D(\tau) \right\rangle_0 , \tag{3.21}$$

for real time τ, and by

$$F_{\hat{O}\hat{O}'}(\tau + i\beta) = \left\langle \hat{O}_D(\tau) \hat{O}'_D(0) \right\rangle_0 \tag{3.22}$$

in the upper line of the strip I_β^+. A similar procedure yields an analytic function $G_{\hat{O}\hat{O}'}(z)$ defined for $z \in I_\beta^- = \{\tau + i\gamma \in \mathbb{C} \mid \beta < \gamma < 0\}$, whic also fulfils specific boundary conditions. In particular, $G_{\hat{O}\hat{O}'}(\tau) = \left\langle \hat{O}_D(\tau) \hat{O}'_D(0) \right\rangle_0$ for real time. The KMS condition is equivalent to

$$F_{\hat{O}\hat{O}'}(\omega) = \exp(-\beta\omega) G_{\hat{O}\hat{O}'}(\omega) , \tag{3.23}$$

in frequency space, as long as there are analytic continuations to the interior of the strips. Our ability to perform the analytic continuation is related to equation (3.17), and a modified version of it for the lower half-plane.

The importance of the KMS condition is that it provides an alternative characterization of thermal equilibrium [161–165]. Crucially, it is a criteria that can be extended to a much broader setting, compared to a naive approach based on Gibbs states, while avoiding technical difficulties. For instance, it provides the correct infinite size limit and rigorous definitions of various phenomena, such as spontaneous symmetry breaking [166, 167]. Our main interest in the KMS condition is that it gives rise to the concept of passive states [168], which will be central to section 3.3.

3.1.4 Fluctuation–Dissipation relation

A direct consequence of the KMS condition is the fluctuation–dissipation relation (FDR). To derive it, let us begin with the following expression

$$\begin{aligned}\big(G_{\hat{O}\hat{O}'}(\omega) - F_{\hat{O}\hat{O}'}(\omega)\big) &= \big(1 - e^{-\beta\omega}\big)G_{\hat{O}\hat{O}'}(\omega) \\ &= \left(\frac{1 - e^{-\beta\omega}}{1 + e^{-\beta\omega}}\right)\big(G_{\hat{O}\hat{O}'}(\omega) + F_{\hat{O}\hat{O}'}(\omega)\big) \\ &= \tanh(\beta\omega/2)\big(G_{\hat{O}\hat{O}'}(\omega) + F_{\hat{O}\hat{O}'}(\omega)\big)\,,\end{aligned} \tag{3.24}$$

which follows directly from equation (3.23). It is the precursor of the FDR, but we need to work to get it in the familiar form, which has physical meaning.

The right hand side of equation (3.24) contains a symmetric combination, and it translates to the expectation value of an anti-commutator in real time. Specifically, it maps to the symmetric correlation function, which is given by

$$S_{\hat{O}\hat{O}'}(\tau) = \frac{1}{2}\langle\{\hat{O}_D(\tau), \hat{O}'_D(0)\}\rangle_0 = \frac{1}{2}\big(\langle\hat{O}_D(\tau)\hat{O}'_D(0)\rangle_0 + \langle\hat{O}'_D(0)\hat{O}_D(\tau)\rangle_0\big)\,, \tag{3.25}$$

and relates to the dynamical fluctuations in the system. We can move to frequency space easily and obtain

$$S_{\hat{O}\hat{O}'}(\omega) = \frac{1}{2}(G_{\hat{O}\hat{O}'}(\omega) + F_{\hat{O}\hat{O}'}(\omega))\,, \tag{3.26}$$

as expected. Hence, the right hand side of equation (3.24) corresponds to the fluctuation part of the FDR.

Notice that the formula for the Kubo response is very similar to equation (3.25), but it has a commutator instead of the anti-commutator. This already suggests that the left hand side of equation (3.24) is related to a response function. In fact, we can derive

$$\chi''_{\hat{O}\hat{O}'}(\omega) = \frac{1}{2}(G_{\hat{O}\hat{O}'}(\omega) - F_{\hat{O}\hat{O}'}(\omega))\,, \tag{3.27}$$

so the left hand side is related to the dissipative part of the response function. Finally, combining equation (3.26) and equation (3.27) leads to

$$\chi''_{\hat{O}\hat{O}'}(\omega) = \tanh(\beta\omega/2)S_{\hat{O}\hat{O}'}(\omega)\,, \tag{3.28}$$

the FDR. Equation (3.28) is extremely important and establishes yet another characterization of thermal equilibrium. It also connects a quantity that is easily measured, the Kubo response function, with another one that is hard to extract, the symmetric correlation function. Recently, there have been proposals to use it to test thermalization in quantum many-body systems, with the help a procedure to measure the anti-commutators [169].

3.2 Protocol for thermal states

In this section we are going to derive our main result. It is the formula that connects the QFI to linear response theory. This is the basis for the protocol for extracting the QFI from quench dynamics which will be put to use in chapter 5. We begin with the derivation of a generalized formula that holds for any well-behaved time-dependent drive. Afterwards, we specialize to the case of an abrupt quench, and discuss various properties of protocol. In particular, we demonstrate various advantageous features of the protocol.

3.2.1 Derivation of the main result

The starting point for our derivation is the formula for $\mathsf{F}_\mathsf{Q}[\hat{\rho}, \hat{\mathrm{O}}]$ in the diagonal bases of the state. As derived in section 2.3, the expression is

$$\mathsf{F}_\mathsf{Q}\big[\hat{\rho}, \hat{\mathrm{O}}\big] = 2\sum_{\mu,\nu} \underbrace{\frac{\rho_\mu - \rho_\nu}{\rho_\mu + \rho_\nu}}_{\text{(I)}} \underbrace{(\rho_\mu - \rho_\nu)|\langle \mu \,|\, \hat{\mathrm{O}} \,|\, \nu\rangle|^2}_{\text{(II)}} \,, \tag{3.29}$$

where the basis states are now eigenstates of the equilibrium Hamiltonian. We have marked two parts of the formula, (I) and (II), which will analyse separately. First, consider the expression (I), for a thermal state it becomes

$$\text{(I)} = \frac{\rho_\mu - \rho_\nu}{\rho_\mu + \rho_\nu} = \frac{e^{-\beta\varepsilon_\mu} - e^{-\beta\varepsilon_\nu}}{e^{-\beta\varepsilon_\mu} + e^{-\beta\varepsilon_\nu}} = \tanh\left(\frac{\beta\omega_{\mu\nu}}{2}\right), \tag{3.30}$$

so we get the same factor as in the FDR. It is essentially a frequency filter that suppresses low frequency contributions. Thus, it discards transitions with $\varepsilon_\mu \approx \varepsilon_\nu$, that is, between states of similar energy . To make sense of the second term, we just need to look at equation (3.14). It shows that (II) amounts to the contribution to $\chi''_{\hat{\mathrm{O}}\hat{\mathrm{O}}'}(\omega)$ from a specific transition.

The Dirac deltas $\delta(\omega - \omega_{\mu\nu})$ in the formula for the dissipative response enforce energy conservation. Therefore, if we integrate $\chi''_{\hat{\mathrm{O}}\hat{\mathrm{O}}'}(\omega)$ against a frequency filter, only valid transitions will contribute. Combining this consideration with equation (3.30) yields,

$$\begin{aligned} \mathsf{F}_\mathsf{Q}\big[\hat{\rho}, \hat{\mathrm{O}}\big] &= \frac{2}{\pi}\int_{-\infty}^{+\infty} \mathrm{d}\omega \tanh\left(\frac{\beta\omega}{2}\right)\chi''_{\hat{\mathrm{O}}\hat{\mathrm{O}}'}(\omega) \\ &= \frac{4}{\pi}\int_{0}^{+\infty} \mathrm{d}\omega \tanh\left(\frac{\beta\omega}{2}\right)\chi''_{\hat{\mathrm{O}}\hat{\mathrm{O}}'}(\omega) \,, \end{aligned} \tag{3.31}$$

where we have used the fact that the integrand is a even function in the second equality. Equation (3.31) was originally derived in [39]. It is also possible to derive a time domain formula by transforming the integral to frequency space, but we will do this shortly with a different approach. Conceptually, these expressions represent a significant advance as they explicitly relate the QFI to correlations encoded in the response functions. However, as mentioned in the beginning of the chapter, their reliance on unequal-time correlation functions, such as $\langle[\hat{O}_D(\tau), \hat{O}_D]\rangle$, hinder their application in some settings. It is worth mentioning that the time domain expression has computational advantages compared to equation (3.31) and has been used for computing the QFI [39, 153].

As indicated, we want to derive a protocol that solely relies on measurements of expectation values $\langle\hat{O}(\tau)\rangle$. We begin this task by deriving the time domain analogue of equation (3.31). Consider the following alternative version of equation (3.30)

$$\frac{\rho_\mu - \rho_\nu}{\rho_\mu + \rho_\nu} = \tanh\left(\frac{\beta\omega_{\mu\nu}}{2}\right) = i\beta^{-1}\int_{-\infty}^{+\infty} d\tau \frac{e^{-i\omega_{\mu\nu}\tau}}{\sinh\left(\frac{\pi\tau}{\beta}\right)} . \tag{3.32}$$

Inserting this formula in equation (3.29), we obtain

$$\begin{aligned} F_Q[\hat{\rho}, \hat{O}] &= 2\beta^{-1}\int_{-\infty}^{+\infty} d\tau \frac{1}{\sinh\left(\frac{\pi\tau}{\beta}\right)} i\sum_{\mu,\nu} e^{-i\omega_{\mu\nu}\tau}(\rho_\mu - \rho_\nu)|\langle\mu \mid \hat{O} \mid \nu\rangle|^2 \\ &= 4\beta^{-1}\int_{0}^{+\infty} d\tau \frac{1}{\sinh\left(\frac{\pi\tau}{\beta}\right)} i\theta(\tau)\sum_{\mu,\nu} e^{-i\omega_{\mu\nu}\tau}(\rho_\mu - \rho_\nu)|\langle\mu \mid \hat{O} \mid \nu\rangle|^2 \\ &= 4\beta^{-1}\int_{0}^{+\infty} d\tau \frac{\chi_{\hat{O}\hat{O}}(\tau)}{\sinh\left(\frac{\pi\tau}{\beta}\right)} , \end{aligned} \tag{3.33}$$

where we have used equation (3.11) to get to the last line.

With equation (3.33) in hands, it is possible to obtain the expressions we need. The insight is that the Kubo formula allows us to rewrite the integral in equation (3.33) in terms of $\Delta O(\tau)$. This is the case because we can apply a deconvolution procedure to the Kubo formula to extract $\chi_{\hat{O}\hat{O}}(\tau)$ from $\Delta O(\tau)$. However, this will require us to modify the integral filter to account for the drive $f(\tau)$.

Once again, we use our favorite trick, the convolution theorem. Applying it to equation (3.10), we obtain

$$\Delta O(\omega) = f(\omega)\chi_{\hat{O}\hat{O}}(\omega) , \tag{3.34}$$

which is the Kubo formula in frequency space. This allows us to formally invert $f(\omega)$ and write

$$\chi_{\hat{O}\hat{O}}(\omega) = f(\omega)^{-1}\Delta O(\omega)\,, \tag{3.35}$$

as an equation of generalized functions, i.e., distributions. Of course, the formula above looks a bit too easy, and this is because it is hiding a lot of complexity. To make sense of it, we must recall that distributions are linear functionals mapping test function into numbers. Hence, $f(\omega)^{-1}$ and equation (3.35), only makes sense when integrated against a test function. Nonetheless, the procedure works for a arbitrary well-behaved drive function $f(\tau)$, as long as it fulfills some properties. Most importantly, $f(\omega)$ can only have isolated zeros in the support of $\chi_{\hat{O}\hat{O}}(\omega)$, for this ensures that $f(\omega)^{-1}$ is well defined as a generalized function. A simple drive that does not fulfill this condition is $f(\tau) = \cos(\omega_0\tau)$ as its Fourier transform only contain contributions from frequencies $\omega = \pm\omega_0$. From a physical standpoint, this simply highlights that the time dependent perturbation under consideration must probe all frequencies of the response function.

Let $v_f(\tau)$ be the inverse Fourier transform of $f(\omega)^{-1}$. It is given by the usual formula,

$$v_f(\tau) = \frac{1}{2\pi}\int_{-\infty}^{+\infty} \mathrm{d}\omega e^{i\omega\tau} f(\omega)^{-1}\,, \tag{3.36}$$

and it is also a generalized distribution. The inverse relation defines $f(\omega)^{-1}$ and encodes that $\varphi * f * v_f = \varphi$ must hold for any well behaved test function φ. Technically, we only need it to hold for the response function, so we could weaken this conditions by imposing physical assumptions—such as causality—onto the test function φ. However, for the examples we consider, this is not necessary. Combining equations (3.35) and (3.36), we have

$$\chi_{\hat{O}\hat{O}}(\tau) = (\Delta O * v_f)(\tau) = \int_{-\infty}^{+\infty} \mathrm{d}\tau' \Delta O(\tau') v_f(\tau - \tau')\,. \tag{3.37}$$

Equation (3.37) is precisely what we require, a deconvolution of the Kubo response function with respect to the drive. Inserting equation (3.37) into equation (3.33) leads to our desired outcome, i.e., a formula for the QFI in terms of

$\Delta O(\tau)$. Specifically,

$$\begin{aligned} F_Q[\hat{\rho}, \hat{O}] &= 4\beta^{-1} \int_0^{+\infty} d\tau' \frac{\chi_{\hat{O}\hat{O}}(\tau')}{\sinh\left(\frac{\pi\tau'}{\beta}\right)} \\ &= 4\beta^{-1} \int_0^{+\infty} d\tau' \frac{1}{\sinh\left(\frac{\pi\tau'}{\beta}\right)} \int_{-\infty}^{+\infty} d\tau \Delta O(\tau) v_f(\tau' - \tau) \\ &= 4\beta^{-1} \int_{-\infty}^{+\infty} d\tau \Delta O(\tau) \int_0^{+\infty} d\tau' \frac{v_f(\tau' - \tau)}{\sinh\left(\frac{\pi\tau'}{\beta}\right)} \\ &= 4\beta^{-1} \int_0^{+\infty} d\tau \Delta O(\tau) \kappa_f(\tau) \,, \end{aligned} \tag{3.38}$$

where we have used causality to drop the negative time integration, and defined a modified filter $\kappa_f(\tau)$. It is simply

$$\kappa_f(\tau) = \int_0^{+\infty} d\tau' \frac{v_f(\tau' - \tau)}{\sinh\left(\frac{\pi\tau'}{\beta}\right)} \,. \tag{3.39}$$

Equation (3.38) is our main results as it provides a method of extracting the QFI from the linear response of a quantum mechanical system. This gives a procedure to certify the presence of entanglement when combined with the multipartite entanglement bounds for the QFI. To obtain a concrete protocol, we now specialize to the case of an instantaneous quench. In this scenario, the drive function is simply $f(\tau) = q\theta(\tau)$ and we need to resolve equation (3.39) to calculate the correct filter.

We have already encountered the Fourier transform of the Heaviside function, and it is straightforward to invert it. Specifically,

$$f(\omega)^{-1} = \frac{1}{q}\left(\pi\delta(\omega) + P\frac{1}{i\omega}\right)^{-1} = \frac{i\omega}{q} \tag{3.40}$$

and we can immediately write

$$v_{\text{quench}}(t) = \frac{\delta'(t)}{q} \tag{3.41}$$

using the derivative of the Dirac delta function, since multiplication in frequency space amounts to a derivate in real time. It is straightforward to check the validity of equation (3.40) in frequency space as $\omega\delta(\omega) = 0$. For a less abstract proof, we

can explicitly calculate $\varphi * \theta * \delta' = \varphi$ in the time domain for an arbitrary test function. We have that

$$\begin{aligned}(\varphi * \theta * \delta')(\tau) &= \int_0^{+\infty} \mathrm{d}\tau_2 \int_0^{+\infty} \mathrm{d}\tau_1 \varphi(\tau_1)\theta(\tau_2 - \tau_1)\delta'(\tau - \tau_2) \\ &= \int_0^{+\infty} \mathrm{d}(\tau - \tau_2) \int_0^{\tau_2} \mathrm{d}\tau_1 \varphi(\tau_1)\delta'(\tau - \tau_2) \\ &= \left(-\frac{\mathrm{d}}{\mathrm{d}\tau_3}\int_0^{\tau_2} \mathrm{d}\tau_1 \varphi(\tau_1)\right)_{\tau_3=\tau-\tau_2=0} \\ &= \left(\frac{\mathrm{d}}{\mathrm{d}\tau_2}\int_0^{\tau_2} \mathrm{d}\tau_1 \varphi(\tau_1)\right)_{\tau_2=\tau} = \varphi(\tau)\end{aligned} \tag{3.42}$$

so δ' is indeed the convolution inverse of θ.

Finally, we have our formula

$$\begin{aligned}\mathsf{F}_{\mathrm{Q}}[\hat{\rho}, \hat{\mathrm{O}}] &= \frac{4}{q\beta}\int_0^{+\infty} \mathrm{d}\tau \Delta\hat{\mathrm{O}}_{\mathrm{quench}}(\tau)\left(-\frac{\mathrm{d}}{\mathrm{d}\tau'}\frac{1}{\sinh(\pi\tau'\beta^{-1})}\right)_{\tau'=\tau} \\ &= \frac{4\pi}{q\beta^2}\int_0^{+\infty} \mathrm{d}\tau \frac{\Delta\hat{\mathrm{O}}_{\mathrm{quench}}(\tau)}{\sinh(\pi\tau\beta^{-1})\tanh(\pi\tau\beta^{-1})}\,,\end{aligned} \tag{3.43}$$

which relates the QFI to the response of the system to an abrupt quench. Thus, we can summarize our protocol into four steps: *(i.)* Prepare a thermal state. *(ii.)* Turn on the quench abruptly. *(iii.)* Measure the evolution of the expectation values. *(iv.)* Integrate results according to equation (3.43). Thermal equilibrium and a perturbation in the linear regime are the only assumptions used for deriving equation (3.38). As such, the quench protocol applies to arbitrary quench operators and quantum many-body systems, including fermionic, bosonic, and spin systems.

It is also convenient to introduce the cumulative response function, which we define as

$$\xi_{\hat{\mathrm{O}}\hat{\mathrm{O}}}(\tau) = \int_0^{\tau} \mathrm{d}\tau' \chi_{\hat{\mathrm{O}}\hat{\mathrm{O}}}(\tau')\,, \tag{3.44}$$

One can check that $\xi_{\hat{\mathrm{O}}\hat{\mathrm{O}}}(\tau) = \Delta\hat{\mathrm{O}}_{\mathrm{quench}}(\tau)/q$, so it is $\xi_{\hat{\mathrm{O}}\hat{\mathrm{O}}}(\tau)$ that enters equation (3.43). Of course, the derivative of the cumulative response function if the Kubo response function. This is consistent with equation (3.41).

3.2.2 Properties of the quench protocol

Our quench protocol has a series of advantageous properties. First of all, only expectation values of $\hat{O}(t)$ are used and access to higher moments is not necessary. This is a great simplification compared to equation (3.31). It reduces the requirements for extracting the QFI in many situations, as no time–time correlations are required. Moreover, the rapid decay of the filter,

$$\kappa_{\text{quench}}(\tau) = \frac{4\pi}{\beta^2}\left(\sinh\left(\frac{\pi\tau}{\beta}\right)\tanh\left(\frac{\pi\tau}{\beta}\right)\right)^{-1} \tag{3.45}$$

implies only short measurement times are required. This feature provides resilience against dissipative effects such as atom loss in experiments with ultracold atoms. At small temperatures, where the required observation times become long, the variance of $\hat{O}$ in the initial state yields a reliable upper bound on the QFI. Our protocol can complement this with a lower bound, by tracking the time evolution up to experimentally accessible times.

Another useful property is that equation (3.43) is additive in the integration time. This implies that, given a cutoff time τ_{cutoff},

$$\underbrace{\frac{4\pi}{q\beta^2}\int_0^{\tau_{\text{cutoff}}} \mathrm{d}\tau \frac{\Delta\hat{O}_{\text{quench}}(\tau)}{\sinh(\pi\tau\beta^{-1})\tanh(\pi\tau\beta^{-1})}}_{=F_Q[\hat{\rho},\hat{O}](\tau_{\text{cutoff}})} \leq \underbrace{\frac{4\pi}{q\beta^2}\int_0^{+\infty} \mathrm{d}\tau \frac{\Delta\hat{O}_{\text{quench}}(\tau)}{\sinh(\pi\tau\beta^{-1})\tanh(\pi\tau\beta^{-1})}}_{=F_Q[\hat{\rho},\hat{O}]}, \tag{3.46}$$

so truncating the integral yields a lower bound for the QFI. It ensures that a limited integration time cannot cause a false negative for entanglement certification. This is because the entanglement bounds come from upper bounds on the QFI that hold for separable states. If one such upper bound is violated by $F_Q[\hat{\rho}, \hat{O}](\tau_{\text{cutoff}})$, then it is also violated by the QFI. Hence, we can safely use truncated integrals to certify entanglement.

The requirement of quenching in the linear regime can be tested by comparing responses with different q-parameters. In principle, $\Delta\hat{O}_{\text{quench}}(\tau)$ contains higher-order corrections, while we are only interested in the part that is described by linear response theory. Formally, one can expand

$$\Delta\hat{O}_{\text{quench}}(\tau) = \sum_{n=1}^{\infty} \Delta\hat{O}^{(n)}_{\text{quench}}(\tau) q^n \,, \tag{3.47}$$

and the term that enters equation (3.43) is $\xi_{\hat{O}\hat{O}}(\tau) = \Delta\hat{O}^{(1)}_{\text{quench}}(\tau)$. Fortunately, the linear part dominates for short times, so the decay of the filter function mitigates any errors coming from non-linear effects. Even more, it is possible to

obtain better estimates on the linear contribution by using different values of the quench parameter q and combining the results through a polynomial fit. This also enables extrapolation to $q = 0$. The simplest application relies on performing the quench with some small q and with $-q$. Both measurements can then be combined to yield

$$\frac{\Delta\hat{\mathrm{O}}_{\mathrm{quench}}(\tau)|_q - \Delta\hat{\mathrm{O}}_{\mathrm{quench}}(\tau)|_{-q}}{2} = \Delta\hat{\mathrm{O}}^{(1)}_{\mathrm{quench}}(\tau)q + \Delta\hat{\mathrm{O}}^{(3)}_{\mathrm{quench}}(\tau)q^3 + \dots \,, \quad (3.48)$$

which removes the quadratic contributions and enables one to get accurate results over larger timescales. One can also apply this principle directly to the values of $\mathsf{F}_{\mathsf{Q}}\big[\hat{\rho}, \hat{\mathrm{O}}\big]$ as any deviations from the correct value, due to higher-order terms, will also depend algebraically on the quench parameter.

In a experiment the quench might not be ideal one $f(\tau) = q\theta(\tau)$, but some ramp $f(\tau) = qr(\tau)$ with a smooth function $r(\tau)$. This is of no concern as long as the timescales when the ramp reaches $r(\tau) \approx 1$ are much smaller than the relevant timescales for the system dynamics. Even when that is not the case, it is possible to account for the ramp rigorously by deriving the correct κ_f for the specific ramp profile. For a ramp $r_{\tau_0}(\tau)$ defined by a time scale τ_0, one has

$$f(\tau) = qr_{\tau_0}(\tau) = qg(\tau/\tau_0) \quad (3.49)$$

where $g(\tau/\tau_0)$ is a function that describes the shape of the ramp as it reaches the final value of the quench. The filter for this ramp is given by $\kappa_f(\tau) = \kappa_{\mathrm{quench}}(\tau) * \bar{g}(\tau/\tau_0)$, where $\bar{g}(t)$ is defined by its Fourier transform

$$\bar{g}(\omega\tau_0) = \left(e^{-i\omega\tau_0} + i\omega\tau_0 \int_0^1 \mathrm{d}y e^{-iy\omega\tau_0} g(y)\right)^{-1} . \quad (3.50)$$

For a linear ramp, $g(\tau/\tau_0) = \tau/\tau_0$, we have $\bar{g}(\omega\tau_0) = i\omega\tau_0/(e^{-i\omega\tau_0} - 1)$.

Additionally, the drive function $f(\tau)$ might not have a simple functional expression and both $f(\tau)$ and $\Delta\hat{\mathrm{O}}_{\mathrm{quench}}(\tau)$ will contain some noise. A direct deconvolution procedure such as the Wiener deconvolution can account for this [170]. It produces an approximation for $v_f(\omega)$ given by

$$v_f(\omega) = \frac{f(\omega)^* S_\chi(\omega)}{|f(\omega)|^2 S_\chi(\omega) + S_n(\omega)} \quad (3.51)$$

where $S_{\chi(n)}(\omega)$ denotes the mean power spectral density of χ (the noise).

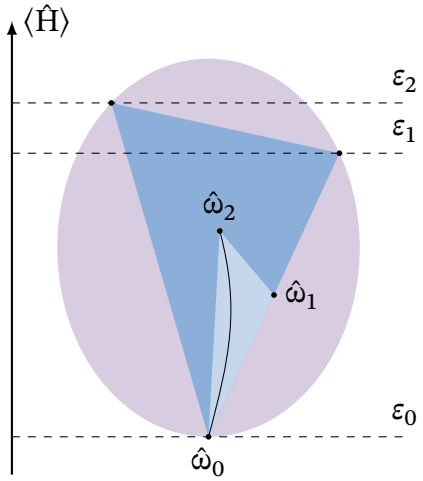

Figure 3.1: Schematic depiction of the simplex of equilibrium states (larger triangle) and the simplex of passive states (smaller triangle) for a three-level system. The curve corresponds to the thermal states, going from the infinite temperature state $\hat{\omega}_2$ to the zero temperature state $\hat{\omega}_0$.

3.3 Extension to passive states

We would like to extend equation (3.43) and the quench protocol to non-thermal equilibrium states. This is highly desirable on a conceptual and a practical level because it is challenging to actually test whether a state is in thermal equilibrium or not. Thus, removing the assumption of a thermal equilibrium would significantly increase in scope of applicability of the quench protocol. Our hypothesis is that it is possible, given some compromises, to extract the QFI using equation (3.43) for a sufficiently generic class of equilibrium ensembles. This is corroborated by existence of expressions connecting the QFI to linear response for other ensembles, such as the eigenstate thermalization hypothesis (ETH) [154].

Here we consider an intermediary step in our endeavor. Specifically, we demonstrate that for a certain class of equilibrium states, know as passive states, there is an effective temperature such that the quench protocol works. Passive states are a class of equilibrium states that defines a weaker thermalization condition [168]. Formally, a state $\hat{\rho}$ is passive if

$$\mathrm{Tr}\big(\hat{U}\hat{\rho}\hat{U}^{\dagger}\hat{H}\big) \leq \mathrm{Tr}\big(\hat{\rho}\hat{H}\big) \tag{3.52}$$

for all unitaries $\hat{U}$ acting on the system. This condition states that it is not possible to lower the energy of a passive state with a reversible process. It also

means that passive states are those that obey the second law in the Kelvin–Planck formulation of thermodynamics [171].

Passive states can also be described more concretely. They are equilibrium states that fulfil an extra equilibration condition, namely that $\rho_\mu \geq \rho_\nu$ whenever $\varepsilon_\nu \geq \varepsilon_\mu$. This can be formulated elegantly using virtual temperatures, which are defined implicitly by

$$\frac{\rho_\mu - \rho_\nu}{\rho_\mu + \rho_\nu} = \tanh\left(\frac{\beta_{\mu\nu}\omega_{\mu\nu}}{2}\right), \tag{3.53}$$

where $\beta_{\mu\nu}$ is the virtual temperature associated to the transition between μ and ν. Using this definition one can check that a state is passive if, and only if, all of its virtual temperatures are positive [172]. The connection with equation (3.52) is that, whenever there is a negative virtual energy, one can lower the energy of the state by inverting the populations of the relevant transition.

Now we introduce the virtual QFI, which we will use to connect passive states to the QFI. For an equilibrium state it is given by

$$\mathrm{F_Q}^{\gamma}\left[\hat{\rho}, \hat{\mathrm{O}}\right] = \frac{4\pi}{q\gamma^2}\int_0^{+\infty} \mathrm{d}\tau \frac{\Delta\hat{\mathrm{O}}_{\mathrm{quench}}(\tau)}{\sinh(\pi\tau\gamma^{-1})\tanh(\pi\tau\gamma^{-1})}, \tag{3.54}$$

where $\gamma \in \mathbb{R}^+$ is some positive number that plays the role of an effective temperature. The choice of the quench formula itself is not particularly critical and it is easy to show that this can be rewritten using other ramps. More importantly, we can write it as

$$\mathrm{F_Q}^{\gamma}\left[\hat{\rho}, \hat{\mathrm{O}}\right] = \sum_{\mu\nu} \tanh\left(\frac{\gamma\omega_{\mu\nu}}{2}\right)(\rho_\mu - \rho_\nu)|\langle\mu \,|\, \hat{\mathrm{O}} \,|\, \nu\rangle|^2, \tag{3.55}$$

which makes the analogy with the QFI of the thermal state explicit.

In the limit when $\gamma \to +\infty$ the tangent hyperbolic in equation (3.55) becomes a sign function. Therefore, the limit is given by

$$\lim_{\gamma\to+\infty} \mathrm{F_Q}^{\gamma}\left[\hat{\rho}, \hat{\mathrm{O}}\right] = \sum_{\mu\nu} \mathrm{sign}(\beta_{\mu\nu})|\rho_\mu - \rho_\nu||\langle\mu \,|\, \hat{\mathrm{O}} \,|\, \nu\rangle|^2, \tag{3.56}$$

and it is positive for passive states. In fact, for passive states this gives an upper bound for the QFI. The limit $\gamma \to 0$ is clearly zero, so we have the following inequality for all passive states

$$\lim_{\gamma\to 0} \mathrm{F_Q}^{\gamma}\left[\hat{\rho}, \hat{\mathrm{O}}\right] \leq \mathrm{F_Q}\left[\hat{\rho}, \hat{\mathrm{O}}\right] \leq \lim_{\gamma\to+\infty} \mathrm{F_Q}^{\gamma}\left[\hat{\rho}, \hat{\mathrm{O}}\right]. \tag{3.57}$$

It follows from inequality (3.57) and the intermediate value theorem that there is a $\tilde{\beta}(\hat{\rho}) \in \mathbb{R}^+$ such that

$$\mathsf{F}_{\mathsf{Q}}\big[\hat{\rho}, \hat{\mathrm{O}}\big] = \mathsf{F}_{\mathsf{Q}}^{\tilde{\beta}(\hat{\rho})}\big[\hat{\rho}, \hat{\mathrm{O}}\big] \,, \tag{3.58}$$

so we can recover the QFI of a passive state using the quench protocol. In particular, we see that the effective temperature $\tilde{\beta}(\hat{\rho})$ contains all the non linearities of the QFI, since the response function are linear on the state. This means that it is not easy to calculate $\tilde{\beta}(\hat{\rho})$, so that we are essentially shifting the complexity from the QFI to it. However, since $\mathsf{F}_{\mathsf{Q}}^{\gamma}\big[\hat{\rho}, \hat{\mathrm{O}}\big]$ is a monotonic increasing function of γ, any $\gamma \leq \tilde{\beta}(\hat{\rho})$ defines a lower bound for the QFI. Thus, we can use approximations $\gamma \lesssim \tilde{\beta}(\hat{\rho})$ to get arbitrarily good approximations of the QFI and this allows us to bypass part of the complexity of the calculation. We can currently studying the properties of $\tilde{\beta}(\hat{\rho})$ as a function of the state by performing random sampling of passive states. This can be done relatively efficiently because the set of passive states defines a simplex (see figure 3.1) [171]. This statistical analysis provides with information about $\tilde{\beta}(\hat{\rho})$ as a function of observables of the system, so that we calculate lower bounds for it with data that would be experimentally accessible. These results, together with the derivation in this section are a part of a work currently in preparation [106].

4 Multipartite mode entanglement

In this chapter we discuss entanglement in the context of indistinguishable particles. This is fundamentally different from the case of qudits due to the presence of particle statistics. Specifically, bosonic and fermionic systems do not admit a Hilbert space with a tensor product decomposition that is compatible with their observables. And this means that an entanglement definition based on tensor product states does not apply. Nonetheless, it is possible to define and characterize entanglement using alternative routes, such as wave function decompositions [96, 97], and the factorization condition [98].

Our focus is the so-called mode entanglement of identical particles. From this perspective, entanglement is a feature of the observables of the system, and their correlation functions. By contrast, particle entanglement is a different characterization of entanglement that focuses on the particles themselves. Which point of view is the correct one, has been a topic of debate since the early 2000s [99]. However, there is substantial evidence by now that mode entanglement is the only consistent criteria for indistinguishable particles [173]. With multiple works successfully employing it to describe entangled states in systems of bosons and fermions [174–177]. Moreover, It has been demonstrated that mode entanglement is a resource for quantum metrology [178–182]. Additionally, techniques such as entanglement witnessing [183, 184] and teleportation [185, 186] have also been extended to indistinguishable particle through the mode entanglement angle.

However, much of the literature focuses on the bipartite case, typically with additional restrictions on the system. In this chapter, we present our results which extend previous techniques to the multipartite case and use it to derive QFI mode entanglement bounds. The presentation is based on our publication, but contains an extended discussion of the theoretical reasoning [105]. The work by Bañuls et al. [98] is of particular importance to us and it is our theoretical reference point. It introduced the factorization condition—as in equation (2.63)—as a criteria for identifying fermionic mode entanglement. Because this technique is agnostic about the structure of the Hilbert space, it bypasses many of the difficulties that come with indistinguishable particles. Additionally, our approach is related to that of Benatti et al. [180], which provides a connection between fermionic mode entanglement and metrology for the two-mode case.

4.1 Indistinguishable particles

The Hilbert space of a system of indistinguishable particles is a Fock space defined by the single-particle states. In the bosonic case, wave functions must be symmetric under permutation, so the Fock space is defined by the symmetrized tensor product. It is a graded vector space given by

$$\bigvee(\mathcal{H}_\mathrm{I}) = \bigoplus_{\mathrm{N}=0}^{\infty} \bigvee^N(\mathcal{H}_\mathrm{I}) = \bigoplus_{\mathrm{N}=0}^{\infty} \mathcal{H}_\mathrm{I} \vee \cdots \vee \mathcal{H}_\mathrm{I} \,, \tag{4.1}$$

where $\mathcal{H}_\mathrm{I}$ denotes the single-particle Hilbert space. Similarly, if the particles are fermions, the Fock space is generated by the exterior algebra of $\mathcal{H}_\mathrm{I}$,

$$\bigwedge(\mathcal{H}_\mathrm{I}) = \bigoplus_{\mathrm{N}=0}^{d} \bigwedge^N(\mathcal{H}_\mathrm{I}) = \bigoplus_{\mathrm{N}=0}^{d} \mathcal{H}_\mathrm{I} \wedge \cdots \wedge \mathcal{H}_\mathrm{I} \,, \tag{4.2}$$

which is the antisymmetric version of the tensor algebra. Here, d denotes the dimension of the single-particle Hilbert space.

The symmetric and antisymmetric product simply realize the standard procedure to obtain bosonic and fermionic wave functions. For instance, the symmetric product of two single-particle states is

$$|\,\psi\rangle \vee |\,\varphi\rangle = |\,\varphi\rangle \vee |\,\psi\rangle \cong \frac{1}{\sqrt{2}}(|\,\psi\rangle \otimes |\,\varphi\rangle + |\,\varphi\rangle \otimes |\,\psi\rangle) \,, \tag{4.3}$$

and generate a bosonic two-particle state. The fermionic counterpart is given by

$$|\,\psi\rangle \wedge |\,\varphi\rangle = -|\,\varphi\rangle \wedge |\,\psi\rangle \cong \frac{1}{\sqrt{2}}(|\,\psi\rangle \otimes |\,\varphi\rangle - |\,\varphi\rangle \otimes |\,\psi\rangle) \,, \tag{4.4}$$

and it defines a antisymmetric wave function. We use the $\cong$ notation above to emphasize that, strictly speaking, the products $|\,\psi\rangle \vee |\,\varphi\rangle$ and $|\,\psi\rangle \wedge |\,\varphi\rangle$ do not belong to the same space as $|\,\psi\rangle \otimes |\,\varphi\rangle$. Nonetheless, there is and embedding of $\mathcal{H}_\mathrm{I} \otimes \mathcal{H}_\mathrm{I}$ into both $\mathcal{H}_\mathrm{I} \vee \mathcal{H}_\mathrm{I}$ and $\mathcal{H}_\mathrm{I} \wedge \mathcal{H}_\mathrm{I}$, and it defines the equivalence in the equations above.

Due to the construction of the Fock space, a $\mathbb{N}$-grading arises naturally. It defines the number operator $\hat{\mathrm{N}}$, which counts the number of particles of a given states. Crucially, it factors through the direct sums in equations (4.1) and (4.2). The number operator is unbounded for bosonic particles, something that introduces some technical challenges, as the dimension of the symmetric Hilbert space is infinite. Nonetheless, it is bounded in the fermionic case due to the Pauli exclusion principle.

Creation and annihilation operators allow us to describe the observables acting on the Fock space. They provide the most efficient way of working with identical particles. This is because they bypass the laborious process of explicitly symmetrizing, or antisymmetrizing, the many-body wave function. Instead, they encode the particle statistics in the canonical commutation relations, in the case of bosons, and in the canonical anticommutation relations, in the case of fermions.

Let us consider two single-particle states $|\varphi\rangle, |\psi\rangle \in \mathcal{H}_\mathrm{I}$. We define bosonic creation and annihilation operators by

$$\begin{aligned}\hat{a}_\varphi\big(|\psi_1\rangle \vee \cdots \vee |\psi_n\rangle\big) =& \langle\varphi|\psi_1\rangle\big(|\psi_2\rangle \vee \cdots \vee |\psi_n\rangle\big) \\ &+ |\psi_1\rangle \vee \hat{a}_\varphi\big(|\psi_2\rangle \vee \cdots \vee |\psi_n\rangle\big) \\ \hat{a}^\dagger_\psi\big(|\psi_1\rangle \vee \cdots \vee |\psi_n\rangle\big) =& |\psi\rangle \vee |\psi_1\rangle \vee \cdots \vee |\psi_n\rangle\,,\end{aligned} \tag{4.5}$$

and they satisfy the canonical commutation relations,

$$[\hat{a}_\varphi, \hat{a}^\dagger_\psi] = \langle\varphi|\psi\rangle\,. \tag{4.6}$$

Similarly, we write fermionic creation and annihilation operators as

$$\begin{aligned}\hat{c}_\varphi\big(|\psi_1\rangle \wedge \cdots \wedge |\psi_n\rangle\big) =& \langle\varphi|\psi_1\rangle\big(|\psi_2\rangle \wedge \cdots \wedge |\psi_n\rangle\big) \\ &- |\psi_1\rangle \wedge \hat{c}_\varphi\big(|\psi_2\rangle \wedge \cdots \wedge |\psi_n\rangle\big) \\ \hat{c}^\dagger_\psi\big(|\psi_1\rangle \wedge \cdots \wedge |\psi_n\rangle\big) =& |\psi\rangle \wedge |\psi_1\rangle \wedge \cdots \wedge |\psi_n\rangle\,,\end{aligned} \tag{4.7}$$

and they satisfy the canonical anticommutation relations,

$$\{\hat{c}_\varphi, \hat{c}^\dagger_\psi\} = \langle\varphi|\psi\rangle\,. \tag{4.8}$$

Fixing a basis of the single particle Hilbert space

$$\mathcal{H}_\mathrm{I} = \bigoplus_{m\in M} \mathbb{C}|\,m\rangle\,, \tag{4.9}$$

we recover the more familiar expressions for equations (4.6) and (4.8). The labels for the basis are called modes. It is also convenient to fix an enumeration for the basis in the fermionic case. This is because an expression like $\prod_{m\in M} \hat{c}^\dagger_m$ is ambiguous in general, due to the antisymmetric nature of the fermions. The ambiguity boils down to a factor of ± 1 that arises when we rearrange the creation operators. Strictly speaking, we only need to fix the parity of the enumeration to remove the ambiguous term, but it is simpler to choose a specific enumeration.

The vacuum state $|\,\rangle$ spans the $\mathrm{N} = 0$ sector. Moreover, it defines the occupation basis that spans higher occupation sectors. Specifically, we have

$$|\,\eta_B\rangle = \hat{\mathrm{a}}^\dagger_{\eta_B}|\,\rangle = \prod_{m\in M} \left(\hat{\mathrm{a}}^\dagger_m\right)^{\eta_B(m)}|\,\rangle \tag{4.10}$$

$$|\,\eta_F\rangle = \hat{\mathrm{c}}^\dagger_{\eta_F}|\,\rangle = \prod_{m\in M} \left(\hat{\mathrm{c}}^\dagger_m\right)^{\eta_F(m)}|\,\rangle\,, \tag{4.11}$$

where η_B, η_F are functions that specify the occupation of the bosonic and fermionic modes. The product of creation operators in equation (4.11) is ordered according to our fixed enumeration. In the bosonic case, $\eta_B(m)$ can be any natural number and $\eta_B \in \mathbb{N}^M$. For fermions, $\eta_F \in 2^M$ since the occupation numbers are restricted to $\eta_B(m) \in \{0, 1\}$. Furthermore, we can define generalized creation operators which can create all possible states from the vacuum. In the fermionic case, they are given by

$$\hat{\mathrm{C}}^\dagger = \sum_{\eta_F} \varphi^\dagger(\eta_F)\hat{\mathrm{c}}^\dagger_{\eta_F}\,, \tag{4.12}$$

where $\varphi^\dagger(\eta_F) \in \mathbb{C}$ is a probability amplitude that corresponds to the many-particle wave function.

4.1.1 Selection and superselection rules

In the case of fermions, an additional subtlety arises due to the parity superselection rule [187]. It forbids the existence of coherence between states with different parity. Concretely, if we write the parity operator as

$$\hat{\mathrm{P}} = (-1)^{\hat{\mathrm{N}}} = \prod_{m\in M} (-1)^{\hat{\mathrm{c}}^\dagger_m \hat{\mathrm{c}}_m}\,, \tag{4.13}$$

then it is not possible to go from the $\mathrm{P} = 1$ sector to the $\mathrm{P} = -1$ sector with physically accessible operations. This has important consequences as it alters the algebra of observables, and the space of states of a fermionic systems.

The fermionic creation and annihilation operators generate a C^*-algebra $\mathsf{CAR}(M)$, but this is not the algebra that describes physical operators. This because the parity superselection rules forbids any operator that can change the superselection section. Therefore, the actual C^*-algebra that describes the physical observables of the fermionic system is

$$\mathcal{A}(M)_F = \left\{\hat{\mathrm{O}} \in \mathsf{CAR}(M) \mid [\hat{\mathrm{O}}, \hat{\mathrm{P}}] = 0\right\}, \tag{4.14}$$

the set of all operators that commute with the parity operator. , not all operators in $\mathsf{CAR}(M)$ are physical. Notice that despite the use of a fixed set of modes in

equations (4.13) and (4.14), the parity operator and the algebra do not depend on a particular choice of modes. Nonetheless, the fixed modes provide a concrete description of $\mathcal{A}(M)_F$. This is because the operators that belong to it can only change the number of particles by multiples of two. And this restricts them to be combinations of even products of creation and annihilation operators. Thus, the elements of $\mathcal{A}(M)_F$ are even polynomials on the creation and annihilation operators associated to the modes.

Fermionic states are normalized positive functionals $\hat{\rho} \in \mathcal{A}(M)_F^*$, which we can represent by density matrices acting on the fermionic Fock space. Due to the parity superselection rule, the states must also commute with the parity operator. As such, all valid fermionic states are of the form

$$\hat{\rho} = \mathsf{p}(+)\hat{\rho}_+ \oplus \mathsf{p}(-)\hat{\rho}_- \,, \tag{4.15}$$

where $\hat{\rho}_\pm$ is a state with fixed parity ± 1. This is a direct consequence of equation (4.14) and the condition that all physical observables commute with $\hat{\mathrm{P}}$. Specifically, the center of $\mathcal{A}(M)_F$[1],

$$\mathcal{Z}(M)_F = \mathcal{A}(M)_F \cap \mathcal{A}(M)_F' = \{\alpha\hat{1} + \beta\hat{\mathrm{P}} \mid \alpha, \beta \in \mathbb{C}\} \,, \tag{4.16}$$

is nontrivial, as it contains $\hat{\mathrm{P}}$, and this induces the decomposition in equation (4.15). As a consequence, it is not possible to connect states with an even number of particles with those with an odd number of particles. It is this fact that prevents one from decomposing the fermionic Fock space into a tensor product of local Hilbert spaces.

Superselection rules are a fundamental feature of physics and apply to all systems. By contrast, selection rules arise in specific situations, such as when a Hamiltonian has a conservation law. Nonetheless, one can use the same formalism to describe both selection and superselection rules. The simplest example of selection rule for identical particles is particle number conservation. In a fermionic system, we can use it to further restrict the algebra of physical operators. We do so by defining

$$\mathcal{A}(M)_F^{\mathrm{N}} = \left\{\hat{\mathrm{O}} \in \mathsf{CAR}(M) \mid [\hat{\mathrm{O}}, \hat{\mathrm{N}}] = 0\right\} \subset \mathcal{A}(M)_F \,, \tag{4.17}$$

which contains the operators that preserve particle number. Naturally, this algebra also has a nontrivial center $\mathcal{Z}(M)_F^{\mathrm{N}}$ that induces a diagonal decomposition like equation (4.15), but in terms of the particle number sectors.

[1]The center of an algebra $\mathcal{Z}(A)$ is the intersection of the algebra with its commutant. As such, it is given by $\mathcal{Z}(A) = A \cap A'$ and it defines a commutative subalgebra.

Bosonic system do not have a superselection rule. This means we can assign

$$\mathcal{A}(M)_B = \mathsf{CCR}(M) \tag{4.18}$$

directly. Thus, the entire algebra generated by bosonic creation and annihilation operators defines physical operators. However, this introduces a technical difficulty of another kind, namely that the operators in the bosonic algebra are unbounded. This because an operator like $\hat{a}_m^\dagger \hat{a}_m$ has arbitrarily large eigenvalues, and this implies that $\mathcal{A}(M)_B$ is not a C^*-algebra, so some care is necessary. Nonetheless, for the applications we have in mind, we can assume that there is a fixed number of particles and this resolved the issues with unbounded operators. This effectively means that we only work with

$$\mathcal{A}(M)_B^{\mathrm{N}} = \left\{\hat{\mathrm{O}} \in \mathsf{CCR}(M) \mid [\hat{\mathrm{O}}, \hat{\mathrm{N}}] = 0\right\} \subset \mathcal{A}(M)_B \,, \tag{4.19}$$

the algebra of bosonic operators that conserve total particle number, i.e., we assume that there is a selection rule in place for bosonic systems.

4.2 Mode entanglement in fermionic systems

In this section, we are going to define multipartite mode entanglement for fermionic systems. We do so by introducing a local net of observables associated to the algebra of parity preserving fermionic operators. This allows us to implement the techniques presented in section 2.4. In particular, we can define a multipartite separability criteria for fermionic modes. This allow us to identify the analogues of product states and use them to derive QFI entanglement bounds for fermionic mode entanglement. The bounds allow us to use the QFI as a tool for certifying multipartite mode entanglement, and we will put them to use in the next chapter.

We derive multipartite entanglement bounds for three different settings, namely:

- Arbitrary fermionic systems.
- Fermionic systems with particle number conservation.
- Fermionic systems with a fixed occupation number.

Each scenario provides increasingly tight bounds on the QFI, which can be adapted to different applications. We provide a concrete algorithm to calculate the bounds systematically. This is a flexible technique that can be adapted to other scenarios. For instance, one can enhance the bounds by introducing additional conserved quantities.

4.2.1 Separability criteria

Let us assume for a moment that the single-particle basis states that define M correspond to localized orbitals in a lattice. It follows that a subset $K \subset M$ amounts to a certain subregion of the lattice, so that we may regard it as a subsystem. The algebra $\mathcal{A}(K)_F$ describes the physical operators with support in this subregion. In particular, there is a local parity operator $\hat{\mathrm{P}}_K$ that defines a superselection rule for the observables of K and the reduced states associated to it. It it constrained by the global parity operator due to the equation

$$\hat{\mathrm{P}} = \hat{\mathrm{P}}_K \hat{\mathrm{P}}_{M\setminus K} = \Big(\prod_{m\in K} (-1)^{\hat{\mathrm{c}}_m^\dagger \hat{\mathrm{c}}_m}\Big)\Big(\prod_{m\notin K} (-1)^{\hat{\mathrm{c}}_m^\dagger \hat{\mathrm{c}}_m}\Big)\,, \tag{4.20}$$

which relates the parity in the global system to the one associated to K and its complement. In any case, this procedure yields a local net of observables that describes the locality structure in the M space, which amount to real space for this particular example.

More broadly, we may consider local net of observables associated to subsets of M regardless of what the modes describe. For instance, in the lattice example, one may consider the basis that is diagonal in momentum space. This yields a net of observables that is local in momentum space, instead of real space. In general, each choice of modes will define a different local net of observables and, consequently, a different notion of entanglement.

A partition of the system amounts to a decomposition of M into various independent subsystems. Specifically, we have

$$M = \bigsqcup_{j\in J} M_j = M_1 \sqcup M_2 \cdots \sqcup M_{|J|}\,, \tag{4.21}$$

with subsets of modes $M_j \subset M$ that are labeled by indexes $j \in J$. The subsets are assumed to be pairwise disjoint, so that we have

$$\mathcal{H}_{\mathrm{I}} = \bigoplus_{j\in J} \mathcal{H}_j = \mathcal{H}_1 \oplus \mathcal{H}_2 \oplus \cdots \oplus \mathcal{H}_{|J|} \tag{4.22}$$

where $\mathcal{H}_j$ is the single-particle Hilbert space spanned by the modes of M_j. This guarantees that the algebras $\mathcal{A}(M_j)_F$ are independent of each other, but only due to the enforcement of the parity superselection rule. It follows that

$$\mathcal{A}(M)_F = \Big(\bigcup_{j\in J} \mathcal{A}(M_j)_F\Big)''\,, \tag{4.23}$$

as expected for a partition of the system. In particular, we can express the parity operator as $\hat{\mathrm{P}} = \hat{\mathrm{P}}_1 \hat{\mathrm{P}}_2 \ldots \hat{\mathrm{P}}_{|J|}$, where $\hat{\mathrm{P}}_j = \hat{\mathrm{P}}_{M_j}$.

Equation (4.23) provide us with a separability criteria for mode entanglement. Specifically, $\{M_j\}$-product states are those that satisfy

$$\langle \prod_{j\in J} \hat{O}_j \rangle_{\hat{\rho}} = \prod_{j\in J} \langle \hat{O}_j \rangle_{\hat{\rho}_j} \tag{4.24}$$

for all operators $\hat{O}_j \in \mathcal{A}(M_j)_F$. If each M_j has at most k modes, we say—by analogy with the procedure in section 2.2— that the partition is a k-partition. And we define the set of k-separable fermionic states Sep_k as the convex hull of all states which are $\{M_j\}$-producible for some k-partition. Finally, a fermionic state has k-partite mode entanglement if it does not belong to Sep_k.

The reduced states $\hat{\rho}_j$ in equation (4.24) must be physical states, i.e., commute the local parity $\hat{P}_j$. This can only occur if they have fixed parities P_j, such that

$$P = P_1 \dots P_{|J|} \,, \tag{4.25}$$

where P is a fixed parity for the state $\hat{\rho}$. In fact, a concrete calculate shows that a partial trace procedure for the fermionic modes is only consistent for states that respect the superselection rule [176]. The necessity to account for the superselection rule in order to obtain a consistent definition of fermionic mode entanglement is a general requirement [98, 174, 176]. The advantage of our formalism is it does this automatically, as we consider the algebras $\mathcal{A}(M_j)_F$ which already handle the parity.

It is worth pointing out that the algebra $\mathsf{CAR}(M)$ is isomorphic to the algebra of a system of d qubits, since the dimension of the fermionic Fock space is 2^d. However, this does not imply that the fermions can be treated as qubits [188]. In particular, it is the superselection rule that induces the local net of observables defined by $\mathcal{A}(K)_F$. This is what differentiates fermions from qubits. One can also see this concretely by mapping the fermionic modes into qubits with a procedure such as the Jordan–Wigner transformation. It sends operators that are local in the fermionic mode picture into nonlocal qubit operators, and vice versa. Thus, the qubit local net of observables, induced by the tensor product structure, is incompatible with the fermionic modes net, which is induced by exterior product structure of the Fock space.

As we have mentioned, the choice of the modes M is critical as inequivalent choices lead to different entanglement criteria. However, due to the generality of our methods, it is not necessary to make any assumptions on M. And, while the majority of works on entanglement focus on modes localized in real-space, there are interesting possibilities for the reciprocal space [182]. This is particularly the case in light of the recent experiments with fermionic atomic species [189].

4.2.2 Entanglement bounds for fermionic systems

Our goal is to derive QFI bounds k-producible states to obtain a way to certify the presence of multipartite mode entanglement. We choose a generator for the QFI that is a generalized version of the generators associated to linear interferometers. Specifically, we employ

$$\hat{O} = \sum_{m \in M} w(m) \hat{c}_m^\dagger \hat{c}_m \,, \tag{4.26}$$

with weights $w(m) \in \mathbb{R}$. This generator is compatible with any partition—as in equation (4.21)—since we can rearrange the occupation numbers into

$$\hat{O} = \sum_j \hat{O}_j = \sum_j \sum_{m \in M_j} w(m) \hat{c}_m^\dagger \hat{c}_m \,, \tag{4.27}$$

such that $\hat{O}_j \in \mathcal{A}(M_j)_F$. In particular, analogously to equation (2.45), it is possible to decompose the QFI of any $\{M_j\}$-producible state into

$$F_Q[\hat{\rho}, \hat{O}] = \sum_{j \in J} F_Q[\hat{\rho}_j, \hat{O}_j] \,, \tag{4.28}$$

using the factorization given by equation (4.24). Thus, we need to find an upper bound on the right-hand side of equation (4.28) that holds for all k-partitions. Moreover, we can use equation (4.15) to decompose the QFI into

$$F_Q[\hat{\rho}, \hat{O}] = p(+) F_Q[\hat{\rho}_+, \hat{O}] + p(-) F_Q[\hat{\rho}_-, \hat{O}] \,, \tag{4.29}$$

so we can assume a fixed parity to obtain the bound.

Just like the qudit case, the fist step is to derive an expression for the QFI of $\{M_j\}$-producible states. We begin by noticing that a state defined by

$$|\psi\rangle = \hat{C}_1^\dagger \hat{C}_2^\dagger \ldots \hat{C}_{|J|}^\dagger |\rangle \tag{4.30}$$

is $\{M_j\}$-producible as long as each generalized creation operator $\hat{C}_j^\dagger$ is restricted to M_j. Specifically, we have

$$\hat{C}_j^\dagger = \sum_{\eta_j} \varphi_j^\dagger(\eta_j) \hat{c}_{\eta_j}^\dagger \,, \tag{4.31}$$

where the sum runs over all $\eta_j \in 2^{M_j}$ with a fixed parity P_j. In fact, every state that is $\{M_j\}$-producible is of this form, as can be easily verified with Wick's theorem. Therefore, it is sufficient to calculate the variance of $\hat{O}$ with respect to $|\psi\rangle$.

The expectation value of the operator $\hat{O}$ follows from Wick's theorem. It is given by

$$\begin{aligned}\langle\psi\,|\,\hat{O}\,|\,\psi\rangle &= \sum_{m\in M} w(m)\langle\,|\,(\prod_j \hat{C}_j)\hat{c}_m^\dagger\hat{c}_m(\prod_j \hat{C}_j^\dagger)\,|\,\rangle \\ &= \sum_j \sum_{m\in M_j} w(m)\langle\,|\,\hat{C}_j\hat{c}_m^\dagger\hat{c}_m\hat{C}_j^\dagger\,|\,\rangle = \sum_j\sum_{\eta_j} w_j(\eta_j)\,\mathsf{p}_j(\eta_j)\,,\end{aligned} \tag{4.32}$$

where we have assumed that the state is normalized, so that $\langle\,|\,\hat{C}_j\hat{C}_j^\dagger\,|\,\rangle = 1$. In the equation above, we introduced random variables

$$w_j(\eta_j) = \sum_{m\in M_j} w(m)\eta_j(m) \tag{4.33}$$

distributed according to the probabilities $\mathsf{p}_j(\eta_j) = \varphi_j^\dagger(\eta_j)\varphi_j(\eta_j)$. A similar calculation yields

$$\begin{aligned}\langle\psi\,|\,\hat{O}^2\,|\,\psi\rangle = &\sum_{j\neq j'}\Big(\sum_{\eta_j} w_j(\eta_j)\,\mathsf{p}_j(\eta_j)\Big)\Big(\sum_{\eta_{j'}} w_{j'}(\eta_{j'})\,\mathsf{p}_j(\eta_{j'})\Big) \\ &+\sum_j\sum_{\eta_j} w_j(\eta_j)^2\,\mathsf{p}_j(\eta_j)\,,\end{aligned} \tag{4.34}$$

and we get

$$\langle\psi\,|\,\hat{O}^2\,|\,\psi\rangle - \langle\psi\,|\,\hat{O}\,|\,\psi\rangle^2 = \sum_j \Delta^2 w_j\,, \tag{4.35}$$

as the crossed terms $j \neq j'$ cancel out. Hence, we conclude that the QFI of $|\,\psi\rangle$ is given by $\mathsf{F}_\mathsf{Q}\big[|\,\psi\rangle\langle\psi\,|,\hat{O}\big] = 4\sum_j \Delta^2 w_j$.

To obtain a useful bound on the QFI, it is necessary to find a bound for $\sum_j \Delta^2 w_j$ that depends neither on the probability distributions p_j nor on the specific partitions M_j, as these are state dependent. Instead, we need a quantity that applies to all k-producible states and the values of the $w(m)$. Our tool of choice for this task is Popoviciu's inequality on variances [190, 191]. It states that

$$\Delta^2 w_j \leq \frac{1}{4}\Big(\max_{\eta_j} w_j(\eta_j) - \min_{\eta_j} w_j(\eta_j)\Big)\,, \tag{4.36}$$

where the maximum and minimum are taken over all allowed configurations. We use this to optimize over all valid k-partitions—while accounting for the constraints from the superselection rule—to obtain a generic bound for equation (4.35).

Consider a fixed partition $\{M_j\}$ and let us divide each M_j into

$$\begin{aligned} M_j^+ &= \{m \in M_j \mid w(m) > 0\} \\ M_j^0 &= \{m \in M_j \mid w(m) = 0\} \\ M_j^- &= \{m \in M_j \mid w(m) < 0\} \,. \end{aligned} \tag{4.37}$$

It follows that

$$\sum_{m\in M_j^-} w(m) \leq w_j(\eta_j) \leq \sum_{m\in M_j^+} w(m) \,, \tag{4.38}$$

and this provides the maximum and minimum necessary for Popoviciu's inequality. If $(-1)^{|M_j^+|} \neq (-1)^{|M_j^-|}$, then the superselection rule allow us improve the bound since the two limits above cannot be reached by states of the same parity. However, we will neglect this for now because we can account for it during the optimization procedure. Combining inequalities (4.36) and (4.38), we have

$$\sum_j \Delta^2 w_j \leq \sum_j \frac{1}{4}\Big(\sum_{m\in M_j^+} w(m) - \sum_{m\in M_j^-} w(m)\Big)^2 = \frac{1}{4}\sum_j \Big(\sum_{m\in M_j} |w(m)|\Big)^2 \,, \tag{4.39}$$

where the sum over M_j^+ corresponds to the maximum of $w(\eta_j)$ over all η_j and the sum over M_j^- to the minimum.

Now we need a global bound that is optimized over all k-partitions. To obtain it, we construct the k-partition that maximizes the right hand side of inequality (4.39). It is given by the algorithm bellow:

1: **procedure** OPT(M, w)
2: $M_\bullet \leftarrow M$
3: $j \leftarrow 1$
4: **while** $M_\bullet \neq \varnothing$ **do**
5: $M_j \leftarrow \varnothing$
6: Move the k modes with highest $|w(m)|$ from $M_\bullet$ to M_j
7: **if** $(-1)^{|M_j^+|} \neq (-1)^{|M_j^-|}$ **then**
8: Move the mode with the lowest $|w(m)|$ from M_j to $M_\bullet$
9: **end if**
10: $j \leftarrow j + 1$
11: **end while**
12: **return** $\{M_j\}$
13: **end procedure**

Optimality is ensured by the step in line 6. It guarantees that each element M_j of the partition has at most k modes, and it concentrates the modes that contribute

the most to inequality (4.39) together. This yields an optimal partition because they will contribute quadratically, and the largest value arises when we square the highest possible number. Lines 7 to 9 makes sure that the bound is as tight as possible. This is because they ensure that the contribution associated to each M_j can be realized by a physical state, that respects the parity superselection rule.

Our optimization procedure generates a parition that is optimal for a global parity given by

$$\mathrm{P} = \prod_j \mathrm{P}_j = \prod_j (-1)^{|M_j^+|} = \prod_j (-1)^{|M_j^-|} \,, \tag{4.40}$$

and it yields a bound

$$\mathsf{F}_{\mathrm{Q}}\big[\hat{\rho}, \hat{\mathrm{O}}\big] \leq \sum_j \Big(\sum_{m \in M_j} |w(m)| \Big)^2 \leq (dk^2 + r^2) \Big(\max_{m \in M} |w(m)| \Big)^2 \tag{4.41}$$

for all k-separable fermionic states. The second bound above is a generic expressions that does not depend explicitly on the optimal partition. Inequality (4.41) follows from our construction due to the convexity of the QFI, and we can use it to certify the presence of multipartite fermionic mode entanglement.

4.2.3 Enhanced bounds at fixed particle number

If we consider a system with particle number conservation, then we can enhance the QFI bound given by inequality (4.41). This is because the algorithm we used to obtain the optimal partition did not factor in any constraints in the occupation numbers. Thus, we can derive a new algorithm that generates an optimal partition for a fixed particle number, and use it to tighten the QFI bound. In particular, the QFI of a state $\hat{\rho}$ that commutes with the number operator follows

$$\mathsf{F}_{\mathrm{Q}}\big[\hat{\rho}, \hat{\mathrm{O}}\big] = \sum_{\mathrm{N}} \mathrm{p}(\mathrm{N})\, \mathsf{F}_{\mathrm{Q}}\big[\hat{\rho}_{\mathrm{N}}, \hat{\mathrm{O}}\big] \,, \tag{4.42}$$

where $\hat{\rho}_{\mathrm{N}}$ is a state with a fixed number of particles and $\mathrm{p}(\mathrm{N})$ is the probability of observing N particles. Therefore, it is sufficient to derive a QFI bound for states with a fixed number of particles, since $\mathrm{p}(\mathrm{N})$ can be easily calculated or measured.

We proceed as before, with the state given by equation (4.30). However, there is an additional requirement, namely that each generalized creation operator $\hat{\mathrm{C}}_j^\dagger$ commutes with the number operator. In practice this means that each $\hat{\mathrm{C}}_j^\dagger$ creates states with a fixed particle number N_j. The global occupation number is $\mathrm{N} = \sum_j \mathrm{N}_j$, and we assume that it is fixed from now on.

The derivations for the expectations values, and the variance of $\hat{\mathrm{O}}$, do not change. However, the lower and upper bounds for $w(\eta_j)$, shown in inequality (4.38), cannot always be reached if there are restrictions on the occupation numbers. In particular, the number of modes in M_j^+ and M_j^- has to be the same and equal to N_j. Otherwise, no choice of occupations η_j can achieve the limits inequality (4.38). We can exploit this to derive tighter bounds for the variance of the state. Effectively, it is necessary to identify what is $\max$ / $\min_{\eta_j} w_j(\eta_j)$ when there is a fixed number of particles.

To obtain the improved bounds, let us again consider an arbitrary partition $\{M_j\}$. Moreover, we fix an allocated number of particles N_j, that add to the global value N. Divide each M_j into

$$M_j = M_j^u \cup M_j^i \cup M_j^l \,, \tag{4.43}$$

where the lower portion M_j^l contains the N_j modes with the lowest weights, the upper portion M_j^u contains the N_j modes with the highest weights, and the intermediary portion M_j^i contains the rest of the modes. It follows that

$$\sum_{m\in M_j^l} w(m) \leq w_j(\eta_j) \leq \sum_{m\in M_j^u} w(m) \,, \tag{4.44}$$

if we only consider occupations η_j compatible with the particle number N_j, that is, such that the creation operator $\mathrm{c}^\dagger_{\eta_j}$ creates exactly N_j particles. Once again, we apply Popoviciu's inequality to obtain

$$\sum_j \Delta^2 w_j \leq \sum_j \frac{1}{4}\Big(\sum_{m\in M_j^u} w(m) - \sum_{m\in M_j^l} w(m)\Big)^2 \,. \tag{4.45}$$

In this case, we cannot benefit from the absolute value and there is an explicit dependence of the occupation numbers.

Now, the task is to find the k-partition M_j that optimizes the right hand side of inequality (4.45). This can be done by concentrating the modes with the highest weights into the same M_j^u and those with the lowest weights into the same M_j^l, in a similar fashion as before. However, we also need to optimize over the allocation of particles to each M_j, since the bound can only depend on the total number N. To do so, we must half-fill as many M_j as possible, giving priority to the M_j that contribute the most. This is because M_j^u and M_j^l overlap when N_j is larger than $\lfloor |M_j|/2 \rfloor$, i.e., when M_j is filled beyond half-filling. And this reduces the bound of inequality (4.45), since some of the terms in the difference will cancel. Similarly, if the filling is below half-filling, there will be modes in M_j^i that do not contribute.

Combining our insights, we can define an algorithm to construct the optimal partition, designed to maximize the righ hand side of inequality (4.45) over all k-partitions and allocations of N particles. It is given by

1: **procedure** OPT(M, N, w)
2: $M_\bullet \leftarrow M$
3: $\mathrm{N}_\bullet \leftarrow \mathrm{N}$
4: $j \leftarrow 1$
5: **while** $M_\bullet \neq \varnothing$ **do**
6: $M_j \leftarrow \varnothing$
7: Move the $\lfloor k/2 \rfloor$ modes with highest $w(m)$ from $M_\bullet$ to M_j
8: Move the $\lfloor k/2 \rfloor$ modes with lowest $w(m)$ from $M_\bullet$ to M_j
9: **if** $\mathrm{N}_\bullet > \lfloor |M_j|/2 \rfloor$ **then**
10: $\mathrm{N}_j \leftarrow \lfloor |M_j|/2 \rfloor$
11: $\mathrm{N}_\bullet \leftarrow \mathrm{N}_\bullet - \lfloor |M_j|/2 \rfloor$
12: **else**
13: $\mathrm{N}_j \leftarrow \mathrm{N}_\bullet$
14: $\mathrm{N}_\bullet \leftarrow 0$
15: **end if**
16: $j \leftarrow j + 1$
17: **end while**
18: **while** $\mathrm{N}_\bullet > 0$ **do**
19: **if** $\mathrm{N}_\bullet > \lceil |M_j|/2 \rceil$ **then**
20: $\mathrm{N}_j \leftarrow \mathrm{N}_j + \lceil |M_j|/2 \rceil$
21: $\mathrm{N}_\bullet \leftarrow \mathrm{N}_\bullet - \lceil |M_j|/2 \rceil$
22: **else**
23: $\mathrm{N}_j \leftarrow \mathrm{N}_\bullet$
24: $\mathrm{N}_\bullet \leftarrow 0$
25: **end if**
26: $j \leftarrow j - 1$
27: **end while**
28: **return** $\{M_j\}$ and $\{\mathrm{N}_j\}$
29: **end procedure**

Lines 7 and 8 allocate up to k modes to M_j in order to maximize the contributions to inequality (4.45). The steps in lines 9 to 15 assign the particles in such manner as to ensure that all M_j—with the possible exception of the last one—are half-filled. If there are particles remaining, lines 18 to 27 allocates them. The loop goes backwards, starting from the M_j with the smallest weights, because this procedure reduces the contributions from the M_j that get filled beyond $|M_j|/2$. This occurs when $\mathrm{N} > |M|/2$ and reduces the value of the upper bound.

Once again, the convexity of the QFI implies that

$$\mathsf{F}_{\mathsf{Q}}\big[\hat{\rho},\hat{\mathrm{O}}\big] \leq \sum_{\mathrm{N}} \mathsf{p}(\mathrm{N}) \underbrace{\sum_{j}\Big(\sum_{m\in M_j^u} w(m) - \sum_{m\in M_j^l} w(m)\Big)^2}_{\text{Optimal partition for N}} , \tag{4.46}$$

for all k-separable states with particle number conservation. And we obtain another family of bounds that can be used to certify fermionic multipartite mode entanglement in quantum many-body systems. They are a refinement of inequality (4.41), since we leveraged the additional information to derive tighter bounds. Our algorithm for the optimal partition also implies that the bound for half-filling $\mathrm{N} = |M|/2$ is a bound for all other occupation values. Thus, it can be used in settings where it is know that there is particle number conservation, but it is no possible to obtain the probabilities $\mathsf{p}(\mathrm{N})$. In particular, we get a generic bound

$$\mathsf{F}_{\mathsf{Q}}\big[\hat{\rho},\hat{\mathrm{O}}\big] \leq \frac{dk^2+r^2}{4}\big(\max_{m\in M} w(m) - \min_{m\in M} w(m)\big)^2 , \tag{4.47}$$

which does not depend on the optimal partitions or the occupation probabilities.

4.3 Considerations for bosonic systems

It is possible apply to adapt our discussion of fermionic mode entanglement to the context of bosons. In particular, we can use the bosonic algebras $\mathcal{A}(M)_B^{\mathrm{N}}$ to define a local net of observables that describes bosonic multipartite mode entanglement. Concretely, we can also write

$$\mathcal{A}(M)_B^{\mathrm{N}} = \Big(\bigcup_{j\in J} \mathcal{A}(M_j)_B^{\mathrm{N}}\Big)'' , \tag{4.48}$$

using a decomposition of the modes as in equation (4.21). This allow us to formulate a factorization condition and use it to define a k-separability criteria for bosons. The condition is the same as its fermionic counterpart in equation (4.24), but with the bosonic algebra instead.

One can also write k-producible bosonic states using generalized creation operators. Specifically, we have

$$|\,\psi\rangle = \hat{\mathrm{A}}_1^\dagger \hat{\mathrm{C}}_A^\dagger \ldots \hat{\mathrm{A}}_{|J|}^\dagger |\,\rangle \tag{4.49}$$

where $\hat{\mathrm{A}}_j^\dagger$ is a generalized creation operators that only acts on the M_j mode. The relevant occupations are $\eta_j \in \mathbb{N}^{M_j}$, so they can arbitrarily large if we do

not add any restrictions. This is why we have to work with the algebras that conserve particle number, for this allows us to bound the spectrum of the bosonic operators.

Using a linear generator for the QFI,

$$\hat{O} = \sum_{m \in M} w(m) \hat{a}_m^\dagger \hat{a}_m \,, \tag{4.50}$$

we can reproduce the same steps as before to find multipartite entanglement bounds. However, there is a problem that needs to be accounted for. For a system with N bosons, the QFI is bounded by

$$F_Q[\hat{\rho}, \hat{O}] \leq \frac{N^2}{4} \Big(\max_{m \in M} w(m) - \min_{m \in M} w(m) \Big)^2 \,, \tag{4.51}$$

and this already realized by a 2-producible state. The reason is that the variance of the superposition $(\hat{a}_{m_{\max}}^\dagger)^N |\,\rangle + (\hat{a}_{m_{\min}}^\dagger)^N |\,\rangle$ already this maximum. Thus, we cannot get useful multipartite mode entanglement bounds, or at least not without some additional work.

The states that realize inequality (4.51) are analogous to *GHZ* spin states, and extremely fragile. By contrast, states that occur in experiments with bosonic atomic species will typically have a smoother particle number distribution. This constrains the occupations $\eta_j \in \mathbb{N}^{M_j}$ that actually occur in the system and allows one to derive multipartite entanglement bounds. After all, this has to be the case, given that experiments with bosonic species have already demonstrated the connection between multipartite entanglement and a metrological enhancement, e.g., using spinor BECs [192]. On the theoretical side, more systematic studies has been conducted for the spin-squeezing parameter and provide multipartite entanglement bounds [88, 193]. In these works, one has effective spins, so that the 2-producible bosonic states that realize inequality (4.46) can be disregarded. We can use our techniques to obtain multipartite entanglement bounds that apply to a more general setting, with arbitrary local occupation numbers.

Let us consider a bosonic system with fixed total particle number N, such that each mode m can be occupied by at most $n_m^{\max}$ particles. This is a generalization of the hard-core bosons case, and should provide an approximation of systems where typical local occupation numbers are bounded. In the hard-core limit, when all $n_m^{\max} = 1$, we can derive a multipartite mode entanglement bound using the same algorithm as the case fermionic case with conserved particle number. This follows from the same partition-optimization procedure, and we can construct optimal partitions for arbitrary local constraints $n_m^{\max}$.

The algorithm that constructs optimal partitions is given by:

procedure OPT($M, \mathrm{N}, w, \mathrm{n}^{\max}$)
  $M_\bullet \leftarrow M$
  $\mathrm{N}_\bullet \leftarrow \mathrm{N}$
  $j \leftarrow 1$
  while $M_\bullet \neq \varnothing$ **do**
    $M_j \leftarrow \varnothing$
    Move the $\lfloor k/2 \rfloor$ modes with highest $w(m)\mathrm{n}_m^{\max}$ from $M_\bullet$ to M_j
    $\mathrm{N}_j^u \leftarrow \sum_{m \in M_j} \mathrm{n}_m^{\max}$
    Move the $\lfloor k/2 \rfloor$ modes with lowest $w(m)\mathrm{n}_m^{\max}$ from $M_\bullet$ to M_j
    $\mathrm{N}_j^l \leftarrow \sum_{m \in M_j} \mathrm{n}_m^{\max} - \mathrm{N}_j^u$
    if $\left|\sum_{m \in M_j^l} w(m)\mathrm{n}_m^{\max}\right| \leq \left|\sum_{m \in M_j^u} w(m)\mathrm{n}_m^{\max}\right|$ **then**
      $\mathrm{N}_j \leftarrow \mathrm{N}_j^u$
    else
      $\mathrm{N}_j \leftarrow \mathrm{N}_j^l$
    end if
    if $\mathrm{N}_\bullet > \mathrm{N}_j$ **then**
      $\mathrm{N}_\bullet \leftarrow \mathrm{N}_\bullet - \mathrm{N}_j$
    else
      $\mathrm{N}_j \leftarrow \mathrm{N}_\bullet$
      $\mathrm{N}_\bullet \leftarrow 0$
    end if
    $j \leftarrow j + 1$
  end while
  while $\mathrm{N}_\bullet > 0$ **do**
    if $\mathrm{N}_\bullet > \mathrm{N}_j^u + \mathrm{N}_j^l - \mathrm{N}_j$ **then**
      $\mathrm{D} \leftarrow \mathrm{N}_j^u + \mathrm{N}_j^l - \mathrm{N}_j$
      $\mathrm{N}_j \leftarrow \mathrm{N}_j + \mathrm{D}$
      $\mathrm{N}_\bullet \leftarrow \mathrm{N}_\bullet - \mathrm{D}$
    else
      $\mathrm{N}_j \leftarrow \mathrm{N}_\bullet$
      $\mathrm{N}_\bullet \leftarrow 0$
    end if
    $j \leftarrow j - 1$
  end while
  return $\{M_j\}$ and $\{\mathrm{N}_j\}$
end procedure

It produces the same type of multipartite mode entanglement bounds as the

fermionic procedures, and can also be calculated efficiently for large quantum many-body systems. Thus, we have

$$\mathsf{F}_{\mathrm{Q}}\big[\hat{\rho}, \hat{\mathrm{O}}\big] \leq \sum_{\mathrm{N}} \mathsf{p}(\mathrm{N}) \underbrace{\sum_{j} \Big(\sum_{m \in M_j^u} w(m) - \sum_{m \in M_j^l} w(m) \Big)^2}_{\text{Optimal partition for N and } \mathrm{n}^{\max}}, \tag{4.52}$$

for all k-separable bosonic states with particle number conservation. This yields a tool for certifying bosonic multipartite mode entanglement in quantum many-body systems.

If the probabilities $\mathsf{p}(\mathrm{N})$ decay sufficiently fast, we can use inequality (4.52) to derive entanglement bounds for the QFI density in continuum systems. This can be done with a regularization procedure based on local constraints $\mathrm{n}_m^{\max} \approx \mathrm{n}(x)$ that depend on the particle density, and the systems volume. We began exploring this approach in the context of Latz's master thesis [109], but it has been expanded and refined since then. The results presented here, including the optimization algorithm, are the outcome of this refinement and we are currently exploring potential applications to atomic systems.

5 Application to a model of interacting fermions

The Fermi–Hubbard model is a paradigmatic model for strongly correlated electrons [150, 194]. It is known to reproduce various qualitative features of solid states systems, but its theoretical description is notoriously challenging. As such, it is a natural candidate for quantum simulation using ultracold atoms [57, 61]. Recent experiments with fermionic species have realized this and pave the way for exploring exotic solid state physics with atomic platforms [195–200]. This opens the possibility of using quantum simulation to characterize entanglement in systems of interacting fermions.

In this chapter, we present our results for the Fermi–Hubbard model. It showcases the techniques discussed in the previous two chapters and demonstrates their viability for current ultracold atoms experiments. Our numerical simulations demonstrate the presence of multipartite mode entanglement at finite temperatures across the phase diagram of the Fermi–Hubbard mode. They suggest a relation between the strongly correlated behavior and the presence of resilient multipartite entanglement. Additionally, we use this as an opportunity to illustrate some of the advantages of the quench protocol that were discussed in chapter 3. The contents presented here are based on our publication and include data taken from it [105].

The first section is a short introduction to the Fermi–Hubbard model, with special attention to its behaviour at large interaction strengths (see the review by Tarruell et al. for further details [61]). This provide us with some intuition about the physics of the model. And suggests which operators will yield good measures of fermionic mode entanglement. Afterwards, we present the numerical results for the QFI obtained with the quench protocol. Besides this, we also discuss some experimental issues and provide numerical results to corroborate the resilience of our quench protocol.

5.1 Fermi–Hubbard model

The Fermi–Hubbard model was introduced in 1960s as a tool to study interacting electrons in metallic systems [201–203]. It displays various nontrivial features and operates as a toy model for more elaborate solid state models. In its simplest version, it describes interacting spin-half fermions in a lattice with nearest neighbour tunneling and a on-site interaction. This corresponds to a tight-binding approximation, whose localized modes correspond to Wannier functions [204], with a cutoff that limits the interaction range.

We consider the one dimensional case of an open chain of size L, so that the fermions live on lattice sites $x = 1, 2, \ldots L$ and have two internal states, $s = \uparrow, \downarrow$. In a ultracold atoms setup, this can be realized with an optical lattice and two addressable atomic levels. The Hamiltonian is given by

$$\hat{\mathrm{H}} = -J \sum_{xs} (\hat{\mathrm{c}}^\dagger_{xs} \hat{\mathrm{c}}_{x+1s} + \mathrm{h.\,c.}) + U \sum_x \hat{\mathrm{n}}_{x\uparrow} \hat{\mathrm{n}}_{x\downarrow} \,, \tag{5.1}$$

where the first term is the kinetic contribution, coupling adjacent sites, and the second corresponds to a on-site interaction potential, which can be attractive or repulsive (see figure 5.1).

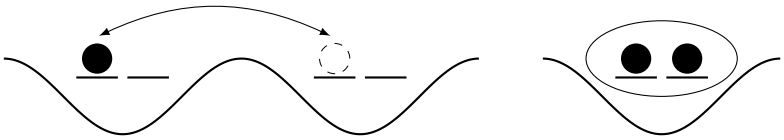

(a) Kinetic energy (b) On-site interaction

Figure 5.1: Diagrammatic representation of the contributions to equation (5.1). The dynamics of the system are defined by the competition between the kinetic energy, diagonal in momentum space, and the on-site interaction, diagonal in real space.

If $U = 0$ then equation (5.1) becomes a free theory, and the $s = \uparrow$ sector decouples from $s = \downarrow$. In momentum space we have

$$\hat{\mathrm{H}}|_{U=0} = \sum_{ks} \varepsilon_k \hat{\mathrm{c}}^\dagger_{ks} \hat{\mathrm{c}}_{ks} \,, \tag{5.2}$$

where $\hat{\mathrm{c}}_{ks} = \sqrt{(1/L)} \sum_x e^{+ikx} \hat{\mathrm{c}}_{xs}$ and $\varepsilon_k = 2J \cos x$, as usual. So that the eigenstates are localized in momentum space. By contrast, for $J = 0$, equation (5.1) is already diagonal and the eigenstates are localized in real space.

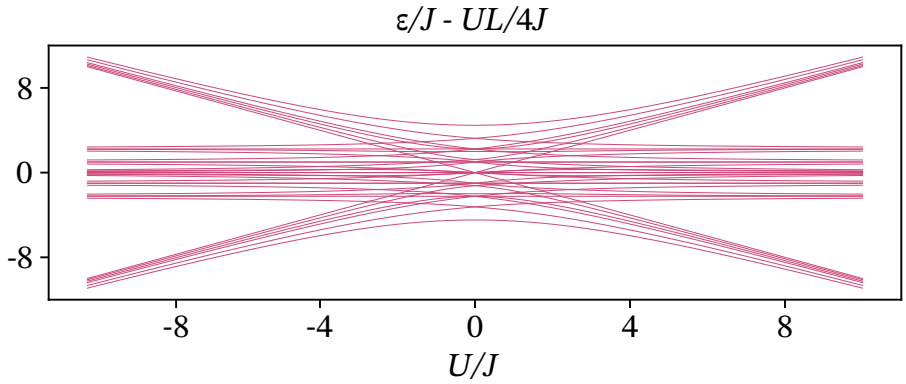

Figure 5.2: Spectrum of a Fermi–Hubbard model with $L = 4$ at half-filling with no magnetic field. The system develops separate bands for large $|U|$ that effectively decouple due to energy gap. The effective antiferromagnetic Hamiltonian of equation (5.4) describes the physics within each band. We add an energy shift proportional to U to make the duality of the system evident. Data was obtained with exact diagonalization.

The occupation number, $\hat{\mathrm{N}} = \sum_x (\hat{\mathrm{n}}_{x\uparrow} + \hat{\mathrm{n}}_{x\downarrow})$, and the magnetic field, $\hat{\mathrm{M}} = \sum_x (\hat{\mathrm{n}}_{x\uparrow} - \hat{\mathrm{n}}_{x\downarrow})$, are conserved by equation (5.1) so we can fix their values. Moreover, the system has particle–hole symmetry, which we can use to our benefit. It allows us to define a duality that relates the repulsive and attractive regime [61]. The transformation is defined by its action on the $s = \downarrow$ sector,

$$\hat{\mathrm{c}}_{x\downarrow} \mapsto (-1)^x \hat{\mathrm{c}}^\dagger_{x\downarrow} , \tag{5.3}$$

and acts trivially for $s = \uparrow$. If we define the doping with respect to half-filling as $\mathrm{D} = \mathrm{N} - L$, then we have a duality between the repulsive and attractive sides that swaps D and M. Therefore, it is sufficient to calculate properties on one side of the phase diagram, since they can be translated to the other side.

5.1.1 Effective description for large interactions

Let us consider the infinitely repulsive limit $U \gg J$ to get a better handle on the physics of the model. Due to the repulsive interaction, the Hamiltonian will prevent pairs from forming. In the half-filling case with no magnetization, $\mathrm{N} = L$ and $\mathrm{M} = 0$, this means that there will be a ground state manifold defined by all possible configurations of the system with only one particle per site. In the opposite limit, when U goes to negative infinity, low energy states will contain

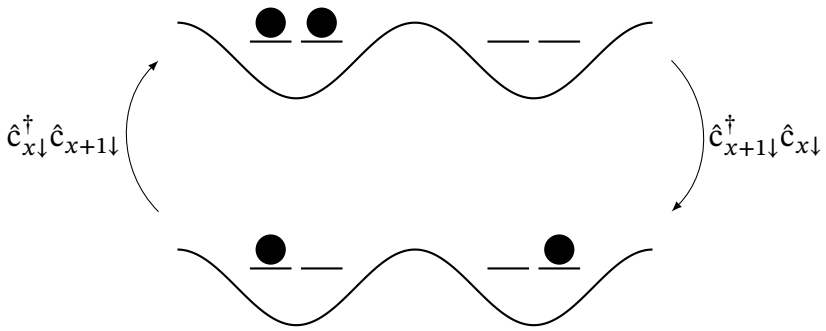

Figure 5.3: Second order perturbative corrections to $U \to \pm\infty$ regime, come from transitions like the one depicted here. The blockage of this process induces the antiferromagnetic interaction of equation (5.4). In the repulsive regime, the bottom state is the low energy one and the one above corresponds to an excitation of energy $|U|$. This is reversed in the attractive case.

as many pairs, created by $\hat{c}^\dagger_{x\uparrow}\hat{c}^\dagger_{x\downarrow}$, as possible. Thus, the ground state manifold will contain all possible permutations of the positions of the pairs. See figure 5.2 for a depiction of the energy levels of the system across the phase diagram. It displays the ground state manifolds for $|U| \gg J$ and the excited bands.

Hence, in the repulsive regime, the density degree of freedom $\hat{n}_{x\uparrow} + \hat{n}_{x\downarrow}$ is frozen and all dynamics occur in the spin sector $\hat{n}_{x\uparrow} - \hat{n}_{x\downarrow}$. The opposite happens in the attractive case, consistent with particle–hole symmetry. It is an manifestation of of spin–charge separation and fractionalization [205] This is a hallmark feature of one dimensional interacting systems and it is predicted by the theory of Tomonaga–Luttinger liquids [206–209]. It has been observed in ultracold atoms experiments with the help of quantum gas microscopy [200].

We can calculate the corrections for finite $|U|$ with perturbation theory. The first correction is of second order and comes from the process depicted in figure 5.3. It results in an antiferromagnetic effective Hamiltonian,

$$\hat{H}_{\text{eff}} \approx \frac{4J^2}{|U|} \sum_x \hat{S}_x \cdot \hat{S}_{x+1} \,, \tag{5.4}$$

where $\hat{S}_x = 1/2 \sum_{n=x,y,z} (\hat{c}^\dagger_{x\uparrow}\ \hat{c}^\dagger_{x\downarrow}) \hat{\sigma}^n_x (\hat{c}_{x\uparrow}\ \hat{c}_{x\downarrow})^T$ is the effective spin vector. The ground states are two-fold degenerate and defined by alternating spin (density) and constant density (spin) in the repulsive (attractive) regime. The antiferromagnetic order has already been observed experimentally in experiments with ultracold atoms [197, 199, 210]. Higher bands correspond to the creation of doublon–holon excitations (breaking of pairs) in the repulsive (attractive) side.

On the attractive side, one can lift the degeneracy in the perturbative regime by applying a spatially modulated shift in the chemical potential. It amounts to

$$\hat{H} \to \hat{H} - \sum_x \mu_x(\hat{n}_{x\uparrow} + \hat{n}_{x\downarrow}) = \hat{H} - q\hat{O}_- \tag{5.5}$$

with a staggered pattern $\mu_x = (-1)^x q$ and $\hat{O}_- = \sum_x (-1)^x(\hat{n}_{x\uparrow} + \hat{n}_{x\downarrow})$. If q is sufficiently small, this will select a reference ground state, but it will not couple the low energy manifold to high energy states. The same strategy applies to the repulsive case, with the spin degree of freedom instead, so we consider

$$\hat{H} \to \hat{H} - \sum_x m_x(\hat{n}_{x\uparrow} - \hat{n}_{x\downarrow}) = \hat{H} - q\hat{O}_+ \tag{5.6}$$

where $\hat{O}_+ = \sum_x (-1)^x(\hat{n}_{x\uparrow} - \hat{n}_{x\downarrow})$ is an alternating magnetic field.

5.2 Numerical results at half-filling

In this section we apply the quench protocol of chapter 3 to the Fermi–Hubbard chain. Thus, we consider a system in thermal equilibrium in the canonical ensemble with an inverse temperature $\beta = 1/T$. The occupation number is fixed to half-filling and the magnetization to zero. To simulate the quench protocol of section 3.2, we consider two generators given by equations (5.5) and (5.6). The motivation is that, as we move from the large interactions regime to $|U| \approx J$, the system will develop fluctuations that destroy the effective description. This suggests that these generators should have a high metrological sensitivity [39]. And that they provide a good probe for multipartite entanglement.

We extract the cumulative response function $\xi(\tau) = \Delta\hat{O}_{\text{quench}}(\tau)/q$ from exact diagonalization by simulating an abrupt quench. This provides the full response, including non linear corrections, and we obtain the linear part by considering sufficiently weak quenches. Integrating with the appropriate filter, yields the QFI as a function of U/J and T/J. The results are summarized in figures 5.4 and 5.5. And demonstrate the presence of multipartite entanglement at finite temperatures.

Figure 5.5 shows the presence of multipartite entanglement that is resilient to thermal fluctuations in the intermediary region $|U| \approx J$. By contrast, entanglement in the perturbative regime decays quickly as the temperature increases. This is because it is related to a fragile GHZ-like ground state that develops due to finite size effects and . Figure 5.6 contain a cut for fixed temperature where this effect is shown clearly.

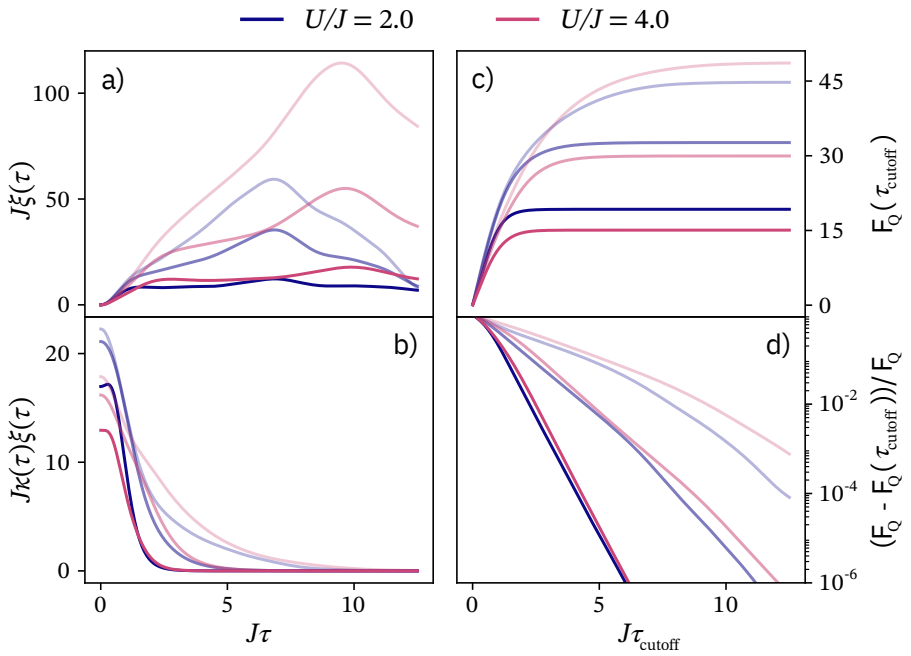

Figure 5.4: Quench protocol for QFI extraction, exemplified at temperatures $T/J = 0.2,\ 0.4,\ 0.8$ (from light to dark shades) for a quench with the staggered magnetization. (a) At time $\tau = 0$, the system is quenched with the operator $\hat{O}_+$ and strength q. Measuring $\langle \hat{O}_+(\tau) \rangle$ and the deviations from the equilibrium expectation value yields the cumulative response function. (b) Using equation (3.43), the QFI can be computed by integrating with the filter function defined by equation (3.45). (c) Cutting off the integral at time τ_{cutoff} produces the lower bound of inequality (3.46). (d) Due to the functional form of $\kappa(\tau) = \kappa_{\text{quench}}(\tau)$, the convergence is exponentially fast with a decay constant set by the temperature, $\mathsf{F}_\mathsf{Q} - \mathsf{F}_\mathsf{Q}(\tau_{\text{cutoff}}) \sim \exp(-\pi T \tau_{\text{cutoff}})$.

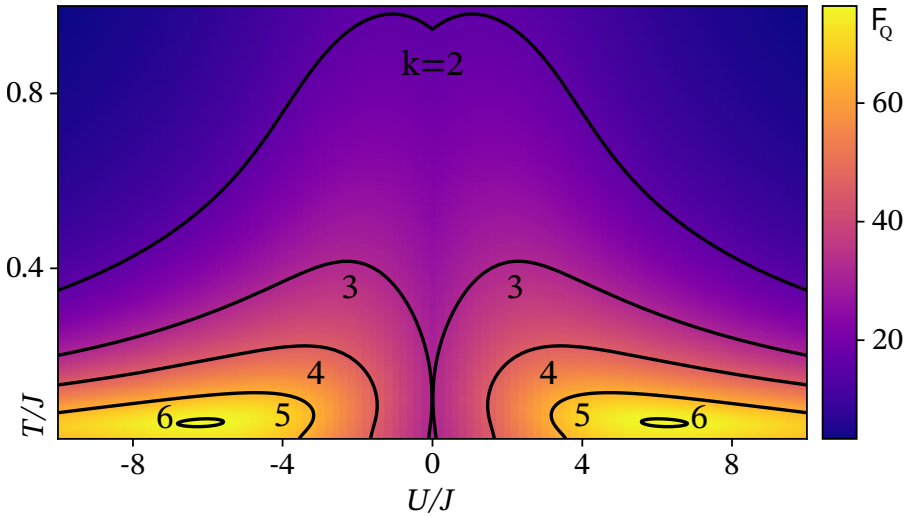

Figure 5.5: Heatmap showing the QFI across the phase diagram. It is calculated using the best generator out of $\hat{O}_{\pm}$. Contour lines show the multipartite entanglement bounds obtained in section 4.2.2 for a fixed particle number. Many-body entanglement is certified up to large temperatures. Data for a chain with $L = 8$.

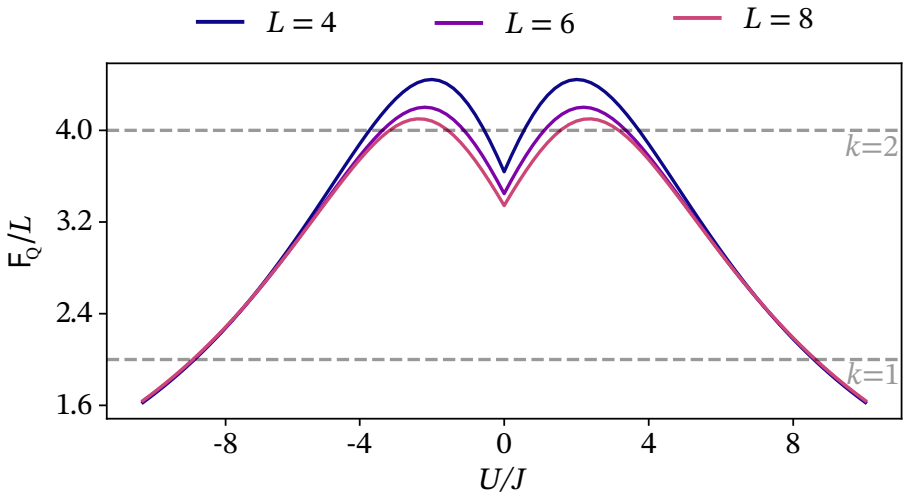

Figure 5.6: QFI density for different system sizes at $T/J = 0.4$ with thresholds for certifying entanglement (dotted lines). Multipartite entanglement is detected in the intermediate region, and the system-size dependence suggests the entanglement is especially robust in it, making it a prime candidate to search for experimental signatures of multipartite entanglement.

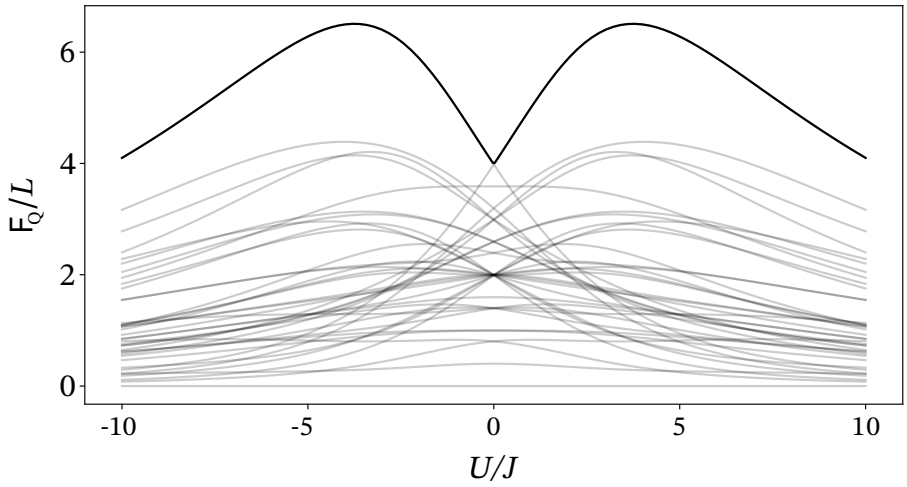

Figure 5.7: Optimization of the QFI generator for fermionic mode entanglement bounds for a chain of size $L = 4$. QFI computed from exact diagonalization for all linear operators with amplitude $w_{xs} = \pm 1$. The dark line denotes the optimized QFI, whereas the gray curves are the QFI for the various generators. It corresponds to the staggered magnetization $\hat{O}_+$ for $U/J > 0$ and to the staggered density $\hat{O}_-$ for $U/J < 0$. This corroborates the suitability of the physical intuition to use operators where large quantum fluctuations can be expected.

The choice of the generator $\hat{O}$ is critical for obtaining useful entanglement bounds. This is a known issue for the study of the QFI and, in general, finding the optimal operator is a computationally challenging task. And it remains a challenge with the restriction on the form of the operator required by the entanglement bounds. For our purposes, we consider a simplified case by considering

$$\hat{O} = \sum_{xs} w_{xs} \hat{n}_{xs} \tag{5.7}$$

with $w_{xs} \in \{-1, +1\}$. The reason for this choice is to consider operators with the same entanglement bound as $\hat{O}_\pm$. In this way, we can investigate the optimal operator for this entanglement bound. As seen in figure 5.7, the optimal operator for the Fermi–Hubbard chain is given by $\hat{O}_\pm$. This corroborates our initial intuition based on the behaviour of the system in the effective perturbative description. Of course, alternative options exist, such as the modulation $w_{xs} = \cos(k_s x + \varphi_s)$ that provides a generalization of the staggered density and magnetization.

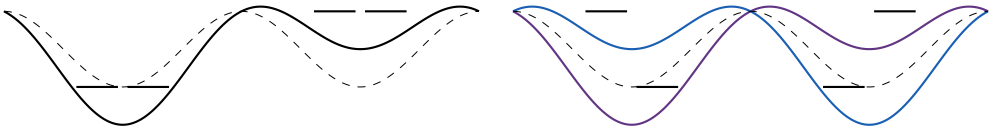

(a) Staggered chemical potential $\mu_x = (-1)^x q$

(b) Staggered magnetic field $m_x = (-1)^x q$

Figure 5.8: Realization of staggered quench specified in the previous section. This can be accomplished with a superlattice in the case of $\hat{O}_-$ to modulate the local chemical potentials in a staggered fashion. In the repulsive regime, it is necessary to use spin-dependent superlattices to modulate the local magnetic field.

5.3 Experimental considerations

Ultracold atoms are now reaching strongly-correlated many-body states of the Fermi–Hubbard model at temperatures as low as $T/J = 0.25$ [197, 199, 200], well within the region where multipartite entanglement can be detected (see figure 5.5). Moreover, as shown in figure 5.4, at such temperatures the QFI converges within few hopping events ($J\tau \lesssim 8$), i.e., on time scales faster than typical decoherence rates [200]. A quench with $\hat{O}_\pm$ amounts to abruptly modifying the chemical potential in a staggered fashion, which can be implemented with superlattices in a straightforward manner, without the need for quantum gas microscopes (see figure 5.8). The relevant observable $\langle \hat{O}_\pm(\tau) \rangle$ can be measured through site-dependent imaging using existing techniques [211–216]. Thus, our quench protocol enables the detection of multipartite entanglement within existing experimental setups.

Nonlinear effects are always present in the quench dynamics, but they are negligible for sufficiently small quench parameters. Figure 5.9 shows a systematic test of the extent to which nonlinear effection have to be accounted for in the QFI extraction. Specifically, it shows the outcome of the quench protocol when performed using quench parameters ranging from $-0.1J$ to $0.1J$. We see that even for $q/J \approx 10\%$, reasonable precision can be achieved for the QFI, with errors on the order of few percent at most. In particular, errors are limited to 5%, except for extreme values of interaction strength. Thus, one can reliably implement the protocol with a finite quench, and still obtain an accurate estimate for the QFI. This is compounded with the fact that the errors are negative, so the value obtained for the QFI can be safely used for entanglement certification. If necessary, accuracy can be further improved by taking several data points at

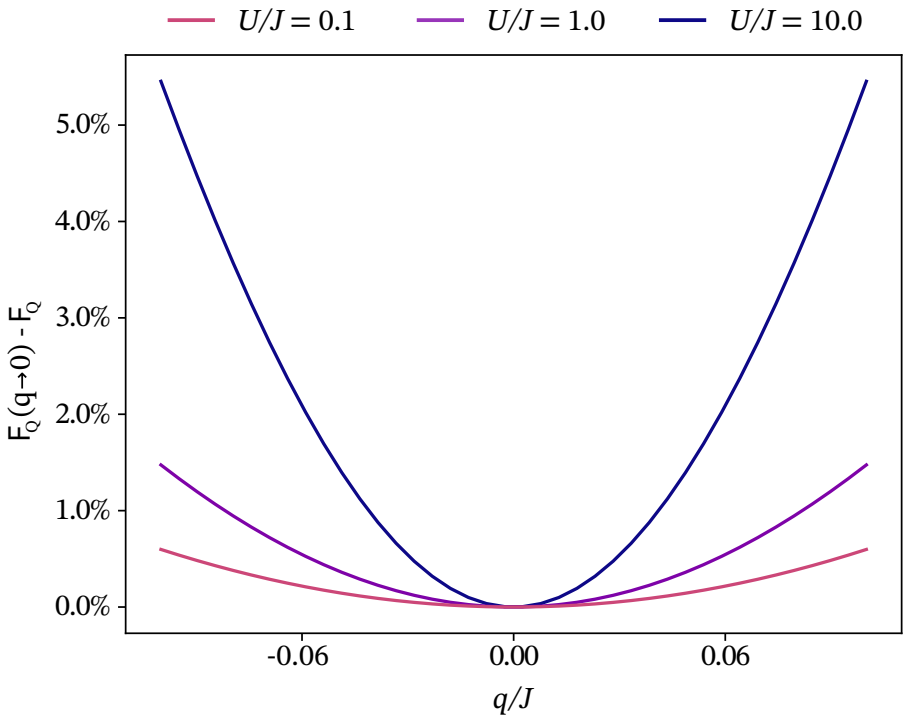

Figure 5.9: QFI extraction with different q for a chain with $L = 4$ at $T/J = 4.0$.. Deviations of $\Delta\hat{O}_{\text{quench}}(\tau)$ from the predictions of linear response theory lead to a q dependent value for F_Q. Here, the errors relative to the correct value are shown. A quadratic correction, coming from the $\Delta\hat{O}^{(3)}_{\text{quench}}(\tau)$ term, dominates at this scale and increases with interaction strength.

$q > 0$ and extrapolating to $q = 0$, as discussed in section 3.2.2.

5.3.1 Resilience against atom loss

Finally, the time evolution of the expectation value of $\hat{O}$ can be subject to decoherence. One strength of our proposal is that only measurements over exponentially short times are required and this significantly mitigates the effects of decoherence. As such, in an experiment with sufficient control so as to ensure a separation of scales, we expect our method to be resilient against deviations from the unitary quench dynamics proposed. Nonetheless, it is worht considering an example to test this hypothesis explicitly.

The time evolution of the system subjected to decoherence is governed by open quantum system dynamics. It can be described with a master equation

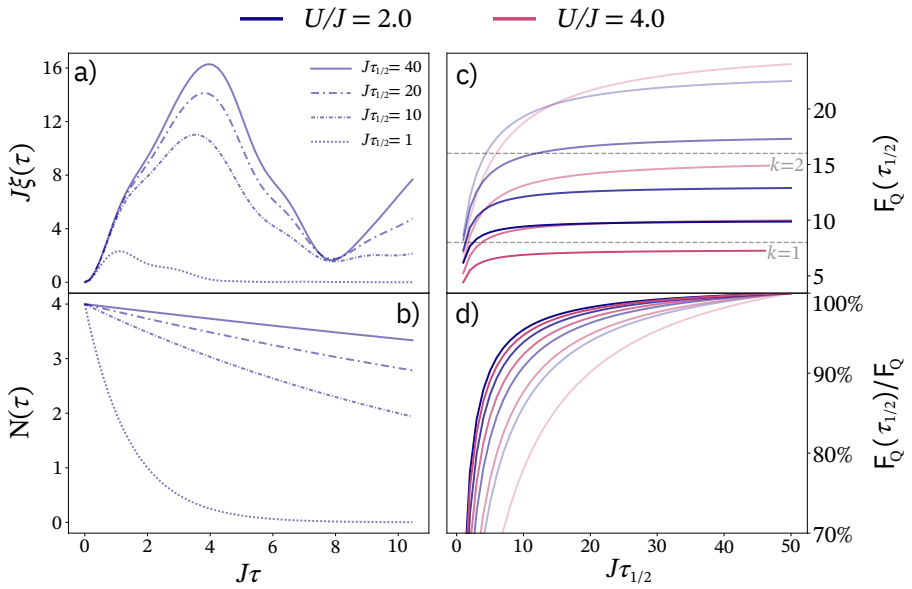

Figure 5.10: QFI extraction subjected to atom loss, exemplified with the the staggered magnetization $\hat{O} = \hat{O}_+$. Data for a chain of size $L = 4$ with temperatures $T/J = 0.2, 0.4, 0.6, 0.8$ (from light to dark shades). (a) As we increase the rate of atom loss (decreasing the half–life $J\tau_{1/2}$), $\xi(\tau)$ decreases but for moderate atom loss rates we retain the signal for short time scales. (b) Here, the rate of atom loss is parameterized by the half-life $\tau_{1/2}$, so that the number of atoms evolves according to $\hat{N}(\tau) = \hat{N}(0)2^{-\tau/\tau_{1/2}}$. (c) We see that entanglement certification is still possible for all but extremely high rates of atom loss $J\tau_{1/2} < 4$. (d) The extent to which the QFI is underestimated is limited to 70% for $J\tau_{1/2} \approx 10$ and only drops so much for the lowest temperatures.

in the Markovian case, which amounts to adding jump operators to the Von Neumann equation. We use this to model the experimentally relevant case of atom loss and perform numerical simulations. Figure 5.10 contains the results and demonstrates that entanglement certification can still be performed on systems subjected to sizable loss. Decoherence coming from atom loss also has the benign property of only decreasing the value obtained for the QFI which prevents any false positives for entanglement certification. We also observe that the QFI for $U/J = 2.0$ is more resilient to atom loss then that of $U/J = 4.0$. This is consistent with the observation that, qualitatively, the entanglement in the strongly correlated region appears to be more robust.

6 Entanglement witnesses for lattice gauge theories

In this chapter, we present our results related to entanglement in lattice gauge theories, and demonstrate how to construct entanglement witnesses for them. This extends the existing framework of entanglement witnesses, typically employed in systems consisting of qubits, to gauge invariant states. It enables the detection of entanglement in lattice gauge theories with simple expectation values of physically accessible observables. As such, it has a considerable advantage over entanglement measures such as the entanglement entropy, which requires knowledge of the physical state that grows exponentially with system size. Thus, we provide an efficient and scalable framework for accessing entanglement in lattice gauge theories.

The interest in studying entanglement in lattice gauge theories, and in gauge theories more generally, is manifold. First, there is evidence that entanglement plays a role in the thermalization and equilibration of gauge theories [217–220], an important topic in the field of high-energy physics. More broadly, given their prominent role as building blocks of the standard model, gauge theories are a natural setting to explore synergies between high-energy physics and quantum information science. Another motivation arises from the rapid development of quantum simulation platforms, and the prospect of realizing a lattice gauge theory in a tabletop experiment [221–228]. Additionally, lattice gauge theories are related to topological quantum computation, and provide the basic models for topological states of matter [41, 229, 230].

From a theoretical standpoint, the application of measures of entanglement to lattice gauge theories has received considerable attention in recent years [101–104, 231–236]. In particular, because the presence of local conservation laws—such as Gauss' law—introduces major subtleties that are of theoretical interests. It gives rise to superselection sectors for the algebra of gauge invariant observables, and this must be accounted by any characterization of entanglement [101, 237]. Here, we employ the formalism introduced in section 2.4, which was used in chapter 4, to achieve this. In particular , It enables us to construct entanglement witness, which are well suited for applications in future experiments performing quantum simulation of lattice gauge theories.

6.1 Lattice gauge theories

Lattice gauge theories are discretized versions of continuum gauge theories defined over a lattice. They were originally introduced by Wilson [238] as a tool to investigate confinement in QCD , and have since found applications in many areas of physics. The basic idea is to model gauge fields using local degrees of freedom assigned to the edges of a lattice [239]. Additionally, an action, or a Hamiltonian, has to be constructed for the lattice in a way that is consistent with the underlying gauge symmetry.

Let us consider a two dimensional square lattice L for concreteness. Wilson loops define canonical gauge invariant degrees of freedom associated to plaquettes of the lattice. They are given by

$$\mathrm{W}[\Gamma_p] = \mathsf{Tr}\Big(P \exp i \oint_{\Gamma_p} \mathrm{d}x^\mu A_\mu\Big) \approx \mathsf{Tr}\Big(\mathrm{U}_{v_0 v_1} \mathrm{U}_{v_1 v_3} \mathrm{U}^\dagger_{v_2 v_3} \mathrm{U}^\dagger_{v_0 v_2}\Big)\,, \tag{6.1}$$

where the integral in equation (6.1) runs over the path $\Gamma_p = \partial p$ outlined by the boundary of the plaquette p. Each U_{vw} amounts to a parallel transport along the edge connecting vertices v and w. Here we assume that there is a irreducible representation of the gauge group G, so that the trace is taken with respect to this representation. The gauge symmetry acts on the U_{vw} degrees of freedom according to

$$\mathrm{U}'_{vw} = \exp\big(+i\alpha_a(v)\lambda^a\big)\mathrm{U}_{vw} \exp\big(-i\alpha_a(w)\lambda^a\big)\,, \tag{6.2}$$

with generators of the symmetry λ^a and an implicit sum over the internal indices a. This gives rises to the Wilson action,

$$S(\mathrm{U}) = -\sum_p \mathsf{Re}\,\mathsf{Tr}\big(\mathrm{U}_{v_0 v_1} \mathrm{U}_{v_1 v_3} \mathrm{U}^\dagger_{v_2 v_3} \mathrm{U}^\dagger_{v_0 v_2}\big)\,, \tag{6.3}$$

which is manifestly gauge invariant. Equation (6.3) is a discretization of the well known Yang–Mills action [240]. As such, it realizes a lattice gauge theory with the plaquette contributions playing the role of the field strength $F^a_{\mu\nu}$.

Besides the action formulation, it is possible to obtain a Hamiltonian formulation of lattice gauge theories [241]. This will be more convenient for our purposes, so we follow this approach from now on. In particular, we consider quantum link models [242]. They provide a Hamiltonian formulation of lattice gauge theories that extends the Wilsonian description and are particularly well suited for quantum simulation [243]. We provide a quick review to introduce the main ingredients following Chandrasekharan et al. [242].

6.1.1 Quantum link models

To define quantum link models, we start with a description that is not gauge invariant and reconstruct a gauge invariant sector from it. We assign local Hilbert space to the edges of the lattice such that we have a global Hilbert space given by

$$\mathcal{H}_L = \bigotimes_{vw \in L_1} \mathcal{H}_{vw} \cong \mathbb{C}^{d^{|L_1|}} , \tag{6.4}$$

where L_1 denotes the set of edges of lattice, and we assume each local degree of freedom is a qudit of dimension d. The parallel transporters amount to G-valued operators $\hat{\mathrm{U}}_{vw}$ acting on this Hilbert space and we can write a Hamiltonian

$$\hat{\mathrm{H}} = \frac{J}{2} \sum_{p \in L_2} \left(\mathsf{Tr}\big(\hat{\mathrm{U}}_{v_1 v_2} \hat{\mathrm{U}}_{v_2 v_4} \hat{\mathrm{U}}^{\dagger}_{v_3 v_4} \hat{\mathrm{U}}^{\dagger}_{v_1 v_3}\big) + \mathrm{h.\,c.} \right) , \tag{6.5}$$

where, once again, the trace is taken with respect to the representation of the group.

Gauge transformations are realized by local generators $\hat{\mathrm{G}}^a_v$ associated to the vertices of the system. They transform parallel transporters according to

$$\hat{\mathrm{U}}'_{vw} = \exp\big(+i\alpha_a(v)\hat{\mathrm{G}}^a_v\big)\hat{\mathrm{U}}_{vw} \exp\big(-i\alpha_a(w)\hat{\mathrm{G}}^a_w\big) , \tag{6.6}$$

which is the analogue of equation (6.2). More generally, we can define a path operator $\hat{\mathrm{U}}_\Gamma$ associated to each path Γ by

$$\hat{\mathrm{U}}_\Gamma = P \prod_{vw \in \Gamma} \hat{\mathrm{U}}_{vw} = \hat{\mathrm{U}}_{v_0 v_1} \hat{\mathrm{U}}_{v_1 v_2} \ldots \hat{\mathrm{U}}_{v_{l-2} v_{l-1}} \hat{\mathrm{U}}_{v_{l-1} v_l} , \tag{6.7}$$

and it will also transform according equation (6.6) if we take $v = v_0$ and $w = v_l$ as the end points of the path. Thus, the operators associated to Wilson loops $\hat{\mathrm{W}}_\Gamma = \mathsf{Tr}_G\, \hat{\mathrm{U}}_\Gamma$ are gauge invariant due to the cyclic property of the trace.

The relevant algebra of operators of the quantum link model is

$$\begin{aligned} [\hat{\mathrm{G}}^a_v, \hat{\mathrm{G}}^b_w] &= \delta_{vw} f_{abc} \hat{\mathrm{G}}^c_v \\ [\hat{\mathrm{U}}_{vw}, \hat{\mathrm{G}}^a_v] &= \lambda^a \hat{\mathrm{U}}_{vw} \\ [\hat{\mathrm{U}}_{vw}, \hat{\mathrm{G}}^a_w] &= \hat{\mathrm{U}}_{vw} \lambda^a , \end{aligned} \tag{6.8}$$

where f_{abc} are the structure constants of the underlying Lie algebra, i.e., they are defined by $[\lambda^a, \lambda^b] = f_{abc}\lambda^c$. The first commutation relation arises since the gauge symmetry should define a local representation of G, so that its generators define a representation of the corresponding Lie algebra. Equation (6.6) is equivalent to

second commutation relation as it defines how the parallel transporters transform after an infinitesimal gauge transformation. Combined, these commutation relations generate the algebra that is necessary to implement the lattice gauge theory. In particular, the algebra of gauge invariant operators is given by

$$\mathcal{A}(L)_G = \left\{ \hat{O} \in \mathcal{B}(L) \mid \forall a \forall v \, [\hat{O}, \hat{G}_v^a] = 0 \right\}, \tag{6.9}$$

and it defines the physical observables of the theory. Of course, it is necessary to obtain a concrete representation of this algebra to get an actual model. This is relatively straight forward for abelian groups, and we will describe the procedure in detail for the U(1) gauge group. However, the basic idea applies more generally and one can also construct quantum link models for for non-abelian theories, such as QCD with the SU(3) gauge group [244].

6.1.2 Example: U(1) quantum link model

If we consider $G = \mathrm{U}(1)$, then the Lie algebra is trivial and we only have one generator $\lambda \cong 1$, so we can drop the group representation indices. Equation (6.8) simplifies and the only nontrivial commutation relations are

$$\begin{aligned} [\hat{U}_{vw}, \hat{G}_v] &= \hat{U}_{vw} \\ [\hat{U}_{vw}, \hat{G}_w] &= -\hat{U}_{vw} \, . \end{aligned} \tag{6.10}$$

This can be realized with a spin algebra, so we assume that each local degree of freedom $\mathcal{H}_{vw}$ corresponds to a spin.

We fix the z component of the spin as the preferred direction which we use to define the gauge generators. Employing this convention, the generators are

$$\begin{aligned} \hat{G}_v &= \sum_{vw \in L_1} \hat{S}^z_{vw} - \sum_{wv \in L_1} \hat{S}^z_{wv} \\ &= \hat{S}^z_{vw_1} + \hat{S}^z_{vw_2} - \hat{S}^z_{w_3 v} - \hat{S}^z_{w_4 v} \, , \end{aligned} \tag{6.11}$$

where we sum over edges attached to v with a ± 1 factor accounts to account for the relative orientation. This is necessary to compensate for the different signs in equation (6.10). For a two dimensional square lattice this reduces to four contributions, two positive ones coming from incoming edges, and two negative ones from the outgoing edges.

The Hamiltonian commutes with the gauge generators by construction, because it has to be gauge invariant. Furthermore, since the group is abelian, the generators commute amongst themselves, i.e., they are gauge invariant. This allows us to associate a physical observable to the contributions to $\hat{G}_v$ coming

from each edge. They are the electric field of the theory and we write $\hat{\mathrm{E}}_{vw} = \hat{\mathrm{S}}^z_{vw}$ to denote this. It follows that each generator amounts to the electric flux across a curve—which acts as Gaussian surface—circling around the vertex. Moreover, we can enforce constraint coming from Gauss' law,

$$\hat{\mathrm{G}}_v|\,\psi\rangle = \big(\hat{\mathrm{E}}_{vw_1} + \hat{\mathrm{E}}_{vw_2} - \hat{\mathrm{E}}_{w_3v} - \hat{\mathrm{E}}_{w_4v}\big)|\,\psi\rangle = 0\,, \tag{6.12}$$

by setting the background charges to zero. This procedure defines the physical states of the theory and the corresponding Hilbert space,

$$\mathcal{H}^{\mathrm{G}}_L = \big\{|\,\psi\rangle \in \mathcal{H}_L \mid \forall v\ \hat{\mathrm{G}}_v|\,\psi\rangle = 0\big\}\,, \tag{6.13}$$

as an eigenspace of the gauge generators.

If we compare equation (6.10) to the commutation relations of spin operators, it becomes clear how to represent the parallel transporters. They correspond to spin raising operators $\hat{\mathrm{U}}_{vw} = \hat{\mathrm{S}}^+_{vw}$ and, in the reverse direction, to spin lowering operators $\hat{\mathrm{U}}_{wv} = \hat{\mathrm{U}}^\dagger_{vw} = \hat{\mathrm{S}}^-_{vw}$. Thus, the plaquette operators are given by

$$\hat{\mathrm{U}}_p = \hat{\mathrm{U}}_{\Gamma_p} = \hat{\mathrm{S}}^+_{v_1v_2}\hat{\mathrm{S}}^+_{v_2v_4}\hat{\mathrm{S}}^-_{v_3v_4}\hat{\mathrm{S}}^-_{v_1v_3}\,, \tag{6.14}$$

and more general Wilson loops arise from the similar expressions.

Fixing $d = 2$, so that the consider spin half, it is possible to get a clear picture of the action of the relevant operators. In particular, we can represent the electric field by its relative orientation to the orientation of the lattice. This is because it can only assume two values. With this convention, equation (6.12) implements the so called two-in-two-out rule. This means that in a physical configuration, each vertex always has two incoming and two outgoing electric fields. The plaquette operator action depends on the orientation of the electric field along the boundary of the plaquette. If there is a well-defined clockwise orientation, $\hat{\mathrm{U}}_p$ flips the orientation of the plaquette, otherwise it annihilates the state. The hermitian conjugate $\hat{\mathrm{U}}^\dagger_p$ acts similarly, but with respect to the opposite orientation. Motivated by this, we introduce

$$\hat{\mathrm{X}}_p = \frac{1}{2}\big(\hat{\mathrm{U}}_p + \hat{\mathrm{U}}^\dagger_p\big) \tag{6.15}$$

which is the operator that flips the orientation of the plaquette. Notice that it is this operator that contributes to the Hamiltonian.

6.2 Separability and gauge symmetries

As we have seen in previous chapters, the algebras of local operators are the fundamental objects that inform the requirements for a well defined separability

criteria. In particular, it is the local net of observables that dictates the enforcement of the factorization condition. If the observables of the algebra have to fulfill certain constraints, due to selection or superselection rules, the factorization condition becomes weaker, and defines a larger set of separable states. This is the case for a lattice gauge theory, since the presence of local conservation laws introduces an extensive number of constraints. With this insight, we are ready to discuss the notion of separability in lattice gauge theories, which will present the theoretical basis for constructing entanglement witnesses for such systems. Our methods apply to general lattice gauge theories, but we will formulate them for the $\mathsf{U}(1)$ case to keep the notation concise.

The first step is to define the local net of observables. This is relatively straight forward because we can regard any subregion of the lattice $R \subset L$ as a subsystem. We assign the algebra of gauge invariant operators with support in R to it. Thus,

$$\mathcal{A}(R)_G = \left\{ \hat{\mathrm{O}} \in \mathcal{B}(R) \mid \forall v \, [\hat{\mathrm{O}}, \hat{\mathrm{G}}_v] = 0 \right\}, \tag{6.16}$$

where we regard $\mathcal{B}(R)$ as a subalgebra of $\mathcal{B}(L)$ in the usual way[1]. Concretely, $\mathcal{A}(R)_G$ is generated by the plaquette operators of plaquettes inside R, and the electric field operators of edges inside it.

With the local net of observables, we can formulate the separability criteria and define entanglement. The aim here is to detect entanglement between two subsystems A and B (see figure 6.2). Therefore, we consider the following factorization condition

$$\langle \hat{\mathrm{O}}_A \hat{\mathrm{O}}_B \rangle_{\hat{\rho}} = \langle \hat{\mathrm{O}}_A \rangle_{\hat{\rho}} \langle \hat{\mathrm{O}}_B \rangle_{\hat{\rho}} = \langle \hat{\mathrm{O}}_A \rangle_{\hat{\rho}_A} \langle \hat{\mathrm{O}}_B \rangle_{\hat{\rho}_B}, \tag{6.17}$$

for all $\hat{\mathrm{O}}_A \in \mathcal{A}(A)_G$ and $\hat{\mathrm{O}}_B \in \mathcal{A}(B)_G$. Notice that A and B do not define a partition of the system, so what we are considering are the quantum correlations inherited by the two subsystems from the global state. Nonetheless, we can easily define a partition by introducing the complement subsystem $C = L \setminus (A \cup B)$, but we are not interested in the observables acting on it. For simplicity, A and B are taken to be two disjoint subregions whose boundaries do not touch directly. This avoids subtleties that occur when dividing a lattice gauge theory into subsystems whose boundaries touch [101, 102, 104, 235]. And it will simplify some discussions and computations later on. Notice that only gauge invariant states are allowed, in the full lattice and also in the subregions, and this guaranteed automatically by the algebraic formalism.

As we shall see, the algebras $\mathcal{A}(A)_G$ and $\mathcal{A}(B)_G$ have nontrivial centers, which induce superselection rules. From the perspective of an observer who lives within

[1] The embedding of $\mathcal{B}(R)$ into $\mathcal{B}(L)$ is the same map described in chapter 2 for the qudit case. Specifically, it maps $\bigotimes_{vw \in R_1} \hat{\mathrm{O}}_{vw}$ into $\bigotimes_{vw \in L_1} \hat{\mathrm{O}}_{vw}$ with $\hat{\mathrm{O}}_{vw} = \hat{\mathrm{I}}_{vw}$ if $vw \notin R_1$

the lattice gauge theory, it is not possible to observe coherence between different sectors. This is because, from this point of view, the gauge symmetry constitutes a fundamental, and inescapable, aspect of the system, so only gauge invariant observables are admissible. However, this is in sharp contrast with physical realizations that may exist, e.g., in an actual laboratory device that performs a gauge theory quantum simulation. An outside experimenter may apply certain rotations on the qubits constituting the device or perform measurements in basis that are incompatible with Gauss' law, which observers within the gauge theory cannot access. Such a procedure might introduce coherence between different superselection sectors. However, this should be disregarded from the point of view of the gauge theory, for it does not translate into nontrivial quantum correlations for gauge invariant observables.

6.2.1 Superselection sector and the center

Equation (6.17) defines the analogues of product states, but it does so implicitly. To be able to compute property of separable states, and derive ways of detecting entangled states, we need a more concrete description. As in the case of fermions, we cannot rely on simple tensor product structure, because such a decomposition does not exist for lattice gauge theories. After all, $\mathcal{H}_L^G$ cannot decompose into a simple tensor product because any such decomposition would violate Gauss' law. This a direct consequence of the defining characteristic of a gauge theory, i.e., the presence of a local gauge symmetry. More specifically, it arises due to the presence of superselection rules, and we need to understand these rules to characterize the separable states.

The superselection rules arise as consequence of the presence of a non-trivial center [101]. In fact, this is precisely the obstruction to the existence of tensor product decomposition and we can use this to our advantage. To make this concrete, let us consider the center of A,

$$\begin{aligned} \mathcal{Z}(A) &= \mathcal{A}(A)_G \cap \mathcal{A}(A)'_G \\ &= \left\{ \hat{Z} \in \mathcal{A}(L)_G \mid \forall \hat{O}_A \in \mathcal{A}(A)_G \;\; [\hat{Z}, \hat{O}_A] = 0 \right\}, \end{aligned} \tag{6.18}$$

and try to identify the nontrivial elements. The first guess would be the gauge generators, since they commute with every gauge invariant operator, but they act trivially on the physical states due to equation (6.12). As an alternative, consider the boundary ∂A and let us assume that it defines a closed loop. If we have a vertex $v \in \partial A$, then the operator $\hat{G}_v$ can be divided into two parts, one coming from the edges inside A, and another one associated to the edgers outside A. Therefore, we can write

$$\hat{G}_v = \hat{G}_{v|A} + \hat{G}_{v|R}\,, \tag{6.19}$$

where $\hat{G}_{v|A} \in \mathcal{A}(A)_G$ and $\hat{G}_{v|R} \in \mathcal{A}(R)_G$. Clearly, $\hat{G}_{v|R} \in \mathcal{A}(A)'_G$ since the operators in $\mathcal{A}(A)_G$ do not act on R. Moreover, Gauss' law implies $\hat{G}_{v|A} = -\hat{G}_{v|R}$ for physical states, so $\hat{G}_{v|A} \in \mathcal{A}(A)'_G$ as well. It follows that $\hat{G}_{v|A}$ is a nontrivial element of the center. The eigenvalues of such operators define superselection sectors for A, since no $\hat{O}_A \in \mathcal{A}(A)_G$ can couple different sectors. The same reasoning also applies to B, and R.

If we consider all $v \in \partial A$, we get a set of generators of the center of A obtained from the split Gauss' operators of equation (6.19). However, for our considerations, it is sufficient to consider some arbitrary set of generators, as long as they are known and act locally. So let us consider arbitrary operators $\hat{Z}_{i|A} \in \mathcal{Z}(A)$ and $\hat{Z}_{j|B} \in \mathcal{Z}(B)$ that generate their respective centers. The labels $i \in I$ and $j \in J$ are not important, but we should keep in mind that the number of labels is proportional to the size of the boundaries. Consider eigenvalues $Z_A = \{Z_{i|A}\}$ and $Z_B = \{Z_{j|B}\}$ for the generators, then we can write

$$\mathcal{H}_L^G = \bigoplus_{(Z_A, Z_R, Z_B)} \mathcal{H}_A^G(Z_A) \otimes \mathcal{H}_R^G(Z_R) \otimes \mathcal{H}_B^G(Z_B) \,, \tag{6.20}$$

where $\mathcal{H}_A^G(Z_A) \subset \mathcal{H}_A^G$ denotes the eigenspace associated to the eigenvalues Z_A, and analogously for R and B. Equation (6.20) holds because, inside the eigenspaces, the generators are proportional to the identity, so that they act trivially. As a consequence, there is no obstruction to a tensor decomposition within a fixed superselection sector.

The eigenvalues Z_R enter equation (6.20) to account for the presence of a nontrivial center of the remaining lattice. Additionally, there is an important caveat, namely the direct sum only runs over compatible combinations (Z_A, Z_R, Z_B) of superselection sectors. For instance, the shared boundary of A and R implies that the generators of $\mathcal{Z}(A)$ are related to operators in $\mathcal{Z}(R)$ so that the values of Z_A and Z_R are not independent (and mutatis mutandis for Z_B and Z_R). Hence, the compatibility rules between Z_B, Z_B and Z_R capture how one can glue gauge invariant states of the subregions to construct a global gauge invariant state. Moreover, it may happen that L itself has superselection rules In principle, this can be accounted for by Z_R, but it is more convenient to fix the global superselection sector from the start.

6.2.2 Representation of the reduced state

We can use equation (6.20) to characterize separable states in a more computational manner. In particular, inside each superselection sector, we have the standard tensor product structure, so we can use the usual formulas. This implies

that the restriction of separable states follows the standard formula after the projection into the eigenspaces. Hence, one can write a separable mixed state restricted to A and B as

$$\hat{\rho}_{A\cup B} = \bigoplus_{(Z_A,Z_B)} p(Z_A,Z_B)\hat{\rho}_A(Z_A)\hat{\rho}_B(Z_B)\,, \tag{6.21}$$

where the direct sum runs over compatible superselection sectors (compare to equation (26) in referece [101]). The distribution of the state into superselection sectors is inherited from the global state and encoded into the probabilities $p(Z_A, Z_B)$.

States described the equation above are exactly those that fulfil the factorization condition in equation (6.17). In some sense, this turns the approach typical of tensor product Hilbert spaces around, where first separability is defined on the state level from which then consequences on observables follow. Importantly, equation (6.21) does not imply that the overall Hilbert space is a tensor product. Specially as the non-trivial structure of equation (6.20) manifests itself through the consistency relations among the different sectors. In any case, we can use equation (6.21) as way to test if a state is separable, and design procedures to detect entanglement witnesses based on this.

6.3 Construction of entanglement witnesses

As briefly mentioned in chapter 2, entanglement witnesses are tool for detecting entangled states. They consist of an operator $\hat{W}$ chosen such that the hyperplane $\langle\hat{W}\rangle_{\hat{\rho}} = 0$ splits the space of quantum states while leaving the convex set of separable states fully contained in one half, typically chosen as $\langle\hat{W}\rangle_{\hat{\rho}} \geq 0$. Under this construction, any state with $\langle\hat{W}\rangle_{\hat{\rho}} < 0$ cannot be separable, and must be entangled. In this way, one can use the measurement of $\hat{W}$ as a tool to diagnose entangled states. Entanglement witnesses are by definition not able to detect all entangled states and do not define an order relation between entangled states. But they imply a significant resource economy: entanglement witnessing entails the measurement of a (more or less complex) physical observable. This is in contrast to the knowledge of the full quantum state that is required for entanglement measures such as entanglement entropy or negativity [22, 23].

Entanglement witnessing is well-established for systems with a tensor product Hilbert space [125–127]. However, some care is necessary in the presence of superselection rules, as in the case with fermions [183, 184]. To develop an entanglement witness for lattice gauge theories, we need to identify observables that

can faithfully divide out the separable states defined according to equation (6.21). We consider witness operators of the form

$$\hat{\mathrm{W}}_{\pm} = \pm\Big(\omega^{\pm}_{\mathrm{sep}}\hat{1} - \sum_m \hat{\mathrm{O}}^m_A \hat{\mathrm{O}}^m_B\Big)\,, \tag{6.22}$$

with observables $\hat{\mathrm{O}}^m_A\hat{\mathrm{O}}^m_B$ designed to capture quantum correlations between subsystems A and B. Most importantly, in the construction of $\hat{\mathrm{W}}_{\pm}$, we must employ only gauge invariant observables that preserve the local superselection rules, i.e., $\hat{\mathrm{O}}^m_A \in \mathcal{A}(A)$ and $\hat{\mathrm{O}}^m_B \in \mathcal{A}(B)$. The constants $\omega^{\pm}_{\mathrm{sep}}$ are chosen to ensure a non-negative expectation value for all separable states. By optimizing over all separable states,

$$\omega^{\pm}_{\mathrm{sep}} = \max_{\hat{\rho}\in\mathrm{Sep}}/\min\Big\langle \sum_m \hat{\mathrm{O}}^m_A \hat{\mathrm{O}}^m_B \Big\rangle_{\hat{\rho}}\,, \tag{6.23}$$

the $\langle \hat{W}_{\pm}\rangle_{\rho} = 0$ hyperplane touches the boundary of the set of separable states (see figure 6.1), thus maximizing the entangled region detected by $\hat{\mathrm{W}}_{\pm}$ [126]. However, for the entanglement witness to be effective, at least some entangled state has to overcome the bounds from equation (6.23), i.e.,

$$\omega^- < \omega^-_{\mathrm{sep}} \text{ or } \omega^+_{\mathrm{sep}} < \omega^+\,, \tag{6.24}$$

where $\omega^{\pm}$ is the maximal/minimal obtained by optimizing over all states.

6.3.1 Optimization of a witness

In general it is not feasible to perform the optimization required of equation (6.23) as the complexity scales poorly with system size [126]. This means that one has to construct witnesses through indirect means. However, in our case, we can leverage the gauge symmetry to our advantage and perform the optimization more efficiently. This is because the direct sum in equation (6.21) enables a substantial simplification of the optimization procedure.

We can solve the optimization procedure for separable states within a fixed pair of compatible superselection sectors Z_A and Z_B,

$$\omega^{\pm}_{\mathrm{sep}}(\mathrm{Z}_B, \mathrm{Z}_B) = \max_{|\mu_A\rangle,|\nu_B\rangle}/\min \sum_m \langle\mu_A|\,\hat{\mathrm{O}}^m_A\,|\mu_A\rangle\langle\nu_B|\,\hat{\mathrm{O}}^m_B\,|\nu_B\rangle\,, \tag{6.25}$$

where we optimize over the states of a basis of $\mathcal{H}^G_A(\mathrm{Z}_A)$ and $\mathcal{H}^G_B(\mathrm{Z}_B)$. Subsequently optimizing over all compatible pairs Z_A) and Z_A), one recovers $\omega^{\pm}_{\mathrm{sep}}$. This procedure is significantly more efficient than performing a single optimization over the set of all separable states. Moreover, in a scenario where there is additional information about the state being evaluated, a more sensitive witness may

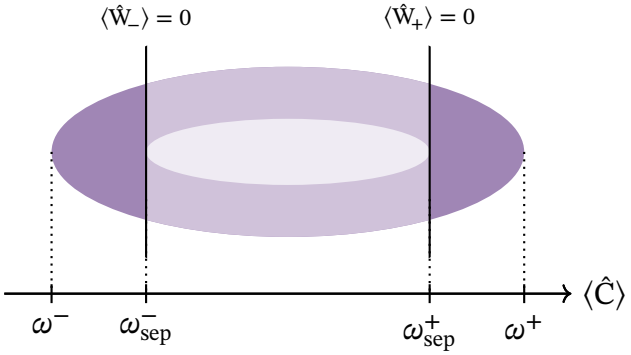

Figure 6.1: Depiction of the entanglement witness optimized over all separable states. Witness operators $\hat{W}_{\pm}$ constructed from a correlator $\hat{C} = \sum_m \hat{O}_A^m \hat{O}_B^m$ as in equation (6.22). The darker shade depict the entangled states detected by the witness, the intermediary shade shows the entangled state that are not detected, and the light shade denotes the set of separable states.

be obtained. For instance, if the probability distribution $p(Z_A, Z_B)$ is known, the constants

$$\omega_{\text{sep}}^{\pm}(p) = \bigoplus_{(Z_A,Z_B)} p(Z_A, Z_B)\omega_{\text{sep}}^{\pm}(Z_B, Z_B) \tag{6.26}$$

yield tighter bounds that may detect entangled states that $\omega_{\text{sep}}^{\pm}$ cannot. In particular, if there is only a single fixed superselection pair for A and B, the bounds from equation (6.25) can be used directly.

Notably, though we focus on the bipartite case, our separability criterion and the construction of the entanglement witness can be easily extended to the multipartite case. Assume a scenario with subregions $R_1 \dots R_k$. We can then define $\hat{W}_{\pm} = \pm(\omega_{\text{sep}}^{\pm}\hat{1} - \sum_m \hat{O}_{R_1}^m \dots \hat{O}_{R_k}^m)$, and use the additional possibilities, since each summand can couple different subregions. To calculate the analogues of equation (6.25), one further needs to compute the compatible superselection sector combinations $(Z_{A_1}, \dots, Z_{A_k})$. This leading to bounds for multipartite separable states and enables the detection of multipartite entanglement in lattice gauge theories.

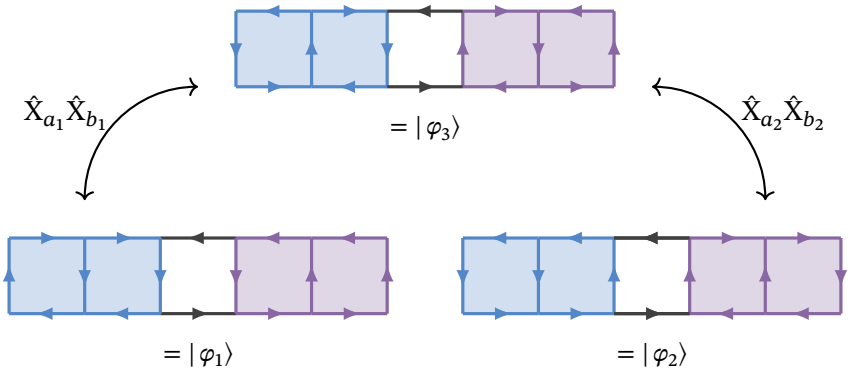

Figure 6.2: Minimal example with the bipartite setup for the entanglement witness with system A in blue and B in purple. The states shown here are the basis for one of the superselection sectors that have non trivial entanglement features. In particular, they define an entangled state $|\psi\rangle = \frac{1}{2}|\varphi_1\rangle + \frac{1}{2}|\varphi_2\rangle + \frac{1}{\sqrt{2}}|\varphi_3\rangle$ which is detected by the witness of equation (6.28) and reaches the maximum value for the correlator $\hat{C}$.

6.3.2 Concrete example for U(1) theories

Given the definitions above, we can construct a valid entanglement witness for the considered U(1) gauge theory. The available gauge invariant observables are the flip operators $\hat{X}_p$, so we consider the following witness

$$\hat{W}_\pm = \pm(\omega^\pm_{\text{sep}}\hat{1} - \hat{C}) = \pm(\omega^\pm_{\text{sep}}\hat{1} - \sum_{p_A p_B} c(p_A, p_B)\hat{X}_{p_A}\hat{X}_{p_B}) \,, \tag{6.27}$$

where the sum runs over plaquettes p_A and p_B in A and B. The function $c(p_A, p_B)$ selects which contributions enter the witness and defines the correlator $\hat{C}$. To employ the witness, it is necessary to evaluate $\langle\hat{C}\rangle$ over all separable states and obtain the constants for equation (6.24). As we have demonstrated, this can be done more efficiently by fixing superselection sectors, and then optimizing.

The simplest example that already yields nontrivial results occurs when both A and B contain two plaquettes. We consider this simple geometry depicted in figure 6.2. In this scenario, that the correlator

$$\hat{C} = \hat{X}_{a_1}\hat{X}_{b_1} + \hat{X}_{a_2}\hat{X}_{b_2} \tag{6.28}$$

witness entanglement in the system. Specifically, we have $\omega^\pm = \pm\sqrt{2}$ and $\omega_{\text{sep}} = \pm 1$, where the nontrivial contributions only come from one pair of compatible

superselection sectors (see figure 6.2). In particular, this superselection sector has dimension 3 and basis states $|\varphi_1\rangle$, $|\varphi_2\rangle$ and $|\varphi_3\rangle$ such that

$$\begin{aligned} \hat{C}|\varphi_1\rangle &= \hat{C}|\varphi_2\rangle = |\varphi_3\rangle \\ \hat{C}|\varphi_3\rangle &= |\varphi_1\rangle + |\varphi_2\rangle \,, \end{aligned} \tag{6.29}$$

so $|\psi\rangle = \frac{1}{2}|\varphi_1\rangle + \frac{1}{2}|\varphi_2\rangle + \frac{1}{\sqrt{2}}|\varphi_3\rangle$ satisfy $\langle\psi|\hat{C}|\psi\rangle = \sqrt{2}$. Thus, it is entangled. This example is just a minimal proof of principle, but the procedure that we used for it can be implemented for larger systems with the help of numerical techniques for optimizing over the superselection sectors (see reference [107]).

7 Conclusion

In this dissertation, we presented some techniques for certifying the presence of entanglement in quantum many-body systems. Conceptually, we tackled two types of question. The issue of how to characterize entanglement in systems that cannot be described by tensor products of local degrees of freedom. And the problem of detecting entanglement in quantum many-body systems with scalable protocols, as opposed to entanglement measures that require near complete knowledge of the quantum state. Our approach aimed at mathematical rigor, while also keeping existing experimental platforms in mind. The techniques discussed in this work are well suited for implementation in, e.g., existing experiments performing quantum simulation.

On the certification side, we demonstrated the possibility of extracting the QFI of certain equilibrium states using engineered dynamics with a protocol that is scalable and experimentally friendly. This was benchmarked with a model of interacting fermions, and we observed the presence of multipartite entanglement at sizeable temperatures. The results further indicate a relation, between the resilience of entanglement to temperature and strongly correlated physics.

The characterization of entanglement was carried out with a formalism that is rigorous, but versatile and applies to quantum systems regardless of their underlying degrees of freedom. It allowed us to define and study multipartite mode entanglement of indistinguishable particles, and obtain bounds that enable the certification of entanglement that is useful for quantum metrology. The bounds were derived with adaptable algorithms, that can be further enhanced for specific situations, giving rise to more effective entanglement certification. Finally, we also studied entanglement in lattice gauge theories, and extended the existing technique of entanglement witnessing to this context.

We are currently in the final stages of implementing the extension of the quench protocol to passive states [106]. This is an important step in pushing the range of applicability of our technique beyond thermal ensembles. Moreover, it fits within our long term research programme of developing a protocol capable of efficiently extracting the QFI that only relies on experimentally verifiable assumptions. Access to such a technique would be a major breakthrough as it would enable certification of entanglement in scalable manner for arbitrary quantum systems.

Furthermore, there are various possibilities to develop the ideas presented in this dissertation. In particular, as already mentioned in chapter 4, the bosonic bounds for the QFI are well suited for existing experiments with bosonic atomic species, and we are currently investigating a good model to test them. This is particularly interesting as a way to explore entanglement in continuum systems in a controlled manner. Moreover, our formalism for entanglement witnesses extends naturally to non-abelian gauge theories, and provides multiple possibilities for future research. Constructing entanglement witnesses for a quantum link model realization of the SU(3) gauge theory is prominent example.

More broadly, the results presented in this work contribute to the ongoing effort to characterize the structure of entanglement in quantum many-body system. This particularly the case in light of the evidence we found of a relation between the thermal stability of entanglement and strongly correlated behaviour. Our contributions are also timely due to the relevance of the problem of entanglement certification to upcoming quantum technologies.

Bibliography

[1] W. Heisenberg, “Über quantentheoretische Umdeutung kinematischer und mechanischer Beziehungen.”, Z. Phys. **33**, 879 (1925).

[2] M. Born et al., “Zur Quantenmechanik”, Z. Phys. **34**, 858 (1925).

[3] M. Born et al., “Zur Quantenmechanik. II.”, Z. Phys. **35**, 557 (1926).

[4] E. Schrödinger, “Quantisierung als Eigenwertproblem”, Ann. Phys. **384**, 361 (1926).

[5] A. Einstein et al., “Can quantum-mechanical description of physical reality be considered complete?”, Phys. Rev. **47**, 777 (1935).

[6] E. Schrödinger, “Discussion of probability relations between separated systems”, Math. Proc. Camb. Philos. Soc. **31**, 555 (1935).

[7] E. Schrödinger, “Probability relations between separated systems”, Math. Proc. Camb. Philos. Soc. **32**, 446 (1936).

[8] M. Born, “Zur Quantenmechanik der Stoßvorgänge”, Z. Phys. **37**, 863 (1926).

[9] D. Bohm, “A suggested interpretation of the quantum theory in terms of ”hidden” variables. I”, Phys. Rev. **85**, 166 (1952).

[10] D. Bohm, “A suggested interpretation of the quantum theory in terms of ”hidden” variables. II”, Phys. Rev. **85**, 180 (1952).

[11] J. S. Bell, “On the Einstein Podolsky Rosen paradox”, Phys. Phys. Fiz. **1**, 195 (1964).

[12] J. S. Bell, “On the problem of hidden variables in quantum mechanics”, Rev. Mod. Phys. **38**, 447 (1966).

[13] J. F. Clauser et al., “Proposed experiment to test local hidden-variable theories”, Phys. Rev. Lett. **23**, 880 (1969).

[14] S. J. Freedman et al., “Experimental test of local hidden-variable theories”, Phys. Rev. Lett. **28**, 938 (1972).

[15] A. Aspect et al., “Experimental realization of Einstein–Podolsky–Rosen–Bohm Gedankenexperiment: a new violation of Bell’s inequalities”, Phys. Rev. Lett. **49**, 91 (1982).

[16] A. Aspect et al., "Experimental test of Bell's inequalities using time- varying analyzers", Phys. Rev. Lett. **49**, 1804 (1982).

[17] G. Weihs et al., "Violation of Bell's inequality under strict Einstein locality conditions", Phys. Rev. Lett. **81**, 5039 (1998).

[18] D. N. Matsukevich et al., "Bell inequality violation with two remote atomic qubits", Phys. Rev. Lett. **100**, 150404 (2008).

[19] M. Giustina et al., "Bell violation using entangled photons without the fair-sampling assumption", Nature **497**, 227 (2013).

[20] B. Hensen et al., "Loophole-free Bell inequality violation using electron spins separated by 1.3 kilometres", Nature **526**, 682 (2015).

[21] R. Horodecki et al., "Quantum entanglement", Rev. Mod. Phys. **81**, 865 (2009).

[22] O. Gühne et al., "Entanglement detection", Phys. Rep. **474**, 1 (2009).

[23] N. Friis et al., "Entanglement certification from theory to experiment", Nat. Rev. Phys. **1**, 72 (2018).

[24] L. Amico et al., "Entanglement in many-body systems", Rev. Mod. Phys. **80**, 517 (2008).

[25] N. Laflorencie, "Quantum entanglement in condensed matter systems", Phys. Rep. **646**, 1 (2016).

[26] G. D. Chiara et al., "Genuine quantum correlations in quantum many-body systems: a review of recent progress", Rep. Prog. Phys. **81**, 074002 (2018).

[27] S. R. White, "Density matrix formulation for quantum renormalization groups", Phys. Rev. Lett. **69**, 2863 (1992).

[28] S. Rommer et al., "Class of ansatz wave functions for one-dimensional spin systems and their relation to the density matrix renormalization group", Phys. Rev. B **55**, 2164 (1997).

[29] I. Affleck et al., "Rigorous results on valence-bond ground states in antiferromagnets", Phys.l Rev. Lett. **59**, 799 (1987).

[30] U. Schollwöck, "The density-matrix renormalization group in the age of matrix product states", Ann. Phys. **326**, 96 (2011).

[31] F. Verstraete et al., "Valence-bond states for quantum computation", Phys. Rev. A **70**, 060302 (2004).

[32] G. Vidal, "Class of quantum many-body states that can be efficiently simulated", Phys. Rev. Lett. **101**, 110501 (2008).

[33] J. Eisert et al., "Colloquium: area laws for the entanglement entropy", Rev. Mod. Phys. **82**, 277 (2010).

[34] S. Sachdev, *Quantum phase transitions*, 2nd ed. (Cambridge University Press (CUP), Mar. 2011).

[35] P. Coleman et al., "Quantum criticality", Nature **433**, 226 (2005).

[36] A. Osterloh et al., "Scaling of entanglement close to a quantum phase transition", Nature **416**, 608 (2002).

[37] G. Vidal et al., "Entanglement in quantum critical phenomena", Phys. Rev. Lett. **90**, 227902 (2003).

[38] F. Verstraete et al., "Entanglement versus correlations in spin systems", Phys. Rev. Lett. **92**, 027901 (2004).

[39] P. Hauke et al., "Measuring multipartite entanglement through dynamic susceptibilities", Nat. Phys. **12**, 778 (2016).

[40] X.-G. Wen, "Colloquium: zoo of quantum-topological phases of matter", Rev. Mod. Phys. **89**, 041004 (2017).

[41] A. Kitaev, "Anyons in an exactly solved model and beyond", Ann. Phys. **321**, 2 (2006).

[42] M. A. Levin et al., "String-net condensation: a physical mechanism for topological phases", Phys. Rev. B **71**, 045110 (2005).

[43] M. A. Nielsen et al., *Quantum computation and quantum information*, 10th ed. (Cambridge University Press (CUP), June 2010).

[44] A. Acín et al., "The quantum technologies roadmap: a european community view", New J. Phys. **20**, 080201 (2018).

[45] Y. I. Manin, "Computable and non-computable", Sov. Radio (1980).

[46] R. P. Feynman, "Simulating physics with computers", Int. J. Theor. Phys. **21**, 467 (1982).

[47] P. W. Shor, "Algorithms for quantum computation: discrete logarithms and factoring", in Proceedings 35th annual symposium on foundations of computer science (Nov. 1994).

[48] D. Deutsch et al., "Rapid solution of problems by quantum computation", Proc. R. Soc. A **439**, 553 (1992).

[49] L. K. Grover, "A fast quantum mechanical algorithm for database search", in Proceedings of the twenty-eighth annual ACM symposium on theory of computing - STOC 96 (1996).

[50] A. Montanaro, "Quantum algorithms: an overview", npj Quantum Inf. **2**, 15023 (2016).

[51] J. Preskill, "Quantum computing in the NISQ era and beyond", Quantum **2**, 79 (2018).

[52] J. I. Cirac et al., "Goals and opportunities in quantum simulation", Nat. Phys. **8**, 264 (2012).

[53] P. Hauke et al., "Can one trust quantum simulators?", Rep. Prog. Phys. **75**, 082401 (2012).

[54] C. Monroe et al., "Programmable quantum simulations of spin systems with trapped ions", Rev. Mod. Phys. **93**, 025001 (2021).

[55] M. Lewenstein et al., *Ultracold atoms in optical lattices* (Oxford University Press, Mar. 2012).

[56] D. Jaksch et al., "Cold bosonic atoms in optical lattices", Phys. Rev. Lett. **81**, 3108 (1998).

[57] T. Esslinger, "Fermi–Hubbard physics with atoms in an optical lattice", Annu. Rev. Condens. Matter Phys. **1**, 129 (2010).

[58] I. Bloch et al., "Quantum simulations with ultracold quantum gases", Nat. Phys. **8**, 267 (2012).

[59] O. Dutta et al., "Non-standard hubbard models in optical lattices: a review", Rep. Prog. Phys. **78**, 066001 (2015).

[60] C. Gross et al., "Quantum simulations with ultracold atoms in optical lattices", Science **357**, 995 (2017).

[61] L. Tarruell et al., "Quantum simulation of the Hubbard model with ultracold fermions in optical lattices", C. R. Phys. **19**, 365 (2018).

[62] K. B. Davis et al., "Bose-einstein condensation in a gas of sodium atoms", Phys. Rev. Lett. **75**, 3969 (1995).

[63] D. S. Jin et al., "Collective excitations of a Bose–Einstein condensate in a dilute gas", Phys. Rev. Lett. **77**, 420 (1996).

[64] L. Pezzé et al., "Quantum metrology with nonclassical states of atomic ensembles", Rev. Mod. Phys. **90**, 035005 (2018).

[65] C. W. Helstrom, "Quantum detection and estimation theory", J. Stat. Phys. **1**, 231 (1969).

[66] C. M. Caves, "Quantum-mechanical noise in an interferometer", Phys. Rev. D **23**, 1693 (1981).

[67] D. F. Walls, "Squeezed states of light", Nature **306**, 141 (1983).

[68] D. J. Wineland et al., "Spin squeezing and reduced quantum noise in spectroscopy", Phys. Rev. A **46**, R6797 (1992).

[69] M. Kitagawa et al., "Squeezed spin states", Phys. Rev. A **47**, 5138 (1993).

[70] D. J. Wineland et al., "Squeezed atomic states and projection noise in spectroscopy", Phys. Rev. A **50**, 67 (1994).

[71] J. Hald et al., "Spin squeezed atoms: a macroscopic entangled ensemble created by light", Phys. Rev. Lett. **83**, 1319 (1999).

[72] J. Estève et al., "Squeezing and entanglement in a Bose–Einstein condensate", Nature **455**, 1216 (2008).

[73] C. Gross et al., "Nonlinear atom interferometer surpasses classical precision limit", Nature **464**, 1165 (2010).

[74] W. Muessel et al., "Scalable spin squeezing for quantum-enhanced magnetometry with Bose-Einstein condensates", Phys. Rev. Lett. **113**, 103004 (2014).

[75] H. Grote et al., "First long-term application of squeezed states of light in a gravitational-wave observatory", Phys. Rev. Lett. **110**, 181101 (2013).

[76] M. Tse et al., "Quantum-enhanced advanced LIGO detectors in the era of gravitational-wave astronomy", Phys. Rev. Lett. **123**, 231107 (2019).

[77] F. Acernese et al. (Virgo Collaboration), "Increasing the astrophysical reach of the advanced virgo detector via the application of squeezed vacuum states of light", Phys. Rev. Lett. **123**, 231108 (2019).

[78] M. G. A. Paris, "Quantum estimation for quantum technology", Int. J. Quantum Inf. **07**, 125 (2009).

[79] G. Tóth et al., "Quantum metrology from a quantum information science perspective", J. Phys. A **47**, 424006 (2014).

[80] M. G. A. Paris, "Entanglement and visibility at the output of a mach-zehnder interferometer", Phys. Rev. A **59**, 1615 (1999).

[81] M. F. Riedel et al., "Atom-chip-based generation of entanglement for quantum metrology", Nature **464**, 1170 (2010).

[82] G. Haack et al., "Parity detection and entanglement with a Mach–Zehnder interferometer", Phys. Rev. B **82**, 155303 (2010).

[83] B. Lücke et al., "Twin matter waves for interferometry beyond the classical limit", Science **334**, 773 (2011).

[84] B. Lücke et al., "Detecting multiparticle entanglement of Dicke states", Phys. Rev. Lett. **112**, 155304 (2014).

[85] H. Strobel et al., "Fisher information and entanglement of non-Gaussian spin states", Science **345**, 424 (2014).

[86] J. G. Bohnet et al., "Quantum spin dynamics and entanglement generation with hundreds of trapped ions", Science **352**, 1297 (2016).

[87] A. Sørensen et al., "Many-particle entanglement with Bose–Einstein condensates", Nature **409**, 63 (2001).

[88] A. S. Sørensen et al., "Entanglement and extreme spin squeezing", Phys. Rev. Lett. **86**, 4431 (2001).

[89] G. Tóth et al., "Optimal spin squeezing inequalities detect bound entanglement in spin models", Phys. Rev. Lett. **99**, 250405 (2007).

[90] L. Pezzé et al., "Entanglement, nonlinear dynamics, and the heisenberg limit", Phys. Rev. Lett. **102**, 100401 (2009).

[91] G. Tóth, "Multipartite entanglement and high-precision metrology", Phys Rev. A **85**, 022322 (2012).

[92] P. Hyllus et al., "Fisher information and multiparticle entanglement", Phys. Rev. A **85**, 022321 (2012).

[93] S. L. Braunstein et al., "Statistical distance and the geometry of quantum states", Phys. Rev. Lett. **72**, 3439 (1994).

[94] M. Cramer et al., "Efficient quantum state tomography", Nat. Commun. **1**, 149 (2010).

[95] C. Schwemmer et al., "Systematic errors in current quantum state tomography tools", Phys. Rev. Lett. **114**, 080403 (2015).

[96] J. Schliemann et al., "Quantum correlations in two-fermion systems", Phys. Rev. A **64**, 022303 (2001).

[97] K. Eckert et al., "Quantum correlations in systems of indistinguishable particles", Ann. Phys. **299**, 88 (2002).

[98] M.-C. Bañuls et al., "Entanglement in fermionic systems", Phys. Rev. A **76**, 022311 (2007).

[99] H. M. Wiseman et al., "Entanglement of indistinguishable particles shared between two parties", Phys. Rev. Lett. **91**, 097902 (2003).

[100] A. P. Balachandran et al., "Algebraic approach to entanglement and entropy", Phys. Rev. A **88**, 022301 (2013).

[101] H. Casini et al., "Remarks on entanglement entropy for gauge fields", Phys. Rev. D **89**, 085012 (2014).

[102] S. Ghosh et al., "On the entanglement entropy for gauge theories", J. High Energy Phys. **2015**, 069 (2015).

[103] K. V. Acoleyen et al., "Entanglement of distillation for lattice gauge theories", Phys. Rev. Lett. **117**, 131602 (2016).

[104] H. Casini et al., "Entanglement entropy and superselection sectors. Part I. Global symmetries", J. High Energy Phys. **2020**, 14 (2020).

[105] R. Costa de Almeida et al., "From entanglement certification with quench dynamics to multipartite entanglement of interacting fermions", Phys. Rev. Research **3**, L032051 (2021).

[106] R. Costa de Almeida et al., "Probing the quantum Fisher information of passive states", (in preparation).

[107] V. Panizza et al., "Entanglement witnessing for lattice gauge theories", J. High Energy Phys. **2022**, 196 (2022).

[108] V. Panizza, "Entanglement witnesses for lattice gauge theories", MA thesis (University of Trento, 2021).

[109] B. M. Latz, "Multipartite entanglement from quench dynamics in spinor bose gases using bogoliubov theory", MA thesis (Heidelberg University, 2019).

[110] A. E. V. Jasso, "Implementing topological entanglement as a resource theory", MA thesis (Heidelberg University, 2020).

[111] M. M. Wilde, *Quantum information theory*, 2nd ed. (Cambridge University Press (CUP), Feb. 2017).

[112] R. Haag, *Local quantum physics, Fields, particles, algebras*, 2nd ed. (Springer Berlin Heidelberg, 1996).

[113] G. J. Murphy, *C*-algebras and operator theory* (Elsevier, 1990).

[114] C. H. Bennett et al., "Communication via one- and two-particle operators on Einstein–Podolsky–Rosen states", Phys. Rev. Lett. **69**, 2881 (1992).

[115] C. H. Bennett et al., "Quantum cryptography: public key distribution and coin tossing", in Proceedings of IEEE international conference on computers, systems and signal processing, Vol. 175 (1984), p. 8.

[116] A. K. Ekert, "Quantum cryptography based on Bell's theorem", Phys. Rev. Lett. **67**, 661 (1991).

[117] C. H. Bennett et al., "Teleporting an unknown quantum state via dual classical and Einstein–Podolsky–Rosen channels", Phys. Rev. Lett. **70**, 1895 (1993).

[118] D. Bouwmeester et al., "Experimental quantum teleportation", Nature **390**, 575 (1997).

[119] D. Boschi et al., "Experimental realization of teleporting an unknown pure quantum state via dual classical and Einstein–Podolsky–Rosen channels", Phys. Rev. Lett. **80**, 1121 (1998).

[120] J.-G. Ren et al., "Ground-to-satellite quantum teleportation", Nature **549**, 70 (2017).

[121] B. S. Cirel'son, "Quantum generalizations of Bell's inequality", Lett. Math. Phys. **4**, 93 (1980).

[122] N. Brunner et al., "Bell nonlocality", Rev. Mod. Phys. **86**, 419 (2014).

[123] A. Peres, "Separability criterion for density matrices", Phys. Rev. Lett. **77**, 1413 (1996).

[124] M. Horodecki et al., "Separability of mixed states: necessary and sufficient conditions", Phys. Lett. A **223**, 1 (1996).

[125] B. M. Terhal, "Bell inequalities and the separability criterion", Phys. Lett. A **271**, 319 (2000).

[126] M. Lewenstein et al., "Optimization of entanglement witnesses", Phys. Rev. A **62**, 052310 (2000).

[127] B. M. Terhal, "Detecting quantum entanglement", Theor. Comput. Sci. **287**, 313 (2002).

[128] H. M. Wiseman et al., "Steering, entanglement, nonlocality, and the Einstein–Podolsky–Rosen paradox", Phys. Rev. Lett. **98**, 140402 (2007).

[129] S. Szalay, "Multipartite entanglement measures", Phys. Rev. A **92**, 042329 (2015).

[130] I. Bengtsson et al., *Geometry of quantum states*, 2nd ed. (Cambridge University Press (CUP), Aug. 2017).

[131] W. Dür et al., "Three qubits can be entangled in two inequivalent ways", Phys. Rev. A **62**, 062314 (2000).

[132] A. Kitaev et al., "Topological entanglement entropy", Phys. Rev. Lett. **96**, 110404 (2006).

[133] M. Levin et al., "Detecting topological order in a ground state wave function", Phys. Rev. Lett. **96**, 110405 (2006).

[134] G. Tóth et al., "Detecting genuine multipartite entanglement with two local measurements", Phys. Rev. Lett. **94**, 060501 (2005).

[135] G. Tóth et al., "Practical methods for witnessing genuine multi-qubit entanglement in the vicinity of symmetric states", New J. of Phys. **11**, 083002 (2009).

[136] R. A. Fisher, "On the mathematical foundations of theoretical statistics", Philos. Trans. R. Soc. A **222**, 309 (1922).

[137] R. A. Fisher, "Theory of statistical estimation", Math. Proc. Camb. Philos. Soc. **22**, 700 (1925).

[138] C. R. Rao, "Information and accuracy attainable in the estimation of statistical parameters", Bull. Calcutta Math. Soc. **35**, 81 (1945).

[139] H. Cramér, *Mathematical methods of statistics*, Vol. 9, Princeton Mathematical Series (Princeton University Press, Dec. 1946).

[140] G. Tóth et al., "Extremal properties of the variance and the quantum fisher information", Phys. Rev. A **87**, 032324 (2013).

[141] V. Giovannetti et al., "Quantum metrology", Phys. Rev. Lett. **96**, 010401 (2006).

[142] P. Zanardi et al., "Quantum tensor product structures are observable induced", Phys. Rev. Lett. **92**, 060402 (2004).

[143] N. Schuch et al., "Nonlocal resources in the presence of superselection rules", Phys. Rev. Lett. **92**, 087904 (2004).

[144] H. Barnum et al., "A subsystem-independent generalization of entanglement", Phys. Rev. Lett. **92**, 107902 (2004).

[145] N. Schuch et al., "Quantum entanglement theory in the presence of superselection rules", Phys. Rev. A **70**, 042310 (2004).

[146] I. M. Gelfand et al., "On the imbedding of normed rings into the ring of operators in Hilbert space", Mat. Sb. **54**, 197 (1943).

[147] I. E. Segal, "Irreducible representations of operator algebras", Bull. Am. Math. Soc. **53**, 73 (1947).

[148] A. Gleason, "Measures on the closed subspaces of a Hilbert space", Indiana Univ. Math. J. **6**, 885 (1957).

[149] R. Haag et al., "An algebraic approach to quantum field theory", J. Math. Phys. **5**, 848 (1964).

[150] M. Lewenstein et al., "Ultracold atomic gases in optical lattices: mimicking condensed matter physics and beyond", Adv. Phys. **56**, 243 (2007).

[151] J. Eisert et al., "Quantum many-body systems out of equilibrium", Nat. Phys. **11**, 124 (2015).

[152] S. Pappalardi et al., "Multipartite entanglement after a quantum quench", J. Stat. Mech.: Theory Exp. **2017**, 053104 (2017).

[153] M. Gabbrielli et al., "Multipartite entanglement at finite temperature", Sci. Rep. **8**, 15663 (2018).

[154] M. Brenes et al., "Multipartite entanglement structure in the eigenstate thermalization hypothesis", Phys. Rev. Lett. **124**, 040605 (2020).

[155] G. Mathew et al., "Experimental realization of multipartite entanglement via quantum fisher information in a uniform antiferromagnetic quantum spin chain", Phys. Rev. Research **2**, 043329 (2020).

[156] M. Yu et al., "Quantum fisher information measurement and verification of the quantum Cramér–Rao bound in a solid-state qubit", npj Quantum Inf. **8**, 56 (2022).

[157] P. Coleman, *Introduction to many-body physics* (Cambridge University Press (CUP), Nov. 2015).

[158] R. Kubo, "Statistical-mechanical theory of irreversible processes. I. general theory and simple applications to magnetic and conduction problems", J. Phys. Soc. Jpn. **12**, 570 (1957).

[159] R. Kubo et al., "Statistical-mechanical theory of irreversible processes. II. response to thermal disturbance", J. Phys. Soc. Jpn. **12**, 1203 (1957).

[160] P. C. Martin et al., "Theory of many-particle systems. I", Phys. Rev. **115**, 1342 (1959).

[161] R. Haag et al., "On the equilibrium states in quantum statistical mechanics", Commun. Math. Phys. **5**, 215 (1967).

[162] H. Araki, "On the equivalence of the KMS condition and the variational principle for quantum lattice systems", Commun. Math. Phys. **38**, 1 (1974).

[163] R. Haag et al., "Stability and equilibrium states", Commun. Math. Phys. **38**, 173 (1974).

[164] H. Araki et al., "Extension of KMS states and chemical potential", Commun. Math. Phys. **53**, 97 (1977).

[165] H. Araki et al., "Equilibrium statistical mechanics of fermion lattice systems", Rev. Math. Phys. **15**, 93 (2003).

[166] N. Landsman, "Spontaneous symmetry breaking in quantum systems: emergence or reduction?", Stud. Hist. Philos. Sci. B - Stud. Hist. Philos. Mod. Phys. **44**, 379 (2013).

[167] K. Landsman, *Foundations of quantum theory, From classical concepts to operator algebras*, 1st ed., Fundamental Theories of Physics (Springer International Publishing, 2017).

[168] W. Pusz et al., "Passive states and KMS states for general quantum systems", Commun. Math. Phys. **58**, 273 (1978).

[169] K. T. Geier et al., "From non-hermitian linear response to dynamical correlations and fluctuation-dissipation relations in quantum many-body systems", 10.48550/arxiv.2104.03983 (2021).

[170] N. Wiener, *Extrapolation, interpolation, and smoothing of stationary time series with engineering applications* (Technology Press of the Massachusetts Institute of Technology, 1964).

[171] M. Perarnau-Llobet et al., "Most energetic passive states", Phys. Rev. E **92**, 042147 (2015).

[172] P. Skrzypczyk et al., "Passivity, complete passivity, and virtual temperatures", Phys. Rev. E **91**, 052133 (2015).

[173] F. Benatti et al., "Entanglement in indistinguishable particle systems", Phys. Rep. **878**, 1 (2020).

[174] N. Friis et al., "Fermionic-mode entanglement in quantum information", Phys. Rev. A **87**, 022338 (2013).

[175] A. P. Balachandran et al., "Entanglement and particle identity: a unifying approach", Phys. Rev. Lett. **110**, 080503 (2013).

[176] N. Friis, "Reasonable fermionic quantum information theories require relativity", New J. Phys. **18**, 033014 (2016).

[177] N. Friis, "Unlocking fermionic mode entanglement", New J. Phys. **18**, 061001 (2016).

[178] F. Benatti et al., "Sub-shot-noise quantum metrology with entangled identical particles", Ann. Phys. **325**, 924 (2010).

[179] F. Benatti et al., "Entanglement and squeezing with identical particles: ultracold atom quantum metrology", J. Phys. B **44**, 091001 (2011).

[180] F. Benatti et al., "Entanglement in fermion systems and quantum metrology", Phys. Rev. A **89**, 032326 (2014).

[181] N. Friis et al., "Heisenberg scaling in gaussian quantum metrology", Phys. Rev. A **92**, 022106 (2015).

[182] D. Braun et al., "Quantum-enhanced measurements without entanglement", Rev. Mod. Phys. **90**, 035006 (2018).

[183] F. Iemini et al., "Quantifying quantum correlations in fermionic systems using witness operators", Quantum Inf. Process. **12**, 733 (2012).

[184] A. Reusch et al., "Entanglement witnesses for indistinguishable particles", Phys. Rev. A **91**, 042324 (2015).

[185] U. Marzolino et al., "Quantum teleportation with identical particles", Phys. Rev. A **91**, 032316 (2015).

[186] T. Debarba et al., "Teleporting quantum information encoded in fermionic modes", Phys. Rev. A **101**, 052326 (2020).

[187] G. C. Wick et al., "The intrinsic parity of elementary particles", Phys. Rev. **88**, 101 (1952).

[188] S. Szalay et al., "Fermionic systems for quantum information people", J. Phys. A **54**, 393001 (2021).

[189] A. Bergschneider et al., "Experimental characterization of two-particle entanglement through position and momentum correlations", Nat. Phys. **15**, 640 (2019).

[190] T. Popoviciu, "Sur les équations algébriques ayant toutes leurs racines réelles", Mathematica **9**, 129 (1935).

[191] R. Bhatia et al., "A better bound on the variance", Am. Math. Mon. **107**, 353 (2000).

[192] H. Strobel, "Fisher information and entanglement of non-Gaussian spin states", PhD thesis (Heidelberg University, 2016).

[193] P. Hyllus et al., "Entanglement and extreme spin squeezing for a fluctuating number of indistinguishable particles", Phys. Rev. A **86**, 012337 (2012).

[194] D. P. Arovas et al., "The Hubbard model", Annu. Rev. Condens. Matter Phys. **13**, 239 (2022).

[195] R. Jördens et al., "A Mott insulator of fermionic atoms in an optical lattice", Nature **455**, 204 (2008).

[196] S. Murmann et al., "Two fermions in a double well: exploring a fundamental building block of the Hubbard model", Phys. Rev. Lett. **114**, 080402 (2015).

[197] A. Mazurenko et al., "A cold-atom Fermi–Hubbard antiferromagnet", Nature **545**, 462 (2017).

[198] C. S. Chiu et al., "Quantum state engineering of a hubbard system with ultracold fermions", Phys. Rev. Lett. **120**, 243201 (2018).

[199] G. Salomon et al., "Direct observation of incommensurate magnetism in Hubbard chains", Nature **565**, 56 (2018).

[200] J. Vijayan et al., "Time-resolved observation of spin-charge deconfinement in fermionic Hubbard chains", Science **367**, 186 (2020).

[201] M. C. Gutzwiller, "Effect of correlation on the ferromagnetism of transition metals", Phys. Rev. Lett. **10**, 159 (1963).

[202] J. Kanamori, "Electron correlation and ferromagnetism of transition metals", Prog. Theor. Phys. **30**, 275 (1963).

[203] J. Hubbard, "Electron correlations in narrow energy bands", Proc. R. Soc. A **276**, 238 (1963).

[204] G. H. Wannier, "Dynamics of band electrons in electric and magnetic fields", Rev. Mod. Phys. **34**, 645 (1962).

[205] C. Castelnovo et al., "Spin ice, fractionalization, and topological order", Annu. Rev. Condens. Matter Phys **3**, 35 (2012).

[206] S.-i. Tomonaga, "Remarks on Bloch's method of sound waves applied to many-fermion problems", Prog. Theor. Phys. **5**, 544 (1950).

[207] J. M. Luttinger, "An exactly soluble model of a many-fermion system", J. Math. Phys. **4**, 1154 (1963).

[208] D. C. Mattis et al., "Exact solution of a many-fermion system and its associated boson field", J. Math. Phys. **6**, 304 (1965).

[209] F. D. M. Haldane, "'Luttinger liquid theory' of one-dimensional quantum fluids. I. properties of the Luttinger model and their extension to the general 1d interacting spinless fermi gas", J. Phys. C: Solid State Phys. **14**, 2585 (1981).

[210] D. Greif et al., "Formation and dynamics of antiferromagnetic correlations in tunable optical lattices", Phys. Rev. Lett. **115**, 260401 (2015).

[211] M. F. Parsons et al., "Site-resolved imaging of fermionic Li_6 in an optical lattice", Phys. Rev. Lett. **114**, 213002 (2015).

[212] G. J. A. Edge et al., "Imaging and addressing of individual fermionic atoms in an optical lattice", Phys. Rev. A **92**, 063406 (2015).

[213] D. Greif et al., "Site-resolved imaging of a fermionic mott insulator", Science **351**, 953 (2016).

[214] L. W. Cheuk et al., "Observation of 2d fermionic mott insulators of ^{40}K with single-site resolution", Phys. Rev. Lett. **116**, 235301 (2016).

[215] M. Boll et al., "Spin- and density-resolved microscopy of antiferromagnetic correlations in Fermi-Hubbard chains", Science **353**, 1257 (2016).

[216] M. F. Parsons et al., "Site-resolved measurement of the spin-correlation function in the Fermi-Hubbard model", Science **353**, 1253 (2016).

[217] J. Berges et al., "Dynamics of entanglement in expanding quantum fields", J. High Energy Phys. **2018**, 145 (2018).

[218] R. Bellwied, "Quantum entanglement in the initial and final state of relativistic heavy ion collisions", J. Phys. Conf. Ser. **1070**, 012001 (2018).

[219] O. K. Baker et al., "Thermal radiation and entanglement in proton-proton collisions at energies available at the CERN large hadron collider", Phys. Rev. D **98**, 054007 (2018).

[220] X. Feal et al., "Thermal behavior and entanglement in pb-pb and p–p collisions", Phys. Rev. C **99**, 015205 (2019).

[221] E. A. Martinez et al., "Real-time dynamics of lattice gauge theories with a few-qubit quantum computer", Nature **534**, 516 (2016).

[222] H. Bernien et al., "Probing many-body dynamics on a 51-atom quantum simulator", Nature **551**, 579 (2017).

[223] N. Klco et al., "Quantum-classical computation of Schwinger model dynamics using quantum computers", Phys. Rev. A **98**, 032331 (2018).

[224] B. Yang et al., "Observation of gauge invariance in a 71-site Bose–Hubbard quantum simulator", Nature **587**, 392 (2020).

[225] M. C. Bañuls et al., "Simulating lattice gauge theories within quantum technologies", Eur. Phys. J. D **74**, 165 (2020).

[226] A. Mil et al., "A scalable realization of local u(1) gauge invariance in cold atomic mixtures", Science **367**, 1128 (2020).

[227] M. Aidelsburger et al., "Cold atoms meet lattice gauge theory", Philos. Trans. R. Soc. A **380**, 20210064 (2021).

[228] J. C. Halimeh et al., "Gauge-symmetry protection using single-body terms", PRX Quantum **2**, 040311 (2021).

[229] M. Freedman et al., "Topological quantum computation", Bull. Am. Math. Soc. **40**, 31 (2002).

[230] W. Lechner et al., "A quantum annealing architecture with all-to-all connectivity from local interactions", Sci. Adv. **1**, e1500838 (2015).

[231] P. Buividovich et al., "Entanglement entropy in gauge theories and the holographic principle for electric strings", Phys. Lett. B **670**, 141 (2008).

[232] W. Donnelly, "Decomposition of entanglement entropy in lattice gauge theory", Phys. Rev. D **85**, 085004 (2012).

[233] A. Gromov et al., "Entanglement entropy in 2D non-abelian pure gauge theory", Phys. Lett. B **737**, 60 (2014).

[234] S. Aoki et al., "On the definition of entanglement entropy in lattice gauge theories", J. High Energy Phys. **2015**, 187 (2015).

[235] R. M. Soni et al., "Aspects of entanglement entropy for gauge theories", J. High Energy Phys. **2016**, 136 (2016).

[236] Đ. Radičević, "Entanglement in weakly coupled lattice gauge theories", J. High Energy Phys. **2016**, 1 (2016).

[237] P. Naaijkens, *Quantum spin systems on infinite lattices*, 1st ed., Lecture Notes in Physics (Springer International Publishing, 2017).

[238] K. G. Wilson, "Confinement of quarks", Phys. Rev. D **10**, 2445 (1974).

[239] J. B. Kogut, "An introduction to lattice gauge theory and spin systems", Rev. Mod. Phys. **51**, 659 (1979).

[240] C.-N. Yang et al., "Conservation of isotopic spin and isotopic gauge invariance", Phys. Rev. **96**, 191 (1954).

[241] J. Kogut et al., "Hamiltonian formulation of Wilson's lattice gauge theories", Phys. Rev. D **11**, 395 (1975).

[242] S. Chandrasekharan et al., "Quantum link models: a discrete approach to gauge theories", Nucl. Phys. B. **492**, 455 (1997).

[243] U.-J. Wiese, "Ultracold quantum gases and lattice systems: quantum simulation of lattice gauge theories", Ann. Phys. **525**, 777 (2013).

[244] R. Brower et al., "QCD as a quantum link model", Phys. Rev. D **60**, 094502 (1999).